THE HEDGEHOG SIGNALING PATHWAY IN THE MOUSE OVARY

A Dissertation
Presented to the Faculty of the Graduate School
of Cornell University
in Fulfillment of the Requirement for the Degree of
Doctor of Philosophy

by
Yi Ren
January 2012

THE HEDGEHOG SIGNALING PATHWAY IN THE MOUSE OVARY

Yi Ren, Ph. D.

Cornell University 2012

The hedgehog (HH) signaling pathway plays critical roles in the *Drosophila* ovary. Previous studies have provided basic information on the pattern of expression of genes within the HH signaling pathway in the mouse ovary and on potential effects of HH signaling on cultured ovarian cells. An in vivo approach with transgenic mice is necessary to determine the function of HH signaling. The studies in this dissertation used the *Amhr2*$^{cre/+}$*SmoM2* transgenic mouse line to investigate phenotypes associated with over-activation of hedgehog signaling in the ovary. Results of these studies determined that HH signaling can influence ovarian follicle development.

Female *Amhr2*$^{cre/+}$*SmoM2* mice are infertile. Although mutant mice had developmental defects in the Mullerian duct, the primary cause of infertility was the failure of ovulation based on the fact that oocytes were trapped in the follicles of superovulated mice. No difference in HH signaling activity was detected between controls and mutants around the time of ovulation. Cumulus expansion was suboptimal but could not explain the complete loss of fertility in the mutants. Luteinization occurred and generated normal levels of progesterone in plasma, although there was a delay in corpus luteum (CL) formation. The major phenotype in the ovaries of mutant mice was reduced mRNA levels of genes typical of smooth muscle in the thecal-interstitial compartment and reduced expression of smooth muscle actin (SMA) associated with blood vessels in the theca, indicating that the thecal vasculature failed to mature. Failure of vascular maturation was most likely the leading cause of anovulation in *Amhr2*$^{cre/+}$*SmoM2* mutant mice.

Vascular maturation failed to occur in the ovaries of mutant mice beginning at the primary stage of follicle development. The *SmoM2-yellow fluorescent protein* (YFP) fusion gene was expressed in the neonatal ovaries of mutant mice and HH signaling

activity was elevated in mutants compared to controls around the time of birth. The vascular network in the cortex of ovaries on days 2 and 4 was of higher density in mutant mice compared to controls. Microarray analyses identified elevated mRNA levels of genes involved in vascular development, particularly genes involved in the formation of vascular networks and in the interaction between endothelial and vascular mesenchymal cells. HH signaling was over-active around the time of birth and may have altered development of the thecal vasculature, possibly leading to the lack of vascular maturation in follicles throughout life.

Around the time of birth, levels of mRNA for genes involved in steroid production were elevated in the ovaries of mutant mice compared to controls. Some of these genes are normally expressed in the fetal adrenal gland, such as *Cyp17a*, *Cyp21a*, *Cyp11b* and *Shh*. Immunohistochemistry of CYP17A, CYP21A and SHH confirmed the expression of these genes in the ovaries of mutant mice but not controls, indicating the presence of adrenal-like cells in the ovaries of mutant mice around the time of birth. This is possibly a result of interrupted cell migration/sorting in the adrenogonadal primordium or differentiation of ovarian cells into adrenal-type cells.

A higher rate of oocyte degeneration and abnormal development of the first wave of follicles occurred in mutant mice. Fewer primordial follicles were present in the ovaries of mutants compared to controls by 24 days of age.

Virgin female *Amhr2*$^{cre/+}$*SmoM2* mutant mice developed ovarian pathology with high frequency. The pathological changes started between 60 to 120 days of age and progressed over time. Clusters of steroidogenic-like cells persisted from 120 days to 1.5 years of age and may contribute to the pathological changes in the ovaries of mutant mice.

In summary, this dissertation provides strong evidence that HH signaling regulates development of the thecal vasculature and its maturation. Over-activation of HH signaling in the embryonic and neonatal ovary led to failure of the thecal vasculature to mature properly, and this was associated with anovulation throughout life. Furthermore, HH may be involved in cell migration/sorting or differentiation of

steroidogenic cells in the embryonic and neonatal ovary. Over-activation of HH signaling activity early in life leads to development of ovarian pathology in aged mice.

BIOGRAPHICAL SKETCH

Yi Ren was born as a single child of the family as were most children born in mainland China during the 1980'. Although she grew up in the middle-sized City Zhengzhou in the Henan Province, her home in the suburbs neighbored land used for crops and animal farms of the Henan Institute of Agricultural Science. Her interest in life science began from a very early stage of her childhood. In elementary school, she dreamed of resurrecting dinosaurs through remnant genetic materials from the fossils of dinosaur eggs. She learned about diverse domesticated as well as wild plants and animals both in the field and at home, from reading, exploring nature, and raising a variety of animals, birds and insects, and was given the title "the zoo minister" by her friends.

After graduating from Henan Experimental High School, she moved on to study at the Department of Animal Science and Technology at China Agricultural University in Beijing. There she worked in projects involving in vitro fertilization and embryo cryopreservation techniques in domestic animals. She also frequented seminars on a variety of topics in biology and was very fortunately inspired by researchers in the field of reproductive biology. Her growing interest in reproductive biology leaded her to Dr. Susan Quirk's laboratory at Cornell University in 2006 to pursue a Ph.D. degree in reproductive physiology. Her Ph.D. projects explore the role of hedgehog signaling in the mammalian ovary using the mouse as a model. She will continue doing research as a postdoctoral fellow after the completion of her Ph.D. degree and she wishes one day to become an independent research scientist and to teach in the field of reproductive biology.

ACKNOWLEDGEMENTS

I am most grateful to my dissertation adviser Dr. Susan Quirk for patiently and artfully teaching me the technique, thinking method, and style of science. She always seems to have the magic ability to inspire my curiosity, to cultivate my confidence, and to strengthen my strength while weakening my weakness. I infinitely appreciate her down-to-every-detailed help with my English, in both spoken and written form; her guidance to the path of a career in science; and her rigorous pursuing for perfection in experimental design and preparation for publication, which I wish to continue to carry on in the future.

I am also very thankful to have the opportunity to learn from and work with other members in Dr. Qurik's laboratory. My special thanks go to Robert Cowan for his fun, patient and creative instruction and demonstration on almost every laboratory technique that I have learned in the last five years. I would also like to offer my thanks to Rebecca Harman, who not only taught me a variety of techniques when I first joined the lab, but also has been an inspiration for working cheerfully and efficiently on a daily basis. I am greatly in debt to Fernando Migone, who has been a tremendous help with managing the mouse room and with my projects. He has taught me a great deal on how to proactively get things done in a timely fashion and to implement positive changes whenever such changes are needed.

I am deeply grateful to my committee members Dr. John Schimenti, Dr. Mariana Wolfner and Dr. Scott Coonrod, for generously spending their time to discuss my projects, helping me with writing, and writing recommendation letter for me. Special acknowledgement goes to Dr. Scott Coonrod for letting me use his confocal microscope for the last two years, without which much of the data in this dissertation could not have been collected.

My gratitude extends to many people in the Department of Animal Science, who have provided me a supportive and warm home for the last five years. Many thanks to Dr. Patricia Johnson and Dr. James Giles, who have kindly let me use their lab

equipment and have been wonderful lab neighbors. I would also like to acknowledge the help of Joanne Parsons and Deloris Bevins, who responded patiently to my request to print papers.

Lastly, I would like to offer my heartfelt gratitude to my family. I want to thank my mother Lily for giving me the roots and wings of life and showing me the positive and perseverant attitude of life. I am also grateful to have spent the last two and half years at Cornell University with my husband Victor Kostyuk, who has supported me infinitely with love.

TABLE OF CONTENTS

LIST OF TABLES

LIST OF FIGURES

CHAPTER ONE:

REVIEW OF LITERATURE AND INTRODUCTION TO CURRENT RESEARCH

The hedgehog signaling pathway

Components of the hedgehog (HH) signaling pathway were first discovered in *Drosophila* by Nusslein-Volhard and Wieschaus using mutagenesis screens (Nusslein-Volhard & Wieschaus, 1980). The name *hedgehog* was given based on the spiky appearance of disorganized denticles during *Drosophila* embryonic development. The hedgehog signaling pathway is highly conserved from flies to vertebrates (Ruel & Therond, 2009). In all species examined to date, secreted HH ligand binds to transmembrane receptor PATCHED (PTC in *Drosophila* melanogaster, PTCH in vertebrates). This binding of HH ligand to PATCHED releases the inhibition of signaling transducer Smoothened (SMO) by PATCHED, and cellular response to HH signaling occurs through changes in expression of HH target genes, such as *Bmp4* (Astorga & Carlsson, 2007), *Vegfa* (Pola *et al.*, 2001), and *N-Myc* (Oliver *et al.*, 2003).

Despite conserved mechanisms described above, divergences in pathway components and in signaling transduction exist between *Drosophila* and mammals (Hooper & Scott, 2005). Instead of a single HH ligand as occurs in *Drosophila*, there are three ligands in mammals, Indian (IHH), Sonic (SHH) and Desert (DHH) HH. While there is only one effector at the transcriptional level in *Drosophila* named Cubitus interruptus (Ci), there are three GLI-Kruppel family members in vertebrates, GLI1, GLI2 and GLI3, which function as transcription factors mediating HH signaling activity (Ruiz i Altaba *et al.*, 2007). Recently, a group of novel, vertebrate-specific HH ligand co-receptors were identified, including BOC, CDO and GAS1, adding a new layer of complexity in the spatial and temporal regulation of HH signaling activity (Allen *et al.*, 2011; Izzi *et al.*, 2011). Moreover, accumulating evidence supports a model in which

the primary cilium is the HH sensoring and regulation center in vertebrates, while this structure is not present in *Drosophila* (Goetz & Anderson, 2010). In vertebrates, key components of the HH pathway are enriched in the primary cilium and their trafficking in the cilium occurs in a HH signaling-dependent manner. Interruption of HH signaling by disturbing intraflagellar transport causes phenotypes similar to those caused by deletion of components of the HH signaling pathway.

One feature of the HH signaling pathway is that its signaling activity is strictly regulated spatially and temporally by a feedback loop (Chuang & McMahon, 1999; Ribes & Briscoe, 2009; Ruiz i Altaba *et al.*, 2007). In the absence of HH ligand, *Gli1* is transcriptionally silent and only *Gli2* and *Gli3* are expressed at considerable levels. The majority of GLI2 is degraded and GLI3 is proteolytically cleaved into a transcription repressor of HH-targeted genes. When HH ligand activates signaling, expression of *Gli1* is elevated. GLI2 and an uncleaved form of GLI3 can function as transcriptional activators and they may contribute to the increased transcription of *Gli1*. GLI1 functions as a potent transcriptional activator, and together with the activator forms of GLI2 and GLI3, induces expression of HH-target genes including several components of the HH pathway itself, such as *Ptch*, hedgehog interacting protein (*Hhip*) and *Gli1*. In addition to its function as a receptor for HH ligands, PTCH1 can bind HH ligands on the cell membrane and facilitate degradation of ligands by endocytosis (Incardona *et al*., 2002). HHIP is anchored in the cell membrane and binds to all three HH ligands, functioning as an inhibitor of HH signaling (Chuang *et al.*, 2003). PTCH and HHIP bind and sequester HH ligands to restrict signaling activity in space and time, thus forming a negative feedback loop (Chuang & McMahon, 1999). Changes in levels of

mRNA for *Ptch*, *Hhip* and *Gli1* are frequently used as measures of changes in HH signaling activity (Ahn & Joyner, 2004; Lee *et al*., 1997).

HH signaling in development, adult homeostasis and disease

The HH signaling pathway is deployed widely during development, adult homeostasis and disease. Examples of other families of signaling pathways with such wide range of functions include the Wnt (combination of 'wingless' and '*INT*'), Notch, bone morphogenic proteins/transforming growth factor β (BMP/TGFβ), fibroblast growth factor (FGF) and epidermal growth factor (EGF) pathways. There is significant interaction among these pathways in a variety of developmental and pathological processes but this review focuses on the regulatory role of HH signaling in mammals.

During embryonic development, the HH signaling pathway is a critical regulator of morphogenesis and patterning of multiple organs and tissues, such as the neural tube, limb bud, and the gastrointestinal tract. In the ventral region of the spinal cord, SHH functions as a morphogen and directs the differentiation of the ventral neural progenitor cells into five neuronal subtypes (Dessaud *et al.*, 2008; Marti & Bovolenta, 2002; Patten & Placzek, 2000). At the posterior margin of the limb bud, SHH secreted from the zone of polarizing activity specifies the digits along the anterior-posterior axis (Francis-West & Hill, 2008; Tickle *et al.*, 1975). SHH and IHH expressed in gut endoderm target the mesenchyme and regulate smooth muscle differentiation and left-right axis formation during embryonic gut development (Ramalho-Santos *et al.*, 2000; van den Brink, 2007). HH signaling also regulates vascular development during embryonic life, and this is reviewed in Chapter 3.

During adult homeostasis, HH signaling plays important roles in processes such as cyclic development of the hair follicle (Fuchs *et al.*, 2001), regenerative repair of the bladder in response to infection (Shin *et al.*, 2011), repair of lung epithelium (Birney *et al.*, 2009), and hematopoiesis (Bhardwaj *et al*., 2001). In humans and mice, mutations that lead to abnormal activation of HH signaling are detected in many types of tumors, such as those of brain, skin, liver, colon, prostate, and the lung (Beachy *et al.*, 2004; Rubin & de Sauvage, 2006; Taipale & Beachy, 2001). Interestingly, these tissues or organs in which abnormal HH signaling activity is associated with cancer are within the same tissues and organs where HH signaling regulates development. It has been hypothesized that HH signaling regulates self-renewal of stem cells or progenitor cells in multiple tissues and this may explain how it contributes to embryonic development, adult homeostasis and pathological process (Beachy *et al.*, 2004). Based on this hypothesis, abnormally activated HH signaling would induce inappropriate expansion of stem cells or progenitor cells and thereby initiate/promote tumorigenesis. Multiple lines of evidence exist in support of this hypothesis. Antagonizing HH signaling using the SMO inhibitor cyclopamine lead to the loss of neuronal stem cells and inhibited tumor growth (Berman *et al.*, 2002). HH signaling was found to maintain tumor stem cell populations in multiple myeloma (Peacock *et al.*, 2007). In cerebellar tumors, mutation of *Gli1* leads to persistent proliferation of granule-cell precursors (Clement *et al.*, 2007). As for melanomas, committed melanocyte precursors in the hair-follicle matrix over-proliferated in response to sustained HH signaling (Stecca *et al.*, 2007). In addition, HH was shown to regulate genes critical in stem cell renewal, such as *nestin* and Bmi1 poly comb ring finger oncogene (*Bmi-1)* (Dave *et al.*, 2011; Michael *et al.*,

2008).

The hedgehog signaling pathway in the ovary

The HH signaling pathway plays critical roles in the *Drosophia* ovary. It maintains the germline stem cell population (King *et al.*, 2001; Narbonne-Reveau *et al.*, 2006), regulates proliferation and differentiation of ovarian somatic stem cells and their progeny (Forbes *et al.*, 1996; Zhang & Kalderon, 2001), and induces mesenchymal precursor cells to differentiate into polar and stalk cells (Tworoger *et al.*, 1999).

In the mammalian ovary, there is evidence for active HH signaling during follicle growth and ovulation, but the role of HH signaling has not yet been determined (Ren *et al.*, 2009; Russell *et al.*, 2007; Spicer *et al.*, 2009; Wijgerde *et al.*, 2005). Beginning at the primary stage of follicle growth, HH ligands, namely *Ihh* and *Dhh*, are expressed in granulosa cells, while targets of HH signaling *Ptch1*, *Gli1* and *Hhip* are mainly expressed in the surrounding mesenchymal compartment. This pattern suggests that the mesenchymal compartment may be the primary target of HH ligands during follicle growth. Shortly after hCG stimulation, mRNA of *Ihh* and *Dhh* is reduced to basal levels and remains low until the time of ovulation; simultaneously, mRNA of *Ptch1* and *Gli1* decreases in the theca-interstitial compartment (Ren *et al.*, 2009 2009; Wijgerde *et al.*, 2005). In vitro studies showed that treatment with SHH promoted proliferation of granulosa cells and the growth of preantral follicles (Russell *et al*., 2007). In addition, treatment of cultured bovine theca-interstitial tissue with SHH stimulated cell proliferation and androgen production (Spicer *et al.*, 2009).

In summary, previous studies have provided basic information about the pattern of

expression for genes within the HH signaling pathway in the mouse ovary, and on the potential effects of HH signaling in cultured ovarian cells. An in vivo approach with transgenic mice is necessary to determine the function of HH signaling in the mouse ovary.

Introduction to current research

In vivo approaches with transgenic mice have been used in the Quirk laboratory to determine the function of HH signaling in the mouse ovary. Two transgenic mouse lines were created, the *Amhr2*$^{cre/+}$Smo$^{null/fox}$ and the *Amhr2*$^{cre/+}$*SmoM2* mouse lines. In the *Amhr2*$^{cre/+}$Smo$^{null/fox}$ mouse line, the HH signal transducer *Smo* is conditionally deleted in the somatic cells of the ovary and the mesenchyme of the Mullerian duct; the female mice are subfertile primarily due to deferred timing of implantation, which leads to embryonic loss (Harman, *et al.*, 2011). In addition, subtle aberrant features of ovarian function have been noted (unpublished). The focus of this dissertation is the ovarian phenotypes in the *Amhr2*$^{cre/+}$*SmoM2* mouse line in which HH signaling is abnormally activated in the ovary and the Mullerian duct.

Female *Amhr2*$^{cre/+}$*SmoM2* mice are infertile. The first aim of the studies reported in this dissertation was to determine the phenotype of *Amhr2*$^{cre/+}$*SmoM2* mice. This included determining the cause of their infertility (Chapter 2). Although mutant mice had developmental defects in the Mullerian duct, we showed that the primary cause of infertility was the failure of ovulation, based on the fact that oocytes were rarely recovered from the oviducts and remained trapped in the follicles of superovulated mice. No apparent morphological abnormality was observed during follicle growth and the

preovulatory period in the ovaries of mutant mice. After stimulation with equine chorionic gonadotropin (eCG) and human chorionic gonadotropin (hCG), cumulus expansion was suboptimal and luteinization was relatively normal. Microarray analyses indicated that mRNA levels of genes typical of smooth muscle were reduced in the mutant mice and real-time RT-PCR and immunohistochemistry of SMA showed that this reduction occurred in the theca-interstitial compartment of the ovary. Immunohistochemistry of platelet endothelial cell adhesion molecule (PECAM-1) and SMA revealed that the reduced expression of SMA was associated with the thecal vasculature, indicating that vessels in theca fail to mature by acquiring the normal complement of vascular smooth muscle cells. We concluded that a mature vasculature in each follicle is necessary for successful ovulation and that defective maturation of the vasculature in growing and preovulatory follicles was likely the major cause of the anovulation phenotype in mutant mice.

The second aim of the dissertation research was to investigate the developmental processes that were altered by dominant activation of HH signaling that could lead to defective maturation of the vasculature in follicles of mutant mice (Chapter 3). Confocal imaging of ovaries on day 2 showed expression of the SMOM2-YFP fusion protein throughout the ovary. HH signaling activity was compared between control and mutant mice at a series of time points during the first several weeks of life by measuring mRNA levels of *Gli1*, *Ptch1* and *Hhip* using real-time RT-PCR. Data showed that HH signaling was elevated in ovaries of mutant mice compared to controls during the first few days of life and then became similar in mutant and control mice. Vascular smooth muscle normally becomes associated with the theca beginning between the primary to

secondary stage of follicle growth. In mutant mice, this maturation fails to occur in all follicles throughout life. Because HH signaling appeared to be elevated in the ovaries of mutant mice compared to controls during the first few days of life and not in growing follicles, the findings suggest that failed maturation of the vasculature in follicles of mutant mice throughout life is caused by change induced during neonatal ovary development. Developmental processes altered in the ovaries of mutant mice were examined by microarray analyses of mRNA extracted from whole ovaries of mice on day 2. Cluster analyses using the DAVID program revealed that the most significantly altered developmental process in the mutants compared to controls was vascular development, and included genes involved in the formation of vascular networks and in the interaction between endothelial and vascular mesenchymal cells. Immunohistochemistry of PECAM-1 showed that a vascular network of higher density formed in the cortex of ovaries from mutant mice. The studies determined that HH signaling was over-activated around the time of birth and that this was associated with altered development of the ovarian vasculature, possibly leading to the lack of vascular maturation in the theca of follicles throughout life.

Cluster analyses of data obtained from microarray analyses also revealed elevated mRNA levels for genes involved in steroid production in the ovaries of mutants compared to controls. Some of these genes are normally expressed in the fetal adrenal, such as *Cyp17a*, *Cyp21a*, *Cyp11b* and *Shh*. Immunohistochemistry showed that the majority of cells positive for CYP17A were also positive for CYP21A, and that SHH-positive cells were within close proximity of CYP17A/CYP21A-positive cells. These results indicated the presence of adrenal-like cells in the ovaries of mutant mice

around the time of birth.

The third aim was to examine changes in ovarian phenotype in aged *Amhr2*$^{cre/+}$*SmoM2* mutant mice (Chapter 4). By 1.5 years of age, virgin female *Amhr2*$^{cre/+}$*SmoM2* mutant mice developed ovarian pathology with high frequency. Histological examination and immunohistochemistry of CYP17A suggested that the pathology of aged female *Amhr2*$^{cre/+}$*SmoM2* mutant mice was associated with steroidogenic-like cells that persisted from 120 days to 1.5 years of age.

References

Ahn S, Joyner AL (2004) Dynamic changes in the response of cells to positive hedgehog signaling during mouse limb patterning. *Cell* **118:** 505-516

Allen BL, Song JY, Izzi L, Althaus IW, Kang JS, Charron F, Krauss RS, McMahon AP (2011) Overlapping Roles and Collective Requirement for the Coreceptors GAS1, CDO, and BOC in SHH Pathway Function. *Dev Cell* **20:** 775-787

Astorga J, Carlsson P (2007) Hedgehog induction of murine vasculogenesis is mediated by Foxf1 and Bmp4. *Development* **134:** 3753-3761

Beachy PA, Karhadkar SS, Berman DM (2004) Tissue repair and stem cell renewal in carcinogenesis. *Nature* **432:** 324-331

Berman DM, Karhadkar SS, Hallahan AR, Pritchard JI, Eberhart CG, Watkins DN, Chen JK, Cooper MK, Taipale J, Olson JM, Beachy PA (2002) Medulloblastoma growth inhibition by hedgehog pathway blockade. *Science* **297:** 1559-1561

Bhardwaj G, Murdoch B, Wu D, Baker DP, Williams KP, Chadwick K, Ling LE, Karanu FN, Bhatia M (2001) Sonic hedgehog induces the proliferation of primitive human hematopoietic cells via BMP regulation. *Nat Immunol* **2:** 172-180

Chuang P, Kawcak T, McMahon AP (2003) Feedback control of mammalian Hedgehog signaling by the Hedgehog-binding protein, Hip1, modulates Fgf signaling during branching morphogenesis of the lung. *Genes and Development* **17:** 342-347

Chuang P, McMahon AP (1999) Vertebrate Hedgehog signalling modulated by induction

of a Hedgehog-binding protein. *Nature* **397:** 617-621

Clement V, Sanchez P, de Tribolet N, Radovanovic I, Ruiz i Altaba A (2007) HEDGEHOG-GLI1 signaling regulates human glioma growth, cancer stem cell self-renewal, and tumorigenicity. *Curr Biol* **17:** 165-172

Dave RK, Ellis T, Toumpas MC, Robson JP, Julian E, Adolphe C, Bartlett PF, Cooper HM, Reynolds BA, Wainwright BJ (2011) Sonic hedgehog and notch signaling can cooperate to regulate neurogenic divisions of neocortical progenitors. *PLoS One* **6:** e14680

Dessaud E, McMahon AP, Briscoe J (2008) Pattern formation in the vertebrate neural tube: a sonic hedgehog morphogen-regulated transcriptional network. *Development* **135:** 2489-2503

Forbes AJ, Lin H, Ingham PW, Spradling AC (1996) *hedgehog* is required for the proliferation and specification of ovarian somatic cells prior to egg chamber formation in *Drosophila*. *Development* **122:** 1125-1135

Francis-West P, Hill R (2008) Uncoupling the role of sonic hedgehog in limb development: growth and specification. *Sci Signal* **1:** pe34

Fuchs E, Merrill BJ, Jamora C, DasGupta R (2001) At the roots of a never-ending cycle. *Dev Cell* **1:** 13-25

Goetz SC, Anderson KV (2010) The primary cilium: a signalling centre during vertebrate development. *Nat Rev Genet* **11:** 331-344

Hooper JE, Scott MP (2005) Communicating with hedgehogs. *Nature Reviews Molecular Cell Biology* **6:** 306-317

Incardona JP, Gruenberg J, Roelink H (2002) Sonic hedgehog induces the segregation of patched and smoothened in endosomes. *Curr Biol* **12:** 983-995

Izzi L, Levesque M, Morin S, Laniel D, Wilkes BC, Mille F, Krauss RS, McMahon AP, Allen BL, Charron F (2011) Boc and gas1 each form distinct shh receptor complexes with ptch1 and are required for shh-mediated cell proliferation. *Dev Cell* **20:** 788-801

King FJ, Szakmary A, Cox DN, Lin H (2001) Yb modulates the divisions of both germline and somatic stem cells through piwi- and hh-mediated mechanisms in the Drosophila ovary. *Molecular Cell* **7:** 497-508

Lee J, Platt KA, Censullo P, Ruiz i Altaba A (1997) Gli1 is a target of Sonic hedgehog that induces ventral neural tube development. *Development* **124:** 2537-2552

Marti E, Bovolenta P (2002) Sonic hedgehog in CNS development: one signal, multiple

outputs. *Trends Neurosci* **25:** 89-96

Michael LE, Westerman BA, Ermilov AN, Wang A, Ferris J, Liu J, Blom M, Ellison DW, van Lohuizen M, Dlugosz AA (2008) Bmi1 is required for Hedgehog pathway-driven medulloblastoma expansion. *Neoplasia* **10:** 1343-1349, 1345p following 1349

Narbonne-Reveau K, Besse F, Lamour-Isnard C, Busson D, Pret AM (2006) fused regulates germline cyst mitosis and differentiation during Drosophila oogenesis. *Mech Dev* **123:** 197-209

Nusslein-Volhard C, Wieschaus E (1980) Mutations affecting segment number and polarity in Drosophila. *Nature* **287:** 795-801

Oliver TG, Grasfeder LL, Carroll AL, Kaiser C, Gillingham CL, Lin SM, Wickramasinghe R, Scott MP, Wechsler-Reya RJ (2003) Transcriptional profiling of the Sonic hedgehog response: a critical role for N-myc in proliferation of neuronal precursors. *Proc Natl Acad Sci U S A* **100:** 7331-7336

Patten I, Placzek M (2000) The role of Sonic hedgehog in neural tube patterning. *Cell Mol Life Sci* **57:** 1695-1708

Peacock CD, Wang Q, Gesell GS, Corcoran-Schwartz IM, Jones E, Kim J, Devereux WL, Rhodes JT, Huff CA, Beachy PA, Watkins DN, Matsui W (2007) Hedgehog signaling maintains a tumor stem cell compartment in multiple myeloma. *Proc Natl Acad Sci U S A* **104:** 4048-4053

Pola R, Ling LE, Silver M, Corbley MJ, Kearney M, Pepinsky RB, Shapiro R, Taylor FR, Baker DP, Asahara T, Isner JM (2001) The morphogen Sonic hedgehog is an indirect angiogenic agent upregulating two families of angiogenic growth factors. *Nature Medicine* **7:** 706-711

Ramalho-Santos M, Melton DA, McMahon AP (2000) Hedgehog signals regulate multiple aspects of gastrointestinal development. *Development* **127:** 2763-2772

Ren Y, Cowan RG, Harman RM, Quirk SM (2009) Dominant activation of the hedgehog signaling pathway in the ovary alters theca development and prevents ovulation. *Molecular Endocrinology* **23:** 711-723

Ribes V, Briscoe J (2009) Establishing and interpreting graded sonic hedgehog signaling during vertebrate neural tube patterning: the role of negative feedback. *Cold Spring Harbor Perspectives in Biology* **1:a002014**

Rubin LL, de Sauvage FJ (2006) Targeting the Hedgehog pathway in cancer. *Nature Reviews Drug Discovery* **5:** 1026-1033

Ruel L, Therond PP (2009) Variations in Hedgehog signaling: divergence and

perpetuation in Sufu regulation of Gli. *Genes Dev* **23:** 1843-1848

Ruiz i Altaba A, Mas C, Stecca B (2007) The Gli code: an information nexus regulating cell fate, stemness and cancer. *Trends Cell Biol* **17:** 438-447

Russell MC, Cowan RG, Harman RM, Walker AL, Quirk SM (2007) The hedgehog signaling pathway in the mouse ovary. *Biology of Reproduction* **77:** 226-236

Shin K, Lee J, Guo N, Kim J, Lim A, Qu L, Mysorekar IU, Beachy PA (2011) Hedgehog/Wnt feedback supports regenerative proliferation of epithelial stem cells in bladder. *Nature* **472:** 110-114

Spicer LJ, Sudo S, Aad PY, Wang LS, Chun SY, Ben-Shlomo I, Klein C, Hsueh AJ (2009) The hedgehog-patched signaling pathway and function in the mammalian ovary: a novel role for hedgehog proteins in stimulating proliferation and steroidogenesis of theca cells. *Reproduction* **138:** 329-339

Stecca B, Mas C, Clement V, Zbinden M, Correa R, Piguet V, Beermann F, Ruiz IAA (2007) Melanomas require HEDGEHOG-GLI signaling regulated by interactions between GLI1 and the RAS-MEK/AKT pathways. *Proc Natl Acad Sci U S A* **104:** 5895-5900

Taipale J, Beachy PA (2001) The Hedgehog and Wnt signalling pathways in cancer. *Nature* **411:** 349-354

Tickle C, Summerbell D, Wolpert L (1975) Positional signalling and specification of digits in chick limb morphogenesis. *Nature* **254:** 199-202

Tworoger M, Larkin MK, Bryant Z, Ruohola-Baker H (1999) Mosaic analysis in the drosophila ovary reveals a common hedgehog-inducible precursor stage for stalk and polar cells. *Genetics* **151:** 739-748

van den Brink GR (2007) Hedgehog signaling in development and homeostasis of the gastrointestinal tract. *Physiol Rev* **87:** 1343-1375

Wijgerde M, Ooms M, Hoogerbrugge JW, Grootegoed JA (2005) Hedgehog signaling in mouse ovary: Indian hedgehog and desert hedgehog induce target gene expression in developing theca cells. *Endocrinology* **146:** 3558-3566

Zhang Y, Kalderon D (2001) Hedgehog acts as a somatic stem cell factor in the *Drosophila* ovary. *Nature* **410:** 599-604

CHAPTER TWO:

DOMINANT ACTIVATION OF THE HEDGEHOG SIGNALING PATHWAY IN THE OVARY ALTERS THECA DEVELOPMENT AND PREVENTS OVULATION

Ren Y, Cowan RG, Harman RM, Quirk SM (2009) Dominant activation of the hedgehog signaling pathway in the ovary alters theca development and prevents ovulation. *Molecular Endocrinology* **23:** 711-723. Reprinted with kind permission of the Endocrine Society.

Summary

The role of the hedgehog (HH) signaling pathway in ovarian function was examined in transgenic mice in which expression of a dominant active allele of the signal transducer smoothened (*SmoM2*) was directed to the ovary and Müllerian duct by cre-mediated recombination (*Amhr2*$^{cre/+}$*SmoM2*). Mutant mice were infertile and had ovarian and reproductive tract defects. Ovaries contained follicles of all sizes and corpora lutea (CL), but oocytes were rarely recovered from the oviducts of superovulated mice and remained trapped in preovulatory follicles. Measures of luteinization did not differ. Cumulus expansion appeared disorganized, and in vitro analyses confirmed a reduced expansion index. Microarray analysis indicated that expression levels of genes typical of smooth muscle were reduced in mutant mice and RT-PCR showed that levels of expression of muscle genes were reduced in the non-granulosa, theca-interstitial cell-enriched fraction. While a layer of cells in the outer theca was positively stained for smooth muscle actin in control ovaries, this staining was reduced or absent in mutant ovaries. Expression of a number of genes in granulosa cells that are known to be important for ovulation did not differ in mutants and controls. Expression of components of the HH pathway was observed in both granulosa cells and in the non-granulosa, residual ovarian tissue and changed in response to treatment with eCG/hCG. The results show that appropriate signaling through the HH pathway is required for development of muscle cells within the theca and that impaired muscle development is associated with failure to release the oocyte at ovulation.

Introduction

The hedgehog (HH) signaling pathway plays a critical role in the development of multiple organs in the embryo and in remodeling processes in adult tissues (King *et al.*, 2008; McMahon *et al.*, 2003). In addition, aberrant HH signaling is associated with the development of cancer (Rubin & de Sauvage, 2006). Processes regulated by HH signaling include cell fate determination, proliferation, and differentiation. HH signaling is critical for ovarian function in Drosophila (McMahon *et al.*, 2003) but its role in the mammalian ovary is not known. Expression of components of the HH signaling pathway have been reported in the mouse ovary, and granulosa and theca cells have been identified as potential targets (Russell *et al.*, 2007; Wijgerde *et al.*, 2005).

In mammals, components of the HH pathway include three secreted protein ligands, sonic, Indian and desert hedgehog (SHH, IHH, DHH), which are differentially expressed in various tissues. There are two transmembrane receptors, patched (PTCH) 1 and 2, which are thought to function similarly, and a transmembrane protein smoothened (SMO) which transduces the signal. In the absence of HH ligand, PTCH inhibits signaling through SMO. Binding of ligand to PTCH relieves inhibition of SMO and signaling occurs. Signaling through SMO is conveyed by modulation of the activity of a family of transcription factors, GLI1, GLI2 and GLI3 (Huangfu & Anderson, 2006). *Gli1* is a transcriptional target of HH signaling and has been used as indicator of activated HH signaling (Ahn & Joyner, 2004; Ikram *et al.*, 2004; Lee *et al.*, 1997; Marigo *et al.*, 1996). While deletion of

Gli1 in the mouse is compatible with normal development (Bai *et al.*, 2002), deletion of *Gli2* and *Gli3* generate phenotypes that mimic deletion of *Shh*, indicating that they are essential for mediating its effects on development (Mo *et al.*, 1997). GLI2 and GLI3 proteins may act as transcriptional activators or may undergo proteolytic processing to shortened forms that function as transcriptional repressors (Pan *et al.*, 2006; Wang *et al.*, 2000).

Gene targeting to alter HH signaling in mice has generally resulted in embryonic lethality, indicating that conditional transgenic approaches are necessary to determine function in adult tissues. The current study analyzed the effect of conditional expression of a dominantly active allele of SMO, known as *SmoM2*, in the ovary. SMOM2 contains a point mutation that prevents inhibition of its activity by PTCH, thus leading to constitutive activation of HH signaling (Xie *et al.*, 1998). The phenotype observed in mice expressing dominant active *SmoM2* indicates that HH signaling is required for proper development of a layer of smooth muscle cells around follicles and for the release of oocytes from follicles at the time of ovulation.

Materials and Methods

Mouse strains and treatments

Amhr2$^{cre/+}$ mice, provided by Dr. Richard Behringer (17) and *GT(ROSA)26Sor*$^{tm1(smo/YFP)Amc}$/J mice (16), purchased from The Jackson Laboratory (Bar Harbor ME), were mated to obtain *Amhr2*$^{cre/+}$*SmoM2* mice (mutants) and *Amhr2*$^{+/+}$*SmoM2* mice (controls). Mice were genotyped from tail DNA using

protocols provided by The Jackson Laboratory. CD-1 mice were purchased from Charles River Laboratories, (Wilmington MA). All animals were maintained in accordance with the National Institutes of Health Guide for the Care and Use of Laboratory Animals. Studies were approved by the Cornell University Institutional Animal Care and Use Committee.

Vaginal smears were obtained daily from mice (45–49 days old) for 3 complete estrus cycles or 20 days, whichever came first. Fertility of mutant females was tested by caging with CD-1 males of proven fertility. In some experiments, tissues were collected from immature mice (21-23 days old) 48 h following ip injection of 5 IU eCG, or from mice treated with eCG followed 48 h later by ip injection of 5 IU hCG, or from mice made pseudopregnant by mating with a vasectomized CD-1 male. In some experiments, granulosa cells were collected from preovulatory follicles at various times after eCG/hCG treatment by puncture with a 27-gauge needle. Subsequently, granulosa cells from smaller follicles were expressed by additional puncture and discarded while the remaining tissue, enriched for theca and stroma, was collected (referred to as “residual tissue”). In other experiments, preovulatory follicles were isolated 24 h after eCG and granulosa cells and theca were obtained by dissection using watchmaker’s forceps. To assess ovulation rate, immature eCG/hCG-primed mice were sacrificed 20 h after hCG and oocytes within the ampulla of the oviduct were flushed and counted. At the time of sacrifice, blood was collected by cardiac puncture. Serum was stored at -20 C until assayed for progesterone using a commercial RIA kit (Siemens Medical Solutions, Los Angeles,

CA).

Assessment of Cre-mediated recombination

Single cell suspensions of uteri, oviducts, and whole ovaries from young mutant and control mice were obtained by digestion with 0.08% trypsin plus 10 μg/ml deoxyribonuclease I in DMEM Ham's F-12 (F12) at 37 C for up to 3 h, with periodic triteration using a pasture pipet. Theca was obtained from preovulatory follicles of immature mice 24 h after injection of eCG by dissection and granulosa cells were obtained by needle puncture. Cell suspensions were fixed in 80% ethanol, and within 24 h of storage at 4 C cells were centrifuged, reconstituted in PBS, and analyzed for YFP using a FACScan flow cytometer (BD Biosciences, San Jose CA). Excitation was at 488 nm and emission detected by FL1 at 530±30 nm. Single cells were selected based on a plot of side scatter vs forward scatter. Plots of side scatter vs FL1A were produced, and an area gate was constructed using matching tissues from control animals which do not express YFP such that approximately 95% of the cells were within the area. This gate was applied to plots from mutant animals, and the proportion of cells with higher FL1A fluorescence, which represents those cells expressing YFP, was determined.

Histology and immunohistochemistry

Tissues were fixed in Bouins for histology or 2% paraformaldehyde for immunohistochemistry, embedded in paraffin and 5 μm sections processed for

staining with hematoxylin and eosin or for immunohistochemistry. For SCC, sections were deparaffinized, rehydrated, and treated for antigen retrieval by boiling in 10 mM citrate buffer for 10 min. Endogenous peroxidase activity was quenched with 0.3% hydrogen peroxide in PBS. Non-specific binding was blocked with 2% normal goat serum. Sections were incubated with rabbit anti-rat SCC antibody (AB1244, Chemicon, Temecula CA), or normal rabbit serum, diluted 1:2000 in PBS-1% BSA at 37 C for 1 h, washed with PBS and then incubated with 0.4 µg/ml goat anti-rabbit IgG conjugated to horseradish peroxidase (Jackson Immunoresearch, West Grove PA) in PBS-1% BSA for 1 h at 37 C. Slides were exposed to Nova Red substrate (Vector Laboratories, Burlingame CA) and counter-stained with Gills hematoxylin. For staining for SCC, sections were deparaffinized, rehydrated and blocked with 2% normal goat serum. Sections were incubated with rabbit anti-human smooth muscle actin (ab15267, prediluted, Abcam Inc., Cambridge MA) or with 1 µg/ml rabbit IgG for 20 min at room temperature, followed by incubation with 0.5 µg/ml Alexa 555 goat anti-rabbit IgG for 30 min at room temperature. Cell nuclei were counterstained with 5 µg/ml Hoechst 33342 dye. For dual staining for SMA and VWB, deparaffinized sections were hydrated, treated with pepsin, and blocked with a Mouse-on-Mouse reagent (Vector Laboratories) followed by 10% NGS. Sections were incubated with mouse anti-human α-SMA (M0851, clone IA4, Dako, Carpinteria CA) diluted 1:20 and rabbit anti-VWB (A0082, Dako) diluted 1:50 at room temp for 25 min, followed by Alexa 488-conjugated goat anti-rabbit IgG and Alexa 595 goat anti-mouse IgG for 40 min. Cell nuclei were counterstained with 10

μg/ml DAPI.

Progesterone production by granulosa cells expressing SmoM2

Granulosa cells from eCG-treated homozygous *SmoM2* mice were plated in 96-well plates ($5x10^4$ cells/well) in DMEM-F12 supplemented with 100 U/ml penicillin, 100 μg/ml streptomycin, 0.25 μg/ml fungizone, 1 mM pyruvate, 2 mM glutamine and containing 10% FBS (all Invitrogen). At the time of plating, cells were infected with recombinant adenovirus expressing *Cre* (Adcre, Microbix Biosystems, Toronto, Canada) or a control adenovirus expressing βgalactosidase (Adβgal; provided by Dr. Wafik El-Deiry) at a dose of $1x10^6$ pfu/well (total volume 50 μl). Four h after infection, additional media containing testosterone (final concentration 1 μM) was added. One day after plating, media was collected and 0 or 10 ng/ml ovine LH (NIDDK-oLH-26; from Dr. A.F. Parlow, Harbor-UCLA Medical Center) was added in serum-free media [DMEM-F12 with additives as above plus 100 ng/ml insulin (Sigma-Aldrich), 5 μg/ml transferrin (Invitrogen), 20 nM sodium selenite (Invitrogen), 0.1% BSA, and 1μM testosterone]. Media was collected on the second and third day after plating and stored at -20 C until assayed for progesterone. In order to determine the efficiency of Adcre-mediated recombination, Adcre- or Adβgal-infected cells were harvested on day 3, and used for flow cytometry to detect YFP.

Microarray analysis

RNA from whole ovaries of untreated, 48 h eCG-treated and 4 h hCG-treated control and mutant mice was prepared using a RNeasy Mini Kit (Qiagen, Valencia CA). RNA was tested prior to pooling equal amounts of RNA from 3 mice of each genotype for microarray analysis; expression of *Lhcgr* mRNA was confirmed to increase after eCG and *Ptgs2* was shown to increase after hCG as expected. Microarray analyses were performed by the Microarray Core Facility of the Cornell University Life Sciences Core Laboratories Center. Labeled cRNA samples were hybridized on mouse genome 430 2.0 GeneChips and scanned by a GeneChip Scanner 3000 according to standard protocol provided by the manufacturer (Affymetrix , Santa Clara, CA). The raw array data was processed by Affymetrix GCOS software to obtain signal values, which were scaled to the default target of 500 and summarized in a pivot table. The signals were log2-transformed after being offset by 64, and log ratios were calculated as the difference between mutant and control samples at each of the 3 time points. Gene filtering was applied to include only 30588 probe sets having at least 1 Present call. Gene ontogeny analysis of log2 differences between transcript levels in mutants and controls was performed using ErmineJ software (Lee *et al.*, 2005).

Analysis of gene expression

RNA was prepared from granulosa cells, theca, residual ovarian tissue, and whole ovaries using a RNeasy Mini Kit. Reverse transcription was performed using a High Capacity cDNA Reverse Transcription Kit (Applied Biosystems, Foster City

CA). Real time RT-PCR was performed on an ABI Prism 7000 using the mouse-specific assays shown in Table 2.1. A standard curve, used in each assay, was constructed from cDNA prepared from RNA of pooled granulosa cells or, for smooth muscle and extracellular matrix genes, from RNA of pooled whole ovaries. Results were standardized by dividing by 18s rRNA concentration and multiplying by 100. Samples from each tissue type were analyzed on the same plate. For each gene, a between plate coefficient of variation was determined by including two common samples on each plate. The between plate coefficients of variation ranged from 1% to 16%; the mean was 10.6±1.4%.

In vitro cumulus expansion assays

Immature *Amhr2*$^{cre/+}$*SmoM2* mutant and *Amhr2*$^{+/+}$*SmoM2* control mice were primed with eCG and COC were isolated at 48 h by needle puncture of large antral follicles. COC were distributed to 24-well plates (approximately 20/well) containing DMEMα (Invitrogen) plus antibiotics and 5% FBS and treated with 0 or 100 ng/ml ovine FSH (NIDDK oFSH-20, from Dr. A.F. Parlow). After 18 h of treatment, COC were scored for the degree of expansion as described previously (Downs, 1989) using a scale of 0 indicating no expansion to a score of 4 indicating full expansion.

In order to test the effect of acute induction of *SmoM2* expression on cumulus expansion, COC were collected from homozygous *SmoM2* mice and infected with $1x10^7$ pfu/ml of Adcre or Adβgal. Cultures were rocked gently for 12 h to prevent

Table 2.1. Quantitative real-time RT-PCR assays

Gene Symbol	Gene name	Assay ID[a]	Exons[b]
Smo	smoothened homolog	Mm01162710_m1	8-9
Ihh	Indian hedgehog	Mm00439613_m1	2-3
Ptch1	patched homolog 1	Mm00436026_m1	17-18
Gli1	GLI-Kruppel family member GLI1	Mm00494645_m1	2-3
Gli3	GLI-Kruppel family member GLI3	Mm00492333_m1	1-2
Hhip	hedgehog-interacting protein	Mm00469580_m1	12-13
Spp	secreted phosphoprotein 1	Mm00436767_m1	2-3
Ptgs2	prostaglandin-endoperoxidase synthase 2	Mm00478374_m1	5-6
Pgr	progesterone receptor	Mm00435625_m1	4-5
Star	steroidogenic acute regulatory protein	Mm00441558_m1	6-7
Lhcgr	luteinizing hormone/ choriogonadotropin receptor	Mm00442931_m1	6-7
Actg2	actin, gamma 2, smooth muscle, enteric	Mm00656102_m1	7-8
Cnn1	calponin 1	Mm00487032_m1	1-2
Des	desmin	Mm00802455_m1	1-2
Tagln	transgelin	Mm00441660_m1	1-2
Tnc	tenascin C	Mm00495662_m1	5-6
Edn2	endothelin 2	Mm00432983_m1	3-4
18s rRNA		4319413E	

[a] Taqman® Gene Expression Assays (Applied Biosystems)
[b] Exons in which forward and reverse primers anneal.

attachment of COC to the plate during infection. Cultures were then treated with 0 or 100 ng/ml FSH and scored for cumulus expansion 18 h later. COC were examined by fluorescence microscopy for expression of YFP.

Cell cycle analysis

Granulosa cells isolated at different times after eCG/hCG treatment of immature mice were analyzed for DNA content by flow cytometry as described previously (Quirk *et al.*, 2006).

Statistical analysis

Serum progesterone concentrations, tissue mRNA concentrations, and cell cycle data were analyzed by randomized (simple) two-way ANOVA. Serum progesterone and tissue mRNA concentrations were log transformed to normalize standard error. Progesterone production by cultured granulosa cells and in vitro cumulus expansion experiments were analyzed by randomized complete block ANOVA, with experimental replicates as blocks; progesterone data were log-transformed. Student-Newman-Keuls test was used to compare individual means if overall significance was indicated (Ott, 2001). All other data were analyzed by unpaired t-test.

Results

Generation of mice with conditional expression of dominant active Smo

Mice in which a dominant active allele of *Smo*, known as *SmoM2*, is conditionally expressed in the ovary were created using a *cre/loxP* strategy. A previously engineered transgenic mouse line was used in which expression of an inserted *SmoM2*-yellow fluorescent protein (*Yfp*) fusion gene is blocked by a *loxP*-flanked stop signal (*SmoM2* mice; (Jeong *et al.*, 2004)). Homozygous *SmoM2* mice were crossed to $Amhr2^{cre/+}$ mice in which *Cre* recombinase sequence was inserted into the *Amhr2* gene (Jamin *et al.*, 2002). The $Amhr2^{cre/+}$ allele was originally shown to direct expression of *Cre* to the gonads and mesenchyme of the Müllerian duct beginning at embryonic day 12.5 (Jamin *et al.*, 2002). Subsequent studies demonstrated $Amhr2^{cre/+}$-mediated recombination in the adult ovary in granulosa cells as well as theca cells (Jorgez *et al.*, 2004) and in the developing and adult reproductive tract (Arango *et al.*, 2005; Deutcher & Yao, 2007). In the current study, sites of *Cre*-mediated recombination in $Amhr2^{cre/+}SmoM2$ mice were determined by examining expression of the *Yfp* fusion gene. Cell suspensions for use in flow cytometry to detect YFP were prepared from whole ovary, oviduct and uterus of newborn mice and from theca and granulosa cells of preovulatory follicles from equine chorionic gonadotropin (eCG)/human chorionic gonadotropin (hCG)-treated immature mice. Cells from genotype-matched control mice lacking *Cre* sequence ($Amhr2^{+/+}SmoM2$) and from liver were analyzed as negative controls. In cells from $Amhr2^{cre/+}SmoM2$ mice, approximately half of the cells expressed detectable levels of YFP while cells from control mice and liver cells from mice of both genotypes showed background fluorescence (Fig. 2.1).

Fertility, ovulation and luteinization

In order to test fertility, *Amhr2*$^{cre/+}$*SmoM2* mutant mice and *Amhr2*$^{+/+}$*SmoM2* control mice were caged continuously with CD-1 males of proven fertility. Vaginal plugs were observed in both mutant and control mice. Control mice had one or two litters within a 2 month period, averaging 9.6±1.0 pups/litter, while mutant mice produced no litters (n=5). In mutant females, mating caused a severe inflammatory response in the reproductive tract (described below). For this reason, subsequent studies on ovarian function were performed using virgin mice in order to eliminate the confounding effect of uterine pathology associated with breeding. Daily vaginal smears showed that estrous cycle length was longer in mutant mice (6.8±0.3 days) than control mice (5.0±0.4 days, $P<0.05$). The percent of days spent in diestrus was greater in mutants than controls (60±3% vs 31±9%) and the percent of days in proestrus was less (12±2% vs 27±4%) (Fig. 2.2).

Response to superovulation was tested by collection of oocytes from the ampulla of eCG-primed prepubertal (21-23 days old) and adult mice (50-60 days old) 20 h after treatment with hCG. Oocytes were readily recovered from immature and adult *Amhr2*$^{+/+}$*SmoM2* control mice (42.7±5.8 and 24.0±1.0 oocytes/mouse, respectively), while only occasional oocytes were recovered from immature and adult *Amhr2*$^{cre/+}$*SmoM2* mutant mice (0.3±0.3 and 0.3±0.3 oocytes/mouse, respectively).

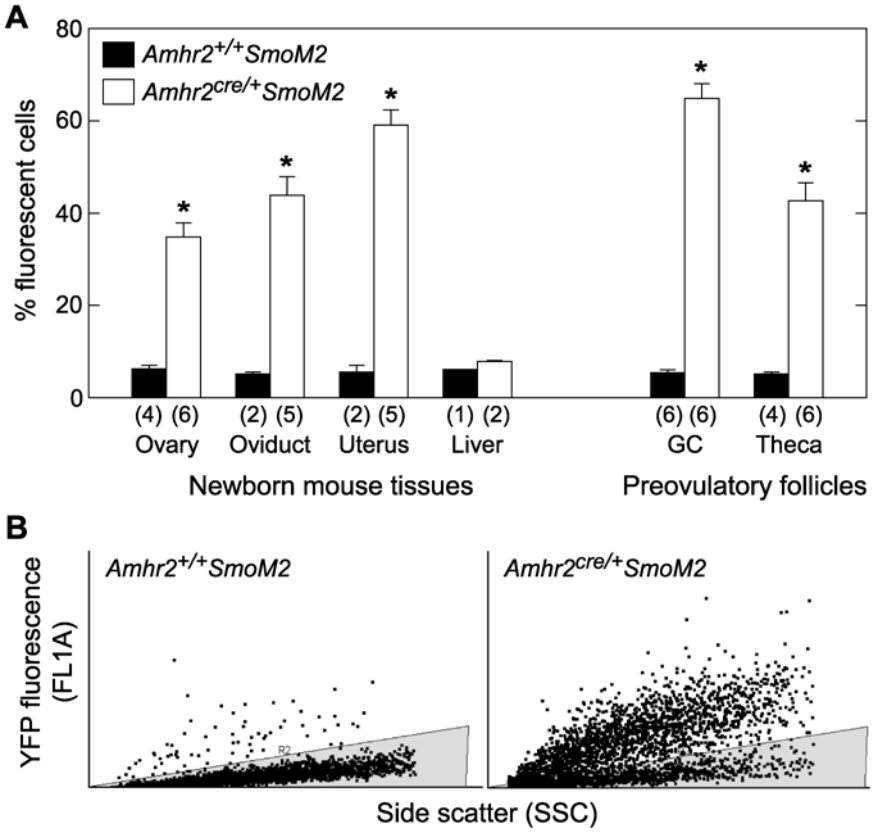
A
80
60
40
20
0
% fluorescent cells
Amhr2+/+SmoM2
Amhr2cre/+SmoM2
*
(4) (6)
Ovary
(2) (5)
Oviduct
(2) (5)
Uterus
(1) (2)
Liver
(6) (6)
GC
(4) (6)
Theca
Newborn mouse tissues
Preovulatory follicles
B
YFP fluorescence (FL1A)
Amhr2+/+SmoM2
Amhr2cre/+SmoM2
R2
Side scatter (SSC)

Figure 1

Fig. 2.1. Assessment of the efficiency of CRE-mediated recombination in *Amhr2*$^{cre/+}$*SmoM2* mice. Dispersed cells from tissues of mutant and control mice were analyzed by flow cytometry to measure fluorescence associated with expression of the *SmoM2/Yfp* reporter gene. **A**) Percent of cells from reproductive tissues expressing YFP. Signal obtained from tissues of control mice and from liver of mice of both genotypes represent background fluorescence. Data are mean ± SEM of (n) replicates. *, $P < 0.05$ vs cells of the same type from *Amhr2*$^{+/+}$*SmoM2* mice. **B**) Representative plots of FL1 fluorescence vs side scatter in granulosa cells. The shaded area is the area representing background fluorescence; cells with fluorescence associated with YFP expression are above the shaded area.

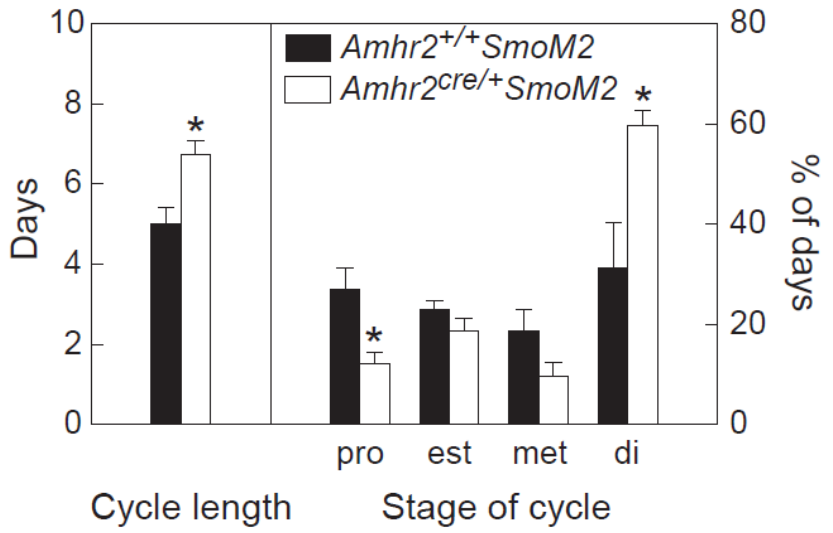

Fig. 2.2. ***Amhr2$^{cre/+}$SmoM2*** **mice have prolonged estrous cycles, characterized by extended periods of diestrus.** Vaginal smears were evaluated for the stage of the estrous cycle in four *Amhr2$^{+/+}$SmoM2* mice and four *Amhr2$^{cre/+}$SmoM2* mice for 3 complete cycles or 20 days. The left panel shows cycle length, and the right panel shows the percent of days mice exhibited smears characteristic of each stage of the cycle. Data are mean ± SEM. *, $P < 0.05$ vs *Amhr2$^{+/+}$SmoM2* mice.

Histological analysis of ovaries isolated 48 h after eCG suggested that preovulatory follicles develop similarly in mutant and control mice (Fig. 2.3A, panels a,b). By 8 h after hCG, cumulus expansion had occurred in control mice but appeared disorganized in mutant mice (Fig. 2.3A, panels c,d). Oocytes within follicles of mutant and control mice resumed meiosis as evidenced by the presence of metaphase chromosomes (Fig. 2.3A, panels c,d). At 20 h after hCG, ovaries of control mice contained newly formed CL, while ovaries of mutant mice lacked new CL and had preovulatory-type follicles containing trapped oocytes (Fig. 2.3A, panels e,f). No sign that follicle rupture had occurred was observed in histological sections from mutant mice. At 44 h after hCG, luteinization had further progressed in control mice, while in mutant mice follicles appeared to be luteinizing but contained blood-filled cavities with trapped oocytes (Fig. 2.3A, panels g,h). CL containing trapped oocytes were observed in adult mutant mice but not in controls (data not shown). These results indicate that ovulation in *Amhr2*$^{cre/+}$*SmoM2* mice is severely reduced and that the process of luteinization may be delayed or prolonged. In order to assess the differentiation of granulosa cells into luteal cells after the LH surge, sections of ovaries were stained for the enzyme cytochrome P_{450}, family 11, subfamily a, polypeptide 1 (CYP11a1), also known as side chain cleavage (SCC), which is essential for progesterone production. At 20 h after hCG, only occasional CL of control and mutant mice stained positively for SCC (Fig. 2.3B, panels i,j). At 44 h, SCC was expressed in CL of control mice and also in CL of mutant mice which sometimes contained blood-filled cavities (Fig. 2.3B, panels k,l).

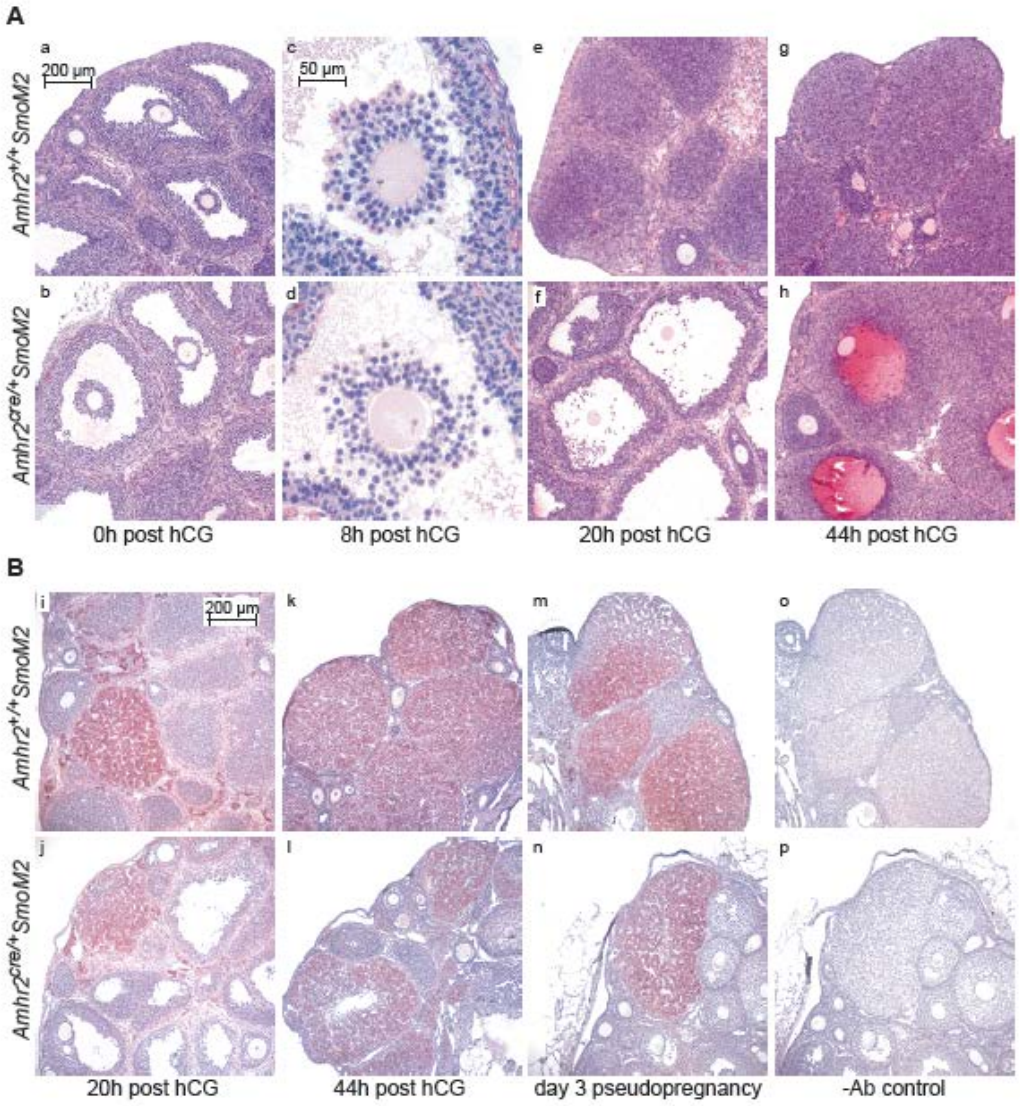
A
a
200 µm
c
50 µm
e
g
Amhr2+/+SmoM2
b
d
f
h
Amhr2cre/+SmoM2
0h post hCG
8h post hCG
20h post hCG
44h post hCG
B
i
200 µm
k
m
o
Amhr2+/+SmoM2
j
l
n
p
Amhr2cre/+SmoM2
20h post hCG
44h post hCG
day 3 pseudopregnancy
-Ab control

Fig. 2.3. Response to superovulation in immature *Amhr2*$^{+/+}$*SmoM2* and *Amhr2*$^{cre/+}$*SmoM2* mice. **A**) Ovaries from *Amhr2*$^{+/+}$*SmoM2* and *Amhr2*$^{cre/+}$*SmoM2* mice stained with hematoxylin and eosin (a-h). Immature (21-23 days old) mice were injected with eCG followed 48 h later by hCG (0 h). Preovulatory follicle formation appears similar in mutant and control mice at 0 h after hCG (a,b), but at 8h expansion of the cumulus in mutant mice appears disorganized compared to control mice (c,d). At 20 h, ovaries of control mice contain newly formed CL while ovaries of mutant mice contain unruptured preovulatory-like follicles with trapped oocytes (e,f). At 44h, CL development had further progressed in control mice while luteinizing follicles of mutant mice have blood-filled cavities with entrapped oocytes (g,h). **B**) Immunohistochemical detection of SCC (reddish brown) in ovaries from mutant and control mice counterstained with hematoxylin (blue). At 20 h after hCG (i,j), occasional CL stained positively for SCC, but most did not. At 44 h (k,l) and in mice on day 3 of pseudopregnancy (m,n), CL of both mutant and control mice showed distinct staining of SCC. Non-specific staining, in which non-immune IgG was added in place of the SCC antibody, is shown (o,p).

On day 3 of pseudopregnancy, CL of mutant and control mice appeared grossly similar; both stained positively for SCC and lacked a central cavity (Fig. 2.3B, panels m,n). Serum concentrations of progesterone following treatment with eCG/hCG and on day 3 of pseudopregnancy were similar in mutant and control mice (Fig. 2.4A).

In *Amhr2*$^{cre/+}$*SmoM2* mice, follicle cells may express *SmoM2* for a prolonged period of time since recombination through *Amhr2*$^{cre/+}$ begins during embryonic development. Therefore, effects of acutely inducing expression of *SmoM2* in granulosa cells in vitro were determined. Granulosa cells were isolated from preovulatory follicles of eCG-primed homozygous *SmoM2* mice and infected in vitro with a recombinant adenovirus expressing *Cre* (Adcre) or with a control adenovirus expressing β-galactosidase (Adβgal) as a control. The concentration of progesterone in culture medium increased over 3 days and was not altered by infection with adenoviruses (Fig. 2.4B). Treatment of parallel cultures with LH after the first day of culture increased the magnitude of progesterone secretion but infection with adenoviruses had no effect (Fig. 2.4C). Activated expression of the *SmoM2-Yfp* fusion gene by Adcre was confirmed by flow cytometry of granulosa cells analyzed 16 h after infection. While the majority of cells infected with Adcre were positive for YFP (71±2%), only background fluorescence was observed in cells infected with Adβgal (5±1%). As indicated above, within a month after caging with males, *Amhr2*$^{cre/+}$*SmoM2* female mice showed signs of distress and bleeding from the vagina. Histological analysis of the reproductive tract showed changes consistent with an

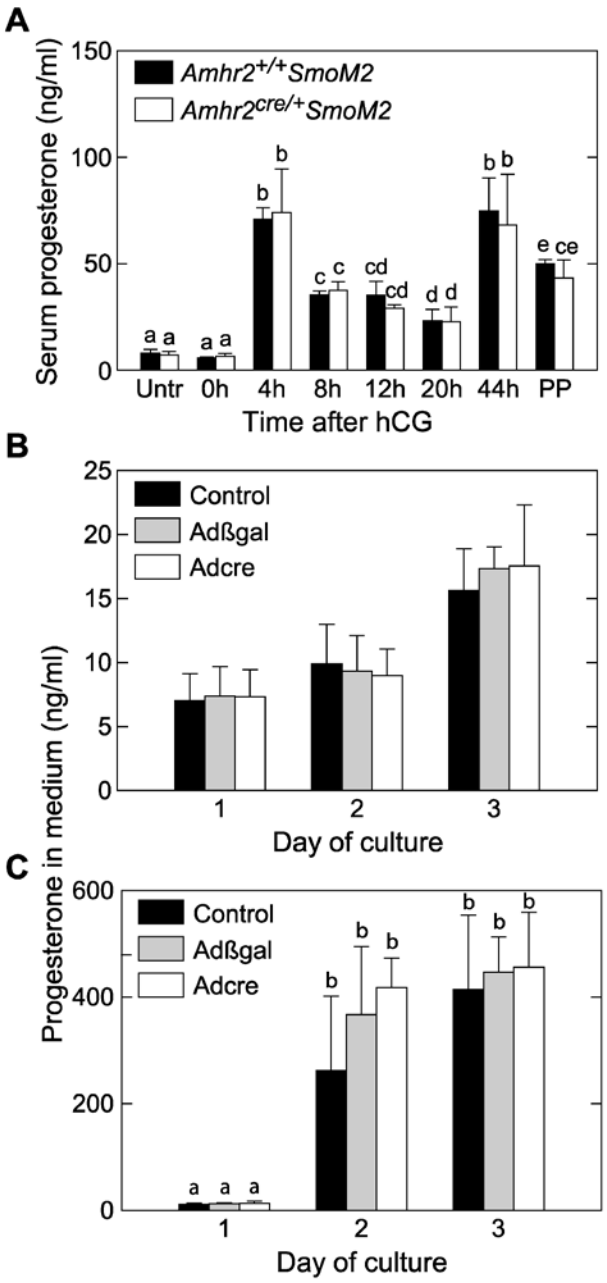
A
Serum progesterone (ng/ml)
150
100
50
0
Amhr2+/+SmoM2
Amhr2cre/+SmoM2
a a
a a
b
b
c c
cd
cd
d d
b b
e ce
Untr
0h
4h
8h
12h
20h
44h
PP
Time after hCG
B
Progesterone in medium (ng/ml)
25
20
15
10
5
0
Control
Adßgal
Adcre
1
2
3
Day of culture
C
Progesterone in medium (ng/ml)
600
400
200
0
Control
Adßgal
Adcre
a a a
b
b
b
b
b
b
1
2
3
Day of culture

Fig. 2.4. Effects of dominant active *SmoM2* on progesterone production.

A) Serum progesterone concentrations do not differ in *Amhr2*$^{cre/+}$*SmoM2* and control mice. Immature (21-23 days old) mice were injected with eCG followed 48 h later by hCG (0 h). n = 4 mice/timepoint. Untr, no hormone treatments; PP, day 3 of pseudopregnancy. **B)** Activation of *SmoM2* expression in cultured granulosa cells does not alter progesterone production. Granulosa cells from *SmoM2* mice were infected with Adcre at the time of plating to induce expression of the *SmoM2/Yfp* fusion gene or with no adenovirus or Adβgal as controls. ANOVA indicated no overall difference. **C**) Granulosa cells from *SmoM2* mice were treated as described for panel B, except that 10 ng/ml oLH was added after 1 and 2 days of culture. For data shown in panels B and C, n = 3 separate granulosa cell preparations tested, each receiving all treatments. Data are mean ± SEM. Bars without common superscripts are significantly different ($P < 0.05$).

extensive inflammatory response within the uterine lumen (Migone, *et al...*, 2011). Aspects of reproductive tract development are altered in mutant mice, a finding consistent with *Cre*-mediated recombination occurring in the developing Müllerian duct, and will be reported in detail elsewhere.

Microarray analysis

Microarray analysis was performed to obtain insight into the cause of ovulatory failure in *Amhr2*$^{cre/+}$*SmoM2 mice*. Single arrays were run using whole ovarian RNA prepared from three groups of immature mutant and control mice; untreated, 48 h after eCG and 4h after hCG in eCG-primed mice. The data were sorted to identify transcripts in which expression differed between mutants and controls for all treatment groups. Six out of the fifteen transcripts that were most prominently down regulated in mutants represent proteins that play a role in muscle function (Table 1, genes shown in bold). Two down regulated transcripts are for extracellular matrix proteins, periostin and tenascin C (TNC). The *Amhr2* transcript is reduced in mutant mice, consistent with the presence of a single functional *Amhr2* allele. Gene ontogeny analysis of microarray data using the ErmineJ program indicated that the three biological processes most significantly different between mutant and control mice were muscle system processes, smooth muscle contraction and muscle development ($p< 1 \times 10^{-12}$). Subsequent quantitative RT-PCR analyses of five selected genes confirmed differences between mutants and controls (Table 2.1).

Table 2.2 Results of microarray analysis of ovarian RNA from *Amhr2*$^{tm1/+}$*smoM2* (mutant) and *Amhr2*$^{+/+}$*smoM2* (control) mice, and confirmation by quantitative RT-PCR.

		Fold difference in array (mutant vs control)				quantitative RT-PCR (arbitrary units)					
						untreated		0h post hCG		4h post hCG	
Gene Symbol	Gene Title	0h	48h	4h	mean	Con	Mut	Con	Mut	Con	Mut
Cnn1	calponin 1	-2.52	-4.55	-3.11	-3.30	74±4^{a}	24±1^{b}	113±15^{c}	21±4^{b}	129±15^{c}	43±8^{d}
Des	desmin	-1.68	-2.66	-5.91	-2.98	69±5^{a}	35±4^{b}	127±3^{c}	34±3^{b}	141±35^{c}	39±8^{b}
Actg2	actin, gamma 2, smooth muscle, enteric	-2.41	-4.20	-2.44	-2.91	62±10^{a}	26±4^{b}	115±8^{c}	30±8^{b}	122±29^{c}	44±5^{ab}
Postn	periostin, osteoblast specific factor	-3.30	-2.43	-1.61	-2.35						
Akr1c13	aldo-keto reductase family 1, member C13	-1.72	-3.82	-1.49	-2.14						
Myh11	myosin, heavy polypeptide 11, smooth muscle	-1.83	-1.99	-2.68	-2.14						
Tnc	tenascin C	-1.91	-1.88	-2.53	-2.09	154±11^{a}	69±5^{b}	70±7^{b}	29±2^{c}	324±44^{d}	115±11^{e}
BC005512	cDNA sequence BC005512	-2.03	-1.91	-2.04	-1.99						
Amhr2	anti-Mullerian hormone type 2 receptor	-1.79	-1.75	-2.43	-1.97						
Tagln	transgelin	-2.06	-2.27	-1.60	-1.95	87±2^{ab}	45±4^{c}	109±17^{a}	33±3^{d}	148±10^{e}	69±11^{b}
Tpm2	tropomyosin 2, beta	-1.91	-2.20	-1.69	-1.92						
Bdnf	brain derived neurotrophic factor	-1.42	-1.79	-2.74	-1.91						
Akr1c12/13	aldo-keto reductase family 1, member C12/C13	-1.56	-3.92	-1.12	-1.90						
Slc2a4	solute carrier family 2 (facilitated glucose transporter), member 4	-2.50	-1.36	-1.94	-1.88						
--	Gene model 879, (NCBI)	-2.15	-1.83	-1.62	-1.82						

Data are presented for 15 genes that were expressed at the lowest levels in mutants compared to controls, based on the geometric mean fold difference. Each fold difference represents single arrays of RNA pooled from ovaries of 3 control or mutant mice. RT-PCR data are mean ± SEM of RNA from each of the 3 control or mutant mice used in the array samples. For RT-PCR data, values without common superscripts are significantly different ($p < 0.05$).

In order to determine the predominant cell type in which changes in muscle gene expression occurred, granulosa cells and residual ovarian tissue were isolated and assayed for smooth muscle marker genes, *Cnn1*, *Des*, *Actg2* and *Tagln*. Expression of muscle genes was low in granulosa cells, did not differ in mutant and control mice, and did change over time after eCG/hCG treatment. Levels of expression of smooth muscle genes were much higher in residual tissue than in granulosa cells and were substantially reduced in mutant mice compared to controls (Fig. 2.5). Minor fluctuations in levels of muscle gene expression were observed after eCG/hCG treatments. *Tnc* expression increased after hCG in both granulosa cells and residual tissue; levels in residual tissue, but not in granulosa cells, were reduced in mutants compared to controls (Fig. 2.5). Expression of endothelin 2 (*Edn2)*, an agonist capable of inducing contraction of follicular muscle cells (Ko *et al.*, 2006; Palanisamy *et al.*, 2006), increased dramatically between 8 and 12 h after hCG in both mutant and control mice and was expressed primarily Table 2.2 in granulosa cells (Fig. 2.5).

Immunohistochemistry of smooth muscle

In order to determine the location of cells with the characteristics of smooth muscle cells, ovarian sections from immature mice were stained for smooth muscle actin α (SMA), which is considered to be a marker for smooth muscle cells, and 4,6-diamidino-2-phenylindole (DAPI), which marks nuclei. In control mice that were untreated or assessed at 48 h after eCG, a SMA-positive layer of cells were

present in the outer theca, consistent with previous studies (Amsterdam *et al.*, 1977; Ko *et al.*, 2006) (Fig. 2.6A and 6B). Co-staining for von Willebrand's factor (VWB), which marks endothelial cells, showed that prominent staining for SMA did not coincide with endothelial cells within the theca layer (Fig. 2.7). Large blood vessels in the stroma stained positively for SMA in the outer layer and positively for VWB in the inner endothelial cell layer (Fig. 2.7). In untreated and eCG-treated mutant mice, SMA staining was absent or dramatically reduced in the theca of the majority of follicles while staining in large blood vessels and low-intensity staining in the vicinity of theca endothelial cells appeared similar to controls (Fig. 2.6A and 6B and Fig. 2.7). In ovaries from eCG-primed immature mutant and control mice that were isolated 12 h after hCG, the pattern of SMA staining was similar to that observed in untreated mice and eCG-treated mice (data not shown). When SMA staining was examined in younger mice, it was found to be undetectable in ovaries of 8 day old control and mutant mice in which primordial and primary follicles predominated (Fig. 2.6C).

On days 12 and 16 of age, SMA was detectable in ovaries of control mice in the outer theca layer of follicles with greater than two layers of granulosa cells (tertiary follicles) and was substantially reduced to non-detectable in follicles of mutant mice (Fig. 2.6C). *Expression of components of the HH signaling pathway*

Expression of components of the HH pathway was detectable in both granulosa cells and residual ovarian tissue, and levels of expression changed in response to treatments with eCG/hCG (Fig. 2.8).

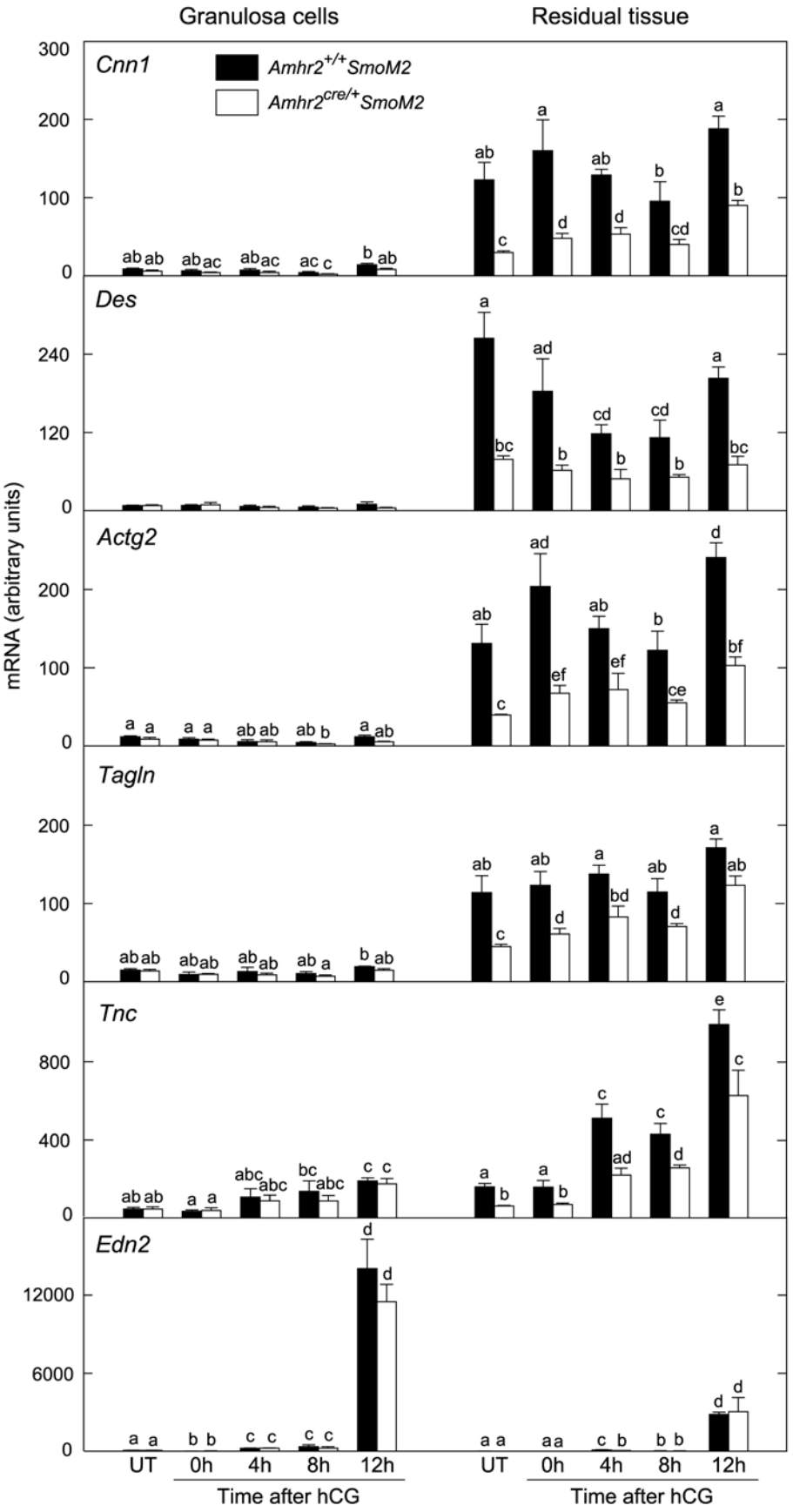
Granulosa cells
Residual tissue
Cnn1
Amhr2+/+SmoM2
Amhr2cre/+SmoM2
Des
Actg2
Tagln
Tnc
Edn2
mRNA (arbitrary units)
UT
0h
4h
8h
12h
Time after hCG
Time after hCG

Fig. 2.5. Expression of genes associated with smooth muscle (*Cnn1*, *Des*, *Actg2*, *Tagln*) or extracellular matrix (*Tnc*) and expression of *Edn2* in granulosa cells and residual ovarian tissue from *Amhr2*$^{+/+}$*SmoM2* and *Amhr2*$^{cre/+}$*SmoM2* mice. Tissues were obtained from untreated mice (UT) or from eCG-primed mice before (0 h) or after injection of hCG. Total RNA was assayed by quantitative real-time RT-PCR. Data are mean ± SEM. n = 3 granulosa cell and residual tissue preparations. Bars without common superscripts are significantly different ($P < 0.05$).

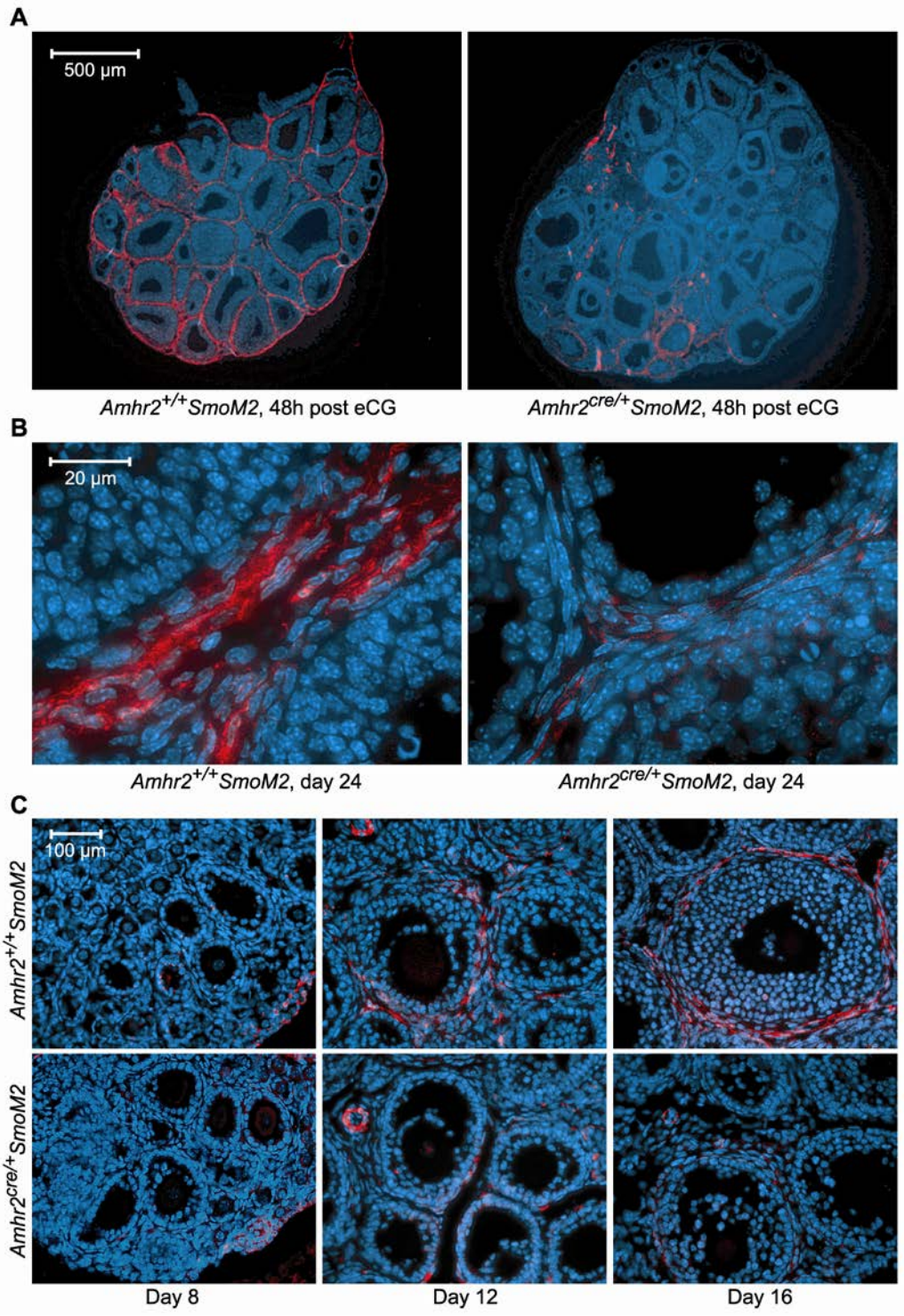
A
500 µm
Amhr2+/+SmoM2, 48h post eCG
Amhr2cre/+SmoM2, 48h post eCG
B
20 µm
Amhr2+/+SmoM2, day 24
Amhr2cre/+SmoM2, day 24
C
100 µm
Amhr2+/+SmoM2
Amhr2cre/+SmoM2
Day 8
Day 12
Day 16

Fig. 2.6. Staining for the smooth muscle marker, SMA, in ovaries of *Amhr2*$^{+/+}$*SmoM2* and *Amhr2*$^{cre/+}$*SmoM2* mice at different ages and in immature mice 48 h after injection of eCG. Sections were counterstained for nuclei with Hoechst 33342 (blue). Results were confirmed in at least 3 mice of each genotype and age.

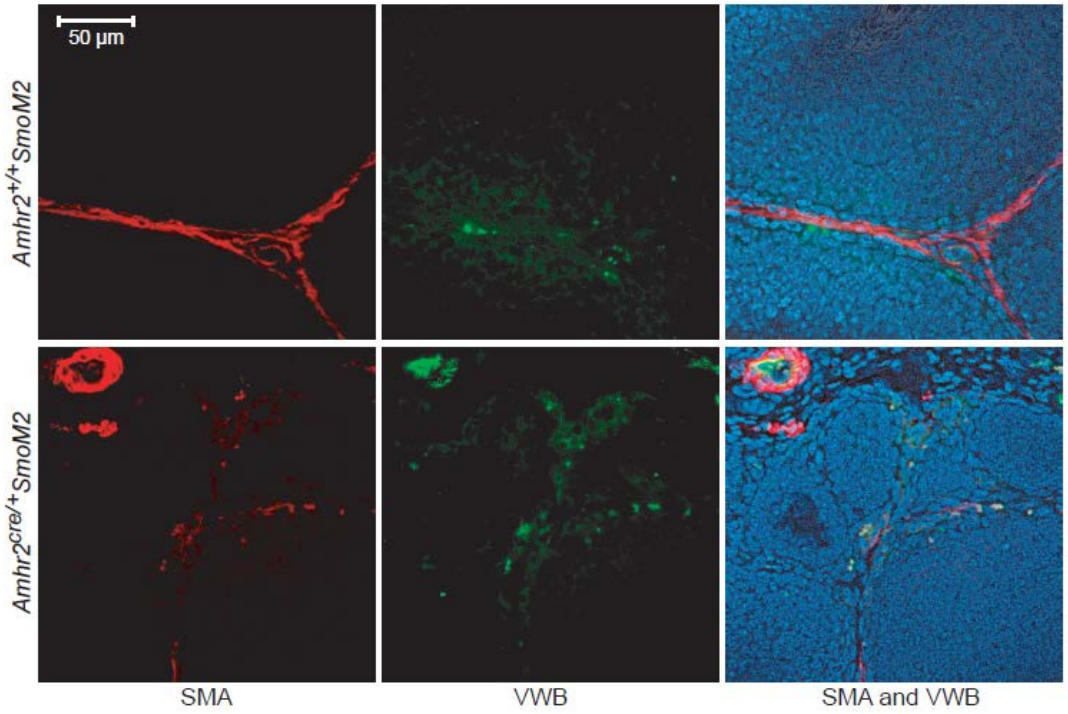

Fig. 2.7. Staining for the smooth muscle marker, SMA, and the endothelial cell marker, VWB, in ovaries of *Amhr2*$^{+/+}$*SmoM2* (top panels) and *Amhr2*$^{cre/+}$*SmoM2* mice (bottom panels). Sections were co-stained for SMA (red) and VWB (green) and for nuclei (DAPI; blue) and individual and merged images are shown. Sections are from ovaries isolated 48 h after injection of eCG to immature mice.

Smo was consistently elevated in granulosa cells of mutant mice relative to controls. *Smo* levels were lower in residual tissue than in granulosa cells and were slightly elevated in mutants relative to controls at several time points. *Ihh* was expressed at substantially higher levels in granulosa cells than in residual tissue; expression in granulosa cells declined between 0 and 4 h after hCG and remained at basal levels thereafter. Levels of *Ptch1*, *Gli3* and *Hhip* were within the same general range in granulosa cells and residual tissue and in mutant and control mice. However, the pattern of changes in gene expression in response to eCG/hCG differed in the two fractions of cells. Levels of *Gli1* were substantially higher in residual tissue compared to granulosa cells and did not differ between mutants and controls. *Gli1* in residual tissue decreased in response to eCG/hCG.

In order to more precisely examine localization of gene expression, theca and granulosa cells were isolated from preovulatory follicles of immature mice 24 h after injection of eCG. *Smo* mRNA was elevated in granulosa cells and theca of mutant mice compared to controls (Fig. 2.9). This result is consistent with *Amhr2cre*-mediated expression of the *SmoM2-Yfp* fusion gene in both granulosa and theca, as shown in Fig. 2.1. Levels of mRNA for genes typically expressed in muscle cells, *Cnn1* and *Actg2*, were expressed predominantly in theca and were reduced in mutants compared to controls (Fig. 2.9).

Expression of genes associated with differentiation of granulosa cells

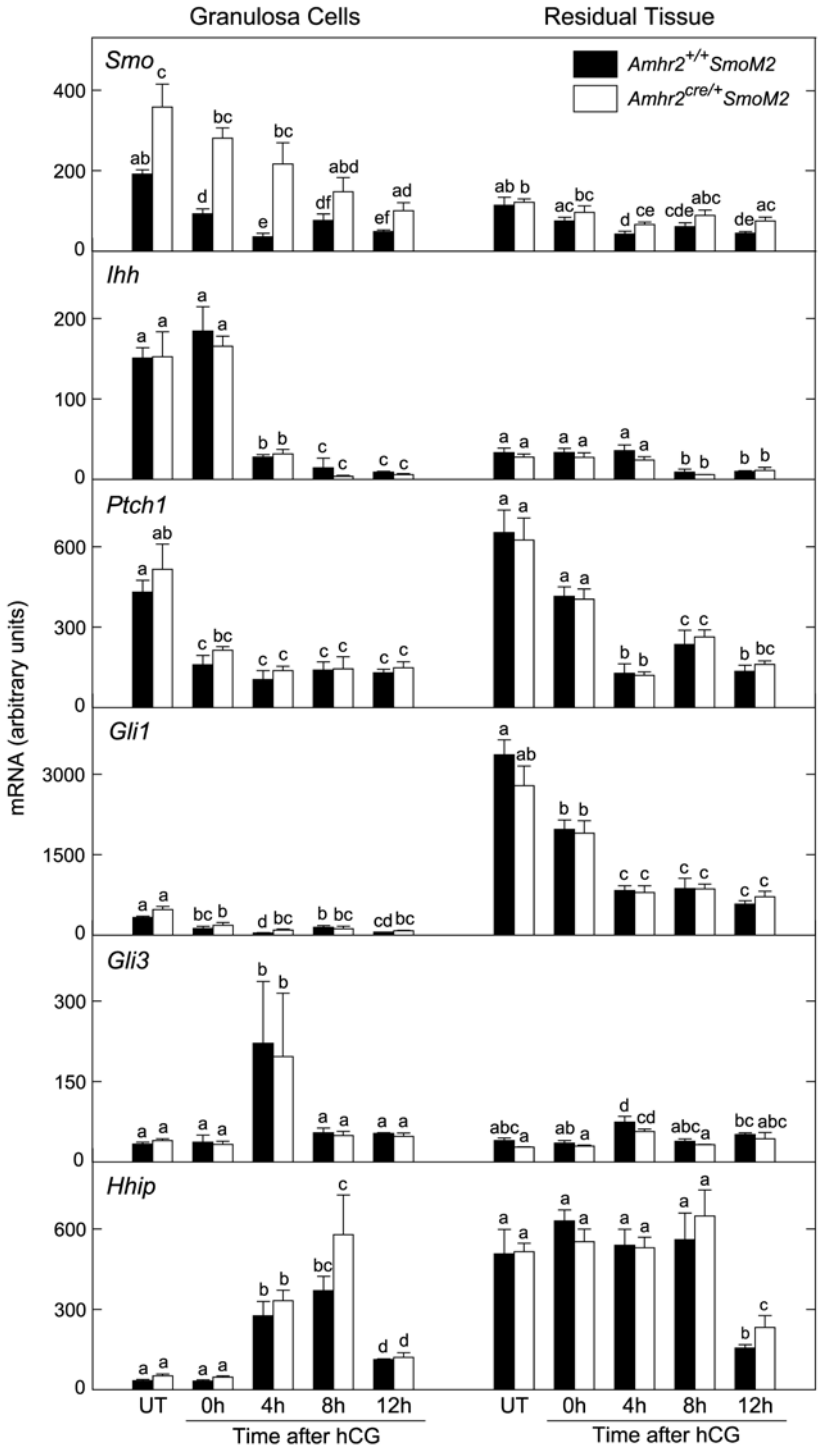
Granulosa Cells
Residual Tissue
Amhr2+/+SmoM2
Amhr2cre/+SmoM2
Smo
Ihh
Ptch1
Gli1
Gli3
Hhip
mRNA (arbitrary units)
UT
0h
4h
8h
12h
Time after hCG

Fig. 2.8. Expression of genes in the HH signaling pathway in granulosa cells and residual ovarian tissue from *Amhr2*$^{+/+}$*SmoM2* and *Amhr2*$^{cre/+}$*SmoM2* mice. Tissues were obtained from untreated mice (UT) or from eCG-primed mice before (0 h) or after injection of hCG. Total RNA was assayed by quantitative real-time RT-PCR. Data are mean ± SEM. n = 3 granulosa cell and residual tissue preparations. Bars without common superscripts are significantly different ($P < 0.05$).

Changes in the pattern of expression of genes known to be involved in ovulation and differentiation were similar in granulosa cells of mutants and controls after injection of hCG including: *Lhcgr*, required for effects of LH on follicle differentiation and ovulation; *Star*, a rate-limiting enzyme required for progesterone production; *Pgr*, known to be required in granulosa cells for ovulation; *Ptgs2* (also known as *Cox-2*), required for cumulus expansion and ovulation; and *Spp1* (also known as osteopontin), a gene known to increase after the LH surge (McRae *et al.*, 2005) and reported to be a target of HH signaling (Yoon *et al.*, 2002) but with unknown function in the follicle (Fig. 2. 10).

Cumulus Expansion

Based on the disorganized appearance of cumulus expansion in histological sections of mutant ovaries, a potential impairment of cumulus expansion was tested in isolated cumulus-oocyte complexes (COC) in vitro. Treatment with FSH induced expansion of COC from control mice as expected, while the magnitude of expansion was reduced in complexes from mutant mice (Fig. 2. 11A). Fluorescent images of representative COC from mutant mice showed bright YFP signal for cells in the plane of focus (Fig. 2.11C). To determine the effect of acute induction of *SmoM2* expression on cumulus expansion in vitro, COC were isolated from preovulatory follicles of eCG-primed mice homozygous for the *SmoM2* allele and cultured with Adcre or Adβgal as control. Analysis of YFP reporter expression in COC by fluorescence microscopy confirmed that *Cre*-mediated activation of *SmoM2*

expression occurred in most cells. Treatment with FSH increased the expansion index in complexes infected with Adβgal while the response to FSH was prevented in complexes infected with Adcre (Fig. 2.11B). Taken together, the results show that *Cre*-mediated activation of *SmoM2* expression in vivo (in *Amhr2*$^{cre/+}$*SmoM2* mice) and in vitro (in Adcre-infected COC from *SmoM2* mice) results in a suboptimal cumulus expansion reaction.

Progression of granulosa cells through the cell cycle

Granulosa cells are reported to exit the cell cycle following exposure to the LH surge, and this is associated with their differentiation into luteal cells (Robker & Richards, 1998). Cell cycle distribution was similar in mutant and control mice with cells present in each stage of the cycle (G0/G1, S and G2/M) at each of the time points examined after treatment with eCG/hCG (Fig. 2.12). Between 8 and 12 h after hCG, the percent cells in S phase decreased and the percent cells in G2/M tended to increase in mutants and controls. Thus, exit from the cell cycle was not complete by 12 h after hCG but movement of a wave of cells from S phase to G2/M appeared to occur between 8 and 12 h.

Discussion

Constitutive expression of dominant active *SmoM2* in the ovary prevented ovulation. The major phenotypic difference identified between mutant and control mice that may contribute to ovulatory failure is the dramatic reduction in the layer of muscle

cells that surround developing follicles. The presence of muscle cells or myofibroblastic-type cells in the theca layer of the follicle has been demonstrated in many mammalian species and an extensive literature exists to suggest a potential role of contractile cells in the process of ovulation (Amsterdam *et al.*, 1977; Espey, 1978). However, a general lack of direct evidence for a requirement for muscle contraction in ovulation, as well as contradictory evidence obtained from different studies, apparently led to decreased effort in this field. Recently, treatment with endothelin-2 (END2) was shown to increase tension development in strips of rat ovarian tissue (Ko *et al.*, 2006). *End2*, expressed by granulosa cells, increases immediately prior to ovulation in the rat (Ko *et al.*, 2006) and mouse (Palanisamy *et al.*, 2006) and receptors for END2 are present within the SMA-positive muscle layer as well as in other cell types within follicles (Ko *et al.*, 2006; Palanisamy *et al.*, 2006). Importantly, injection of an END2 antagonist into the rat ovary decreased the rate of ovulation in vivo and reduced contraction of follicular smooth muscle was postulated to be responsible (Ko *et al.*, 2006). Furthermore, systemic injection of an END2 antagonist to mice decreased ovulation rate (Palanisamy *et al.*, 2006). A number of genetically altered mice have been created in which ovulation is impaired and these studies have revealed important information about the signaling pathways involved in ovulation. However, the end-points affected which directly prevent ovulation have often remained undetermined. The mice generated in the current study provide a unique model to directly test the effects of impaired follicular muscle development on ovulation.

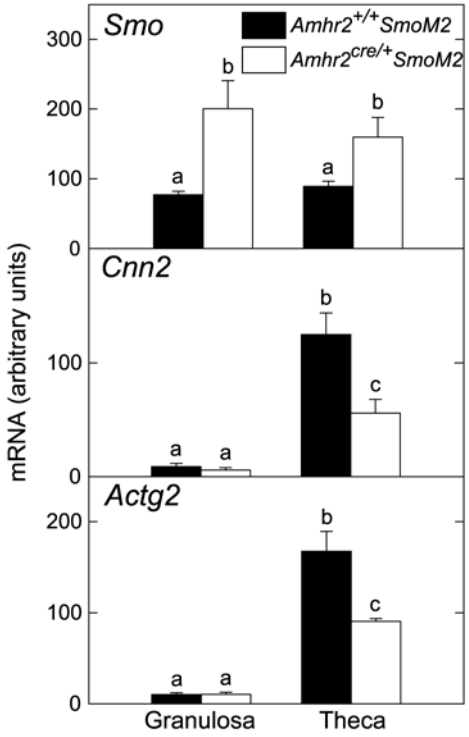

Fig. 2.9. Expression of genes in isolated granulosa and theca cells of preovulatory follicles from *Amhr2*$^{+/+}$*SmoM2* and *Amhr2*$^{cre/+}$*SmoM2* mice. Cells were isolated from preovulatory follicles of immature mice 24 h after injection of eCG. Total RNA was assayed by quantitative real-time RT-PCR. Data are mean ± SEM. n = 3 granulosa cell and theca preparations. Bars without common superscripts are significantly different ($P < 0.05$).

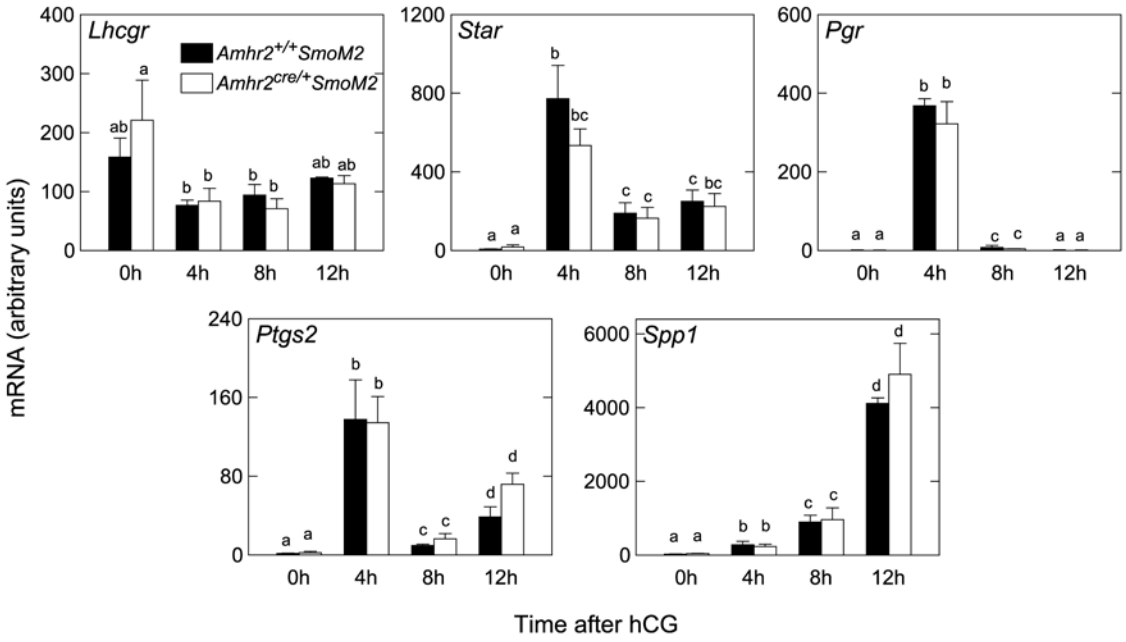

Fig. 2.10. Expression of genes associated with ovulation and luteinization in granulosa cells from eCG-primed *Amhr2*$^{+/+}$*SmoM2* and *Amhr2*$^{cre/+}$*SmoM2* mice obtained after injection of hCG. Total RNA was assayed by quantitative real-time RT-PCR. Data are mean ± SEM. n = 3 granulosa cell preparations. Bars without common superscripts are significantly different ($P < 0.05$).

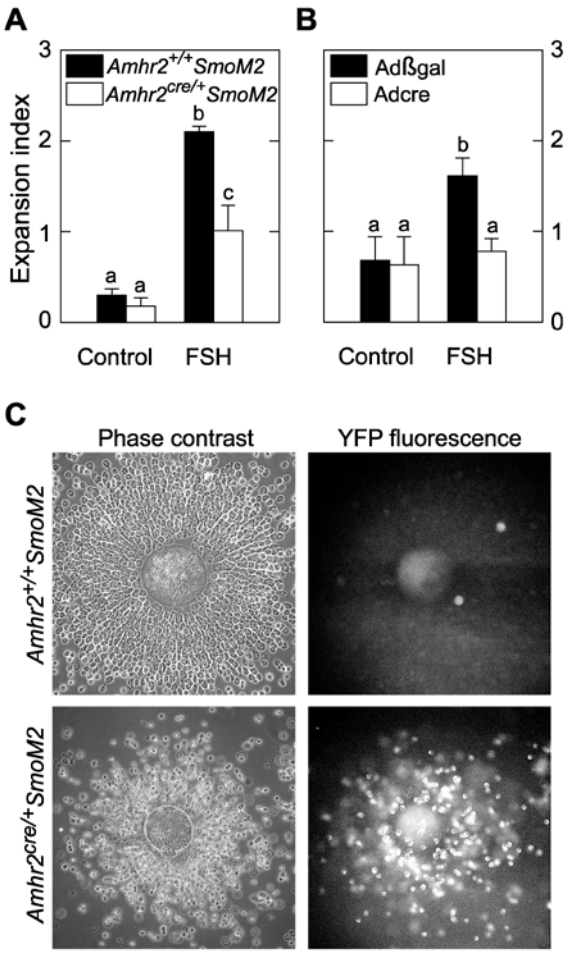
A
B
C
Expansion index
Amhr2+/+SmoM2
Amhr2cre/+SmoM2
Adßgal
Adcre
Control
FSH
Phase contrast
YFP fluorescence
Amhr2+/+SmoM2
Amhr2cre/+SmoM2

Fig. 2.11. Cumulus expansion is reduced in COC expressing *SmoM2*. **A**) COC were obtained from *Amhr2*$^{+/+}$*SmoM2* and *Amhr2*$^{cre/+}$*SmoM2* mice 48 h after injection with eCG and incubated with 0 or 100 ng/ml oFSH. Cumulus expansion was scored on a scale of 0 (no expansion) to 4 (full expansion) 20-24 h later. For each treatment, a total of 60–79 COC from three separate COC preparations were scored. **B**) COC were obtained from *SmoM2* mice 48 h after injection with eCG and incubated for 6 h with Adβgal or Adcre. At 6 h, 0 or 100 ng/ml oFSH was added, and cumulus expansion examined at 24 h. For each treatment, a total of 20-34 COC from three separate COC preparations were scored. Data are mean ± SEM. Bars without common superscripts are significantly different ($P < 0.05$). **C**) Phase contrast and fluorescent images of representative COC from *Amhr2*$^{+/+}$*SmoM2* mice (significant expansion, no fluorescent signal observed) and *Amhr2*$^{cre/+}$*SmoM2* mice (minimal expansion, positive YFP signal observed; note cells in the plane of focus show bright signal for YFP).

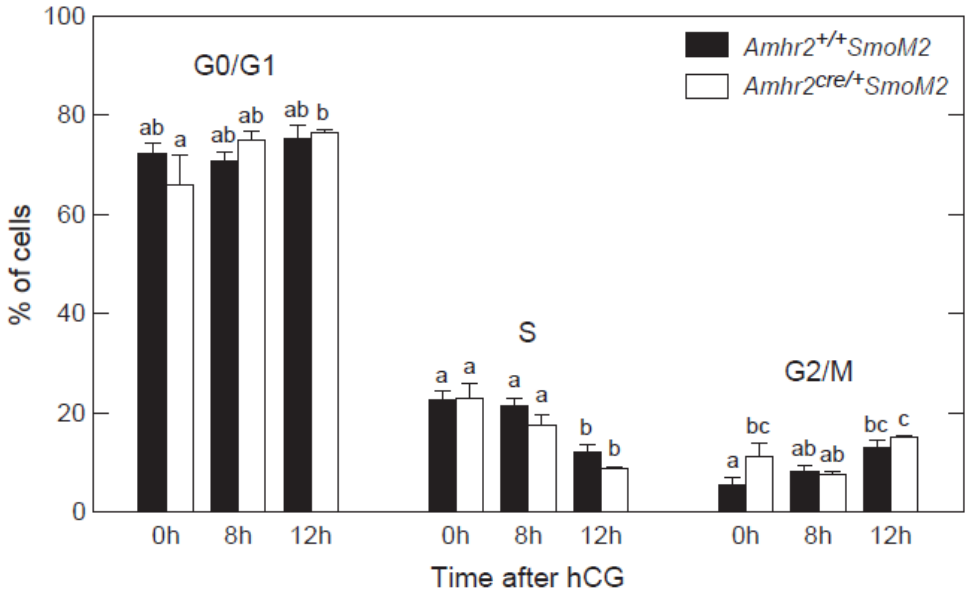

Fig. 2.12. Granulosa cells from preovulatory follicles of eCG-primed *Amhr2*$^{+/+}$*SmoM2* and *Amhr2*$^{cre/+}$*SmoM2* mice begin to exit the cell cycle in a similar manner after injection of hCG. Cell cycle stage was determined by flow cytometric analysis of propidium iodide binding to cellular DNA. Data are mean ± SEM. n = 3-8 granulosa cell preparations from individual animals. Within each cell cycle stage, bars without common superscripts are significantly different ($P < 0.05$).

HH signaling regulates smooth muscle differentiation in a number of organ systems. In the developing gut, ureter and bladder, SHH directs radial patterning of mesoderm by stimulating the proliferation of mesenchymal cell precursors and preventing their differentiation into smooth muscle cells (Shiroyanagi *et al.*, 2007; Sukegawa *et al.*, 2000; Yu *et al.*, 2002). In each of these systems, mesenchymal cells located most distant from the source of SHH in the epithelium differentiate into muscle cells, while cells closer to the epithelium adopt non-muscle cell fates. These findings are consistent with a well-documented aspect of HH effects on tissue patterning; a concentration gradient of HH ligand is established and differentiation of target cells is dependent on their position within the gradient (King *et al.*, 2008). Further direct evidence that expression of dominant active *SmoM2* can inhibit differentiation of smooth muscle was provided by experiments in which expression of *SmoM2* in *Xenopus* embryos increased proliferation of midgut mesenchymal cells and attenuated expression of the differentiation marker smooth muscle actin (Zhang & Kalderon, 2001).

The theca is presumed to be derived from mesenchymal cells present in the newborn ovary at the time that fragmentation of ovigerous cords to form primordial follicles occurs (Mazaud *et al.*, 2005), although theca progenitor cell(s) have not been definitively identified and studied (Hirshfield, 1991a; Magoffin, 2005). Primordial follicles are composed of a quiescent oocyte surrounded by a flattened layer of pregranulosa cells and enclosed by a basement membrane. Although the theca cell layer that will form outside the basement membrane is not yet discernable,

mesenchymal cells in close association with primordial follicles include theca cell precursors (Hirshfield, 1991b). Factors determining the fate of cells within the theca as fibroblastic, steroidogenic or myoid have not been determined. In growing primary follicles, a layer of dividing mesenchymal cells surrounding the basement membrane was detected in rats infused with tritiated thymidine, suggesting that an early layer of theca precursors is intimately associated with the follicle at this stage (Hirshfield, 1991b). Components of the HH signaling pathway are detectable by real time RT-PCR in newborn mouse ovaries(Russell *et al.*, 2007). During the first days of life, the ovigerous cords break down and formation of primordial follicles is complete within 4 days. In situ hybridization showed that expression of *Dhh* and *Ihh* is first detectable in granulosa cells of primary follicles and *Ptch1* and *Gli1* are expressed in the theca (Wijgerde *et al.*, 2005). Therefore, at least as early as the primary stage, and possibly earlier, HH signaling might regulate the differentiation of mesenchymal cells and thereby influence thecal development. Results of the current study show that theca muscle cells are detectable in control mice by immunohistochemistry for SMA as early as day 12 of age while staining is substantially reduced in mutant mice. Appropriate temporal and spatial signaling through the HH signaling pathway appears to be critical for cell fate determination and/or differentiation of smooth muscle cells within the theca layer of the follicle. Furthermore, development of this cell layer is likely to be essential for ovulation.

Quantitative gene expression analyses showed that levels of *Smo* mRNA in granulosa cells of *Amhr2*$^{cre/+}$*SmoM2* mice were elevated at all time points examined

after eCG/hCG-treatment compared to control mice, confirming constitutive expression of *SmoM2*. In contrast, *Smo* levels in residual tissue were substantially lower than in granulosa cells and were only slightly elevated in mutants compared to controls at several time points (Fig. 2.8). *SmoM2* was clearly expressed in the theca of mutant mice since the YFP reporter protein was detected in theca of preovulatory follicles by flow cytometry (Fig. 2.1) and expression of *Smo* mRNA was elevated in isolated theca of mutants compared to controls (Fig. 2.9). Failure to observe increased expression of *Smo* in residual tissue of mutant mice may reflect dilution of theca within the residual tissue with other cell types.

Components of the HH signaling pathway were expressed in the granulosa cells as well as the theca, in agreement with a previous report (Russell *et al.*, 2007). The LH surge appears to trigger changes in HH signaling; *Ihh* decreased within 4 h after hCG and *Hhip* and *Gli3* simultaneously increased. HHIP binds HH ligands and is thought to function as an antagonist (Chuang & McMahon, 1999), and GLI3 often acts as a transcriptional repressor. While in a number of contexts HH signaling reduces expression of *Gli3* mRNA (Bastida *et al.*, 2004; Marigo *et al.*, 1996; Ohba *et al.*, 2008), a primary means of regulation is by processing of GLI3 protein. The regulation of GLI3 processing by HH signaling is a critical determinant of many aspects of development (Koziel *et al.*, 2005; Litingtung *et al.*, 2002; Wang *et al.*, 2000; Wang *et al.*, 2007). In the absence of HH signaling, full-length GLI3 is processed to form a truncated repressor (GLI3R) by phosphorylation at multiple sites mediated by cAMP-dependent protein kinase A (PKA), CKI and GSK3 (Tempe *et al.*, 2006;

Wang *et al.*, 2000; Wang & Li, 2006). In this regard, it is interesting that ovarian PKA activity increases in response to the LH surge (Gonzalez-Robayna *et al.*, 1999; Richards, 1994). *Gli1* and *Patch1* are reported to be transcriptional targets of HH signaling (Ahn & Joyner, 2004; Ikram *et al.*, 2004; Lee *et al.*, 1997; Marigo *et al.*, 1996). While levels of *Gli1* were much higher in residual tissue than in granulosa cells, levels of *Ptch1* were within the same range in the two cell fractions. The relationship between levels of *Ptch1* mRNA and HH signaling is complex; *Ptch1* is a transcriptional target of HH signaling, while PTCH protein inhibits signaling through SMO, generating a negative feedback loop in which HH attenuates its own activity (Chen & Struhl, 1996; Jeong & McMahon, 2005). The significance of potential changes in HH signaling in both the granulosa and residual tissue after the LH surge remains to be determined.

The disorganized appearance of cumulus expansion in *Amhr2*$^{cre/+}$*SmoM2* mice detected by histology was confirmed by in vitro assays. The fact that elevated HH signaling interfered with normal cumulus expansion is consistent with a report that expression of *Ihh* and *Dhh* decrease in COC of mice after hCG (Hernandez-Gonzalez *et al.*, 2006). A number of genetically altered mice in which ovulation is impaired were also reported to have reduced cumulus expansion, including mice null for *Ptgs2* (Davis *et al.*, 1999), *Rip140* (Tullet *et al.*, 2005), *Adamts1* (Mittaz *et al.*, 2004) and petraxin 3 (Varani *et al.*, 2002) and mice with defective EGFR signaling (Hsieh *et al.*, 2007), but the basis for this association has not been defined. While impaired cumulus expansion may contribute to ovulatory failure in *Amhr2*$^{cre/+}$*SmoM2* mice, it

is likely that failed development of the theca muscle cells is primarily responsible. Microarray and RT-PCR analyses showed that expression of *Tnc*, which encodes a protein that can contribute to hyaluronan cross-linking in the extracellular matrix, was reduced in mutant mice in the residual tissue but not in mural granulosa cells. TNC was previously identified at high levels in theca externa of rats (Yasuda *et al.*, 2005). This is of potential relevance to ovulation since in a number of tissues TNC is associated with tissue remodeling and wound healing (Schellings *et al.*, 2004). TNC was also localized to the cumulus matrix of mice and women suggesting that it may play a role in cumulus expansion (Familiari *et al.*, 1996; Hernandez-Gonzalez *et al.*, 2006; Relucenti *et al.*, 2005). The transcript for periostin (*Postn*), which encodes an extracellular matrix protein that belongs to the same family as TNC, was also reduced in mutant mice (Table 2). The possibility that extracellular matrix components of the follicle are regulated by HH signaling requires further investigation.

In *Amhr2*$^{cre/+}$*SmoM2* mice, expression of a number of genes changed similarly after hCG to that observed in controls, including *Ptgs2* and *Pgr*, which are essential for ovulation (Jefferson *et al.*, 2006; Lim *et al.*, 1997; Lydon *et al.*, 1995), *Lhcgr*, which is required for differentiation (Richards, 1994) and *End2*, which is thought to be involved in stimulating muscle contraction and follicle rupture (Ko *et al.*, 2006). Microarray data revealed no difference between mutant and control mice in expression of *Cyp17a1*, encoding cytochrome P_{450} 17α-hydroxylase/17, 20-lyase, the enzyme required for androgen synthesis in the theca. Furthermore, oocyte maturation appeared to be initiated normally and cell cycle analysis revealed no

differences in granulosa cell proliferation. Measurements of *Star* mRNA, SCC and serum progesterone indicated no alteration in luteinization in mutant mice. Furthermore, in vitro induction of *SmoM2* expression by granulosa cells had no effect on progesterone production. These findings, as well as ovarian histology, suggest that many aspects of follicle development to the preovulatory stage occurred fairly normally in mutant mice, and that some of the early events in response to the LH surge were not altered. It is not yet determined why estrous cycle length is prolonged in mutant mice. Careful morphometric analysis of follicle development in mutant and control ovaries will be necessary to address this question.

The fact that blood-filled cavities were prominent in follicles of eCG/hCG treated mutant mice suggested that development of the vasculature might be abnormal, leading to increased leakage of blood cells into the antral cavity. However, the concentration of serum progesterone did not differ in mutant and control mice, indicating that vascular development was adequate to promote the normal release of progesterone into the circulation. This reasoning is supported by the findings that impaired vascular development of CL in various strains of transgenic mice and in sheep is associated with decreased levels of progesterone in the circulation (Hsieh *et al.*, 2005). In addition, immunostaining for endothelial cells indicated no obvious differences in preovulatory follicles of mutant and control mice.

In summary, dominant activation of HH signaling in developing follicles likely blocks the differentiation of precursor cells into muscle cells that normally reside in the outer theca layer of the follicle. This possibility is consistent with known effects

of HH signaling on smooth muscle differentiation in other developmental systems. Although follicles develop to the preovulatory stage and undergo many changes in response to eCG/hCG normally, they fail to release the oocyte. These findings lend support to the theory that muscle cells within the theca layer are required for release of the oocyte at the time of ovulation.

Acknowledgements

The authors thank Dr. Richard R. Behringer, University of Texas M.D. Anderson Cancer Center, Houston Texas, for providing *Amhr2*$^{cre/+}$ mice, and Patricia Fisher, NYSCVM, Cornell University, for performing SMA/VWB immunohistochemistry.

References

Ahn S, Joyner AL (2004) Dynamic changes in the response of cells to positive hedgehog signaling during mouse limb patterning. *Cell* **118:** 505-516

Amsterdam A, Lindner HR, Groschel-Stewart U (1977) Localization of actin and myosin in the rat oocyte and follicular wall by immunofluorescence. *Anat Rec* **187:** 311-328

Arango NA, Szotek PP, Manganaro TF, Oliva E, Donahoe PK, Teixeira J (2005) Conditional deletion of β-catenin in the mesenchyme of the developing mouse uterus results in a switch to adipogenesis in the myometrium. *Developmental Biology* **288:** 276-283

Bai CB, Auerbach W, Lee JS, Stephen D, Joyner AL (2002) Gli2 , but not Gli1 , is required for initial Shh signaling and ectopic activation of the Shh pathway. *Development* **129:** 4753-4761

Bastida MF, Delgado MD, Wang B, Fallon JF, Fernandez-Teran M, Ros MA (2004) Levels of Gli3 repressor correlate with Bmp4 expression and apoptosis during limb development. *Developmental Dynamics* **231:** 148-160

Chen Y, Struhl G (1996) Dual roles for Patched in sequestering and transducing

hedgehog. *Cell* **87:** 553-563

Chuang P, McMahon AP (1999) Vertebrate Hedgehog signalling modulated by induction of a Hedgehog-binding protein. *Nature* **397:** 617-621

Davis BJ, Lennard DE, Lee CA, Tiano HF, Morham SG, Wetsel WC, Langenbach R (1999) Anovulation in cyclooxygenase-2-deficient mice is restored by prostaglandin E 2 and interleukin-1 *Endocrinology* **140:** 2685-2695

Downs SM (1989) Specificity of epidermal growth factor action on maturation of the murine oocyte and cumulus oophorus in vitro. *Biology of Reproduction* **41:** 371-379

Espey LL (1978) Ovarian contractility and its relationship to ovulation: a review. *Biology of Reproduction* **19:** 540-551

Familiari G, Verlangia C, Nottola SA, Renda T, Micara G, Aragona C, Zardi L, Motta PM (1996) Heterogeneous distribution of fibronectin, tenascin-C, and laminin immunoreactive material in the cumulus-corona cells surrounding mature human oocytes from IVF-ET protocols - evidence that they are composed of different subpopulations: an immunohistochemical study using scanning confocal laser and fluorescence microscopy. *Molecular Reproduction and Development* **43:** 392-402

Gonzalez-Robayna IJ, Alliston TN, Buse P, Firestone GL, Richards JS (1999) Functional and subcellular changes in the A-kinase-signaling pathway: relation to aromatase and Sgk expression during the transition of granulosa cells to luteal cells. *Molecular Endocrinology* **13:** 1318-1337

Hernandez-Gonzalez I, Gonzalez-Robayna I, Shimada M, Wayne CM, Ochsner SA, White L, Richards JS (2006) Gene expression profiles of cumulus cell oocyte complexes during ovulation reveal cumulus cells express neuronal and immune-related genes: Does this expand their role in the ovulation process? *Molecular Endocrinology* **20:** 1300-1321

Hirshfield AN (1991a) Development of follicles in the mammalian ovary. *International Review of Cytology* **124:** 43-101

Hirshfield AN (1991b) Theca cells may be present at the outset of follicular growth. *Biology of Reproduction* **44:** 1157-1162

Hsieh M, Boerboom D, Shimada M, Lo Y, Parlow AF, Luhmann UFO, Berger W, Richards JS (2005) Mice null for frizzled4 (fzd4 -/-) are infertile and exhibit impaired corpora lutea formation and function. *Biology of Reproduction* **73:** 1135-1146

Hsieh M, Lee D, Panigone S, Horner K, Chen R, Theologis A, Lee DC, Threadgill DW, Conti M (2007) Luteinizing hormone-dependent activation of the epidermal growth factor network is essential for ovulation. *Molecular and Cellular Biology* **27:** 1914-1924

Huangfu D, Anderson KV (2006) Signaling from Smo to Ci/Gli: conservation and divergence of Hedgehog pathways from Drosophila to vertebrates. *Development* **133:** 3-14

Ikram MS, Neill GW, Regl G, Eichberger T, Frischauf AM, Aberger F, Quinn A, Philpott M (2004) Gli2 is expressed in normal human epidermis and BCC and induces Gli1 expression by binding to its promoter. *Journal of Investigative Dermatology* **122:** 1503-1509

Jamin SP, Arango NA, Mishina Y, Hanks MC, Behringer RR (2002) Requirement of Bmpr1a for Mullerian duct regression during male sexual development. *Nature Genetics* **32:** 408-410

Jefferson W, Newbold R, Padilla-Banks E, Pepling M (2006) Neonatal genistein treatment alters ovarian differentiation in the mouse: inhibition of oocyte nest breakdown and increased oocyte survival. *Biophysical Journal* **74:** 161-168

Jeong J, Mao J, Tenzen T, Kottmann AH, McMahon AP (2004) Hedgehog signaling in the neural crest cells regulates the patterning and growth of facial primordia. *Genes and Development* **18:** 937-951

Jeong J, McMahon AP (2005) Growth and pattern of the mammalian neural tube are governed by partially overlapping feedback activities of the hedgehog antagonists patched1 and Hhip1. *Development* **132:** 143-154

Jorgez CJ, Klysik M, Jamin SP, Behringer RR, Matzuk MM (2004) Granulosa cell-specific inactivation of follistatin causes female fertility defects. *Molecular Endocrinology* **18:** 953-967

King PJ, Guasti L, Laufer E (2008) Hedehog signaling in endocrine development and disease. *Journal of Endocrinology* **198:** 439-450

Ko CM, Gieske MC, Al-Alem L, Hahn YK, Su W, Gong MC, Iglarz M, Koo Y (2006) Endothelin-2 in ovarian follicle rupture. *Endocrinology* **147:** 1770-1779

Koziel L, Wuelling M, Schneider S, Vortkamp A (2005) Gli3 acts as a repressor downstream of Ihh in regulating two distinct steps of chondrocyte differentiation. *Development* **132:** 5249-5260

Lee HK, Braynen W, Keshav K, Pavlidis P (2005) ErmineJ: tool for functional analysis of gene expression data sets. *BMC Bioinformatics* **6:** 269

Lee J, Platt KA, Censullo P, Ruiz i Altaba A (1997) Gli1 is a target of Sonic hedgehog that induces ventral neural tube development. *Development* **124:** 2537-2552

Lim H, Paria BC, Das SK, Dinchuk JE, Langenbach R, Trzaskos JM, Dey SK (1997) Multiple female reproductive failures in cyclooxygenase 2-deficient mice. *Cell* **91:** 197-208

Litingtung Y, Dahn RD, Li Y, Fallon JF, Chiang C (2002) Shh and Gli3 are dispensable for limb skeleton formation but regulate digit number and identity. *Nature* **418:** 979-983

Lydon JP, DeMayo FJ, Funk CR, Mani SK, Hughes AR, Montgomery CA, Jr., Shyamala G, Conneely OM, O'Malley BW (1995) Mice lacking progesterone receptor exhibit pleiotropic reproductive abnormalities. *Genes and Development* **9:** 2266-2278

Magoffin DA (2005) Cells in focus: ovarian theca cell. *International Journal of Biochemistry and Cell Biology* **37:** 1344-1349

Marigo V, Johnson RL, Vortkamp A, Tabin CJ (1996) Sonic hedgehog differentially regulates expression of Gli and Gli3 during limb development. *Developmental Biology* **180:** 273-283

Mazaud S, Guyot R, Guigon CJ, Coudouel N, Le Magueresse-Battistoni B, Magre S (2005) Basal membrane remodeling during follicle histogenesis in the rat ovary: contribution of proteinases of the MMP and PA families. *Dev Biol* **277:** 403-416

McMahon AP, Ingham PW, Tabin CJ (2003) Developmental roles and clinical significance of Hedgehog signaling. *Current Topics in Developmental Biology* **53:** 1-114

McRae RS, Johnston HM, Mihm M, O'Shaughnessy PJ (2005) Changes in mouse granulosa cell gene expression during early luteinization. *Endocrinology* **146:** 309-317

Mittaz L, Russell DL, Wilson T, Brasted M, Tkalcevic J, Salamonsen LA, Hertzog PJ, Pritchard MA (2004) Adamts-1 is essential for the development and function of the urogenital system. *Biology of Reproduction* **70:** 1096-1105

Mo R, Freer AM, Zinyk DL, Crackower MA, Michaud J, Heng HHQ, Chik KW, Shi X, Tsui L, Cheng SH, Joyner AL, Hui C (1997) Specific and redundant functions of

Gli2 and Gli3 zinc finger genes in skeletal patterning and development. *Development* **124:** 113-123

Ohba S, Kawaguchi H, Kugimiya F, Ogasawara T, Kawamura N, Saito T, Ikeda T, Fujii K, Miyajima T, Kuramochi A, Miyashita T, Oda H, Nakamura K, Takato T, Chung Ui (2008) Patched1 haploinsufficiency increases adult bone mass and modulates Gli3 repressor activity. *Developmental Cell* **14:** 689-699

Ott RL (2001) *An introduction to statistical methods and data analysis, 5th ed*, Vol. 5, Belmont, CA: Duxbury Press.

Palanisamy GS, Cheon YP, Kim J, Kannan A, Li Q, Sato M, Mantena SR, Sitruk-Ware RL, Bagchi MK, Bagchi IC (2006) A novel pathway involving progesterone receptor, endothelin-2, and endothelin receptor B controls ovulation in mice. *Molecular Endocrinology* **20:** 2784-2795

Pan Y, Bai CB, Joyner AL, Wang B (2006) Sonic hedgehog signaling regulates Gli2 transcriptional activity by suppressing its processing and degradation. *Molecular and Cellular Biology* **26:** 3365-3377

Quirk SM, Cowan RG, Harman RM (2006) The susceptibility of granulosa cells to apoptosis is influenced by oestradiol and the cell cycle. *Journal of Endocrinology* **189:** 441-453

Relucenti M, Heyn R, Correr S, Familiari G (2005) Cumulus oophorus extracellular matrix in the human oocyte: a role for adhesive proteins. *Italian Journal of Anatomy and Embryology* **110:** 219-224

Richards JS (1994) Hormonal control of gene expression in the ovary. *Endocrine Reviews* **15:** 725-751

Robker RL, Richards JS (1998) Hormone-induced proliferation and differentiation of granulosa cells: a coordinated balance of the cell cycle regulators cyclin D2 and p27 Kip1 *Molecular Endocrinology* **12:** 924-940

Rubin LL, de Sauvage FJ (2006) Targeting the Hedgehog pathway in cancer. *Nature Reviews Drug Discovery* **5:** 1026-1033

Russell MC, Cowan RG, Harman RM, Walker AL, Quirk SM (2007) The hedgehog signaling pathway in the mouse ovary. *Biology of Reproduction* **77:** 226-236

Schellings MW, Pinto YM, Heymans S (2004) Matricellular proteins in the heart: possible role during stress and remodeling. *Cardiovasc Res* **64:** 24-31

Shiroyanagi Y, Liu B, Cao M, Agras K, Li J, Hsieh MH, Willingham EJ, Baskin LS (2007) Urothelial sonic hedgehog signaling plays an important role in bladder smooth muscle formation. *Differentiation* **75:** 968-977

Sukegawa A, Narita T, Kameda T, Saitoh K, Nohno T, Iba H, Yasugi S, Fukuda K (2000) The concentric structure of the developing gut is regulated by Sonic hedgehog derived from endodermal epithelium. *Development* **127:** 1971-1980

Tempe D, Casas M, Karaz S, Blanchet-Tournier MF, Concordet JP (2006) Multisite protein kinase A and glycogen synthase kinase 3beta phosphorylation leads to Gli3 ubiquitination by SCFbetaTrCP. *Mol Cell Biol* **26:** 4316-4326

Tullet JMA, Pocock V, Steel JH, White R, Milligan S, Parker MG (2005) Multiple signaling defects in the absence of RIP140 impair both cumulus expansion and follicle rupture. *Endocrinology* **146:** 4127-4137

Varani S, Elvin JA, Yan C, DeMayo J, DeMayo FJ, Horton HF, Byrne MC, Matzuk MM (2002) Knockout of pentraxin 3, a downstream target of growth differentiation factor-9, causes female subfertility. *Molecular Endocrinology* **16:** 1154-1167

Wang B, Fallon JF, Beachy PA (2000) Hedgehog-regulated processing of Gli3 produces an anterioir/posterior repressor gradient in the developing vertebrate limb. *Cell* **100:** 423-434

Wang B, Li Y (2006) Evidence for the direct involvement of áTrCP in Gli3 protein processing. *Proceedings of the National Academy of Sciences* **103:** 33-38

Wang C, R [illegible] Wang B (2007) The Shh-independent activation of the full length Gli3 protein and its role in vertebrate limb digit patterning. *Developmental Biology* **305:** 460-469

Wijgerde M, Ooms M, Hoogerbrugge JW, Grootegoed JA (2005) Hedgehog signaling in mouse ovary: Indian hedgehog and desert hedgehog induce target gene expression in developing theca cells. *Endocrinology* **146:** 3558-3566

Xie J, Murone M, Luoh SM, Ryan A, Gu Q, Zhang C, Bonifas JM, Lam CW, Hynes M, Goddard A, Rosenthal A, Epstein EH, Jr., de Sauvage FJ (1998) Activating Smoothened mutations in sporadic basal-cell carcinoma. *Nature* **391:** 90-92

Yasuda K, Hagiwara E, Takeuchi A, Mukai C, Matsui C, Sakai A, Tamotsu S (2005) Changes in the distribution of tenascin and fibronectin in the mouse ovary during folliculogenesis, atresia, corpus luteum formation and luteolysis. *Zoological Science* **22:** 237-245

Yoon JW, Kita Y, Frank DJ, Majewski RR, Konicek BA, Nobrega MA, Jacob H, Walterhouse D, Iannaccone P (2002) Gene expression profiling leads to identification of GLI1-binding elements in target genes and a role for multiple downstream pathways in GLI1-induced cell transformation. *Journal of Biological Chemistry* **277:** 5548-5555

Yu J, Carroll TJ, McMahon AP (2002) Sonic hedgehog regulates proliferation and differentiation of mesenchymal cells in the mouse metanephric kidney. *Development* **129:** 5301-5312

Zhang Y, Kalderon D (2001) Hedgehog acts as a somatic stem cell factor in the *Drosophila* ovary. *Nature* **410:** 599-604

CHAPTER THREE: OVER-ACTIVATION OF HEDGEHOG SIGNALING AFFECTS DEVELOPMENT OF OVARIAN VASCULATURE AND LEADS TO THE PRESENCE OF ADRENAL-LIKE CELLS IN THE OVARY

Summary

To understand the role of HH signaling in the mammalian ovary, we previously created mice expressing a dominant active allele of the signal transducer, *Smoothened* (*Smo*), named *SmoM2*, in the ovary and the reproductive tract by driving its expression with the *anti-Mullerian hormone receptor type II* (*Amhr2*) promoter. Mutant mice fail to ovulate. This phenotype is associated with reduced expression of smooth muscle genes and smooth muscle actin within the thecal layer of growing follicles. The deficiency in thecal smooth muscle is evident beginning at the secondary stage of follicle development and continues as follicles develop to preovulatory status, suggesting that developmental defects occur during early life in mutant mice. Along these lines, no difference was detected in expression of the HH target genes *Gli1*, *Ptch1* and *Hhip* in preovulatory follicles, suggesting that over-activation of HH signaling that leads to the phenotype in mutant mice may be restricted to early ovarian development. The present study aimed to determine whether HH signaling activity was altered before the onset of follicle growth, and to address the nature of the developmental defects in the ovaries of mutant mice. The results showed that HH signaling is abnormally activated in the ovaries of mutant mice compared to controls around the time of birth. Microarray analyses revealed that levels of mRNA for genes involved in vascular network formation and endothelial-mesenchymal interaction are elevated in mutants compared to their levels in controls in ovaries from mice at 2 days of age. Consistent with this finding, a capillary network of higher density was formed in the cortex of the neonatal ovary in

mutant mice. Reduced expression of smooth muscle actin in the theca of mutant mice represented vascular smooth muscle, indicating aberrant maturation of thecal vasculature. Interestingly, adrenal-like cells were present in neonatal ovaries of mutant mice as indicated by their expression of genes normally expressed in the adrenal gland, such as C*yp11b1*, *Cyp21* and *Shh*. An increased rate of oocyte degeneration occurred in mutant mice compared to controls during follicle assembly, resulting in a reduced primordial follicle pool at 24 days of age. The first wave of follicular development was abnormal in mutant mice, with increased incidence of atresia, multiple-oocyte-follicles and abnormal morphology of follicles grown to the secondary stage. These results indicate that over-activation of HH signaling around the time of birth may alter vascular development, and this may contribute to defects in the thecal vasculature throughout life that are associated with anovulation. In addition, the data suggest that HH signaling may be a mediator of cell migration or/and sorting in the adrenogonadal primordium, or alternatively, that it can induce differentiation of cells within the ovary to a fate typical of adrenal cells.

Introduction

In an attempt to understand the function of HH signaling in the ovary, we previously created mice expressing a dominantly active allele of the signal transducer *Smo*, named *SmoM2*, in the Mullarian duct and the ovary by driving its expression with the *anti-Mullerian hormone receptor type II* (*Amhr2*) promoter (Ren *et al*., 2009). The resultant *Amhr2*$^{cre/+}$*SmoM2* mutant mice are infertile and fail to ovulate. The

failure of ovulation in mutant mice is accompanied by reduced expression of smooth muscle genes in the thecal layer of growing follicles in the mutants compared to controls. This abnormality begins in follicles from the secondary stage, when theca begins to acquire an extensive vasculature. In addition, no difference in the levels of mRNA for components of HH pathway was detected in preovulatory follicles around the time of ovulation. These observations indicate that the failure of ovulation in *Amhr2*$^{cre/+}$*SmoM2* mutant mice is due to altered HH signaling activity during development rather than around the time of ovulation. The purpose of the current study was to determine whether HH signaling activity is altered in mutant mice and whether this alteration contributes to the failure of ovulation in later life.

HH signaling has potent pro-angiogenic effects and regulates multiple aspects of vascular development. In the murine yolk sac, HH signaling is necessary for the differentiation of embryoid bodies into blood islands (Byrd *et al.*, 2002). In avain and murine embryos, HH signaling is required for the formation of endothelial tubes during initial vasculogenesis and for subsequent angiogenesis (Nagase *et al*., 2006; Vokes *et al*., 2004). HH signaling promotes formation of vascular networks in a great number of tissues during development, adult homeostasis and tumorigenesis. In the hindbrain choroid plexus, SHH induces vascular outgrowth that is critical for the function of the choroid plexus (Nielsen & Dymecki, 2010). During development of the lung, HH signaling in coordination with FGF9 regulates the growth and patterning of the pulmonary capillary network (White *et al*., 2007), which is critical for tubular branching morphogenesis (van Tuyl *et al*., 2007). HH signaling also

controls vascularization of the cartilage (Joeng & Long, 2009). In murine melanoma, SHH promotes proliferation of endothelial cells in vivo and in vitro (Geng *et al*.,2007). Recently, Chen *et al*. (Chen *et al*., 2011) showed that HH signaling promotes tumorigenesis by enhancing tumor angiogenesis. Finally, HH signaling can induce the specification of endothelial cells to become arterial, rather than venous cells (Williams *et al*., 2010).

One mechanism through which HH signaling exerts its compound effects on vascular development is by promoting the differentiation, migration and proliferation of endothelial precursor cells (Asai *et al*., 2006; Byrd & Grabel, 2004). Accumulating evidence indicates that effects of HH signaling on vascular development are not through direct effects on endothelial cells but are often achieved, at least in part, through direct action on vascular mural cells or the mesenchymal-interstitial cells surrounding the vasculature. During the formation of the pulmonary capillary network, SHH and FGF9 signal to the lung mesenchyme to regulate the growth and patterning of the distal capillary network (White *et al*., 2007). In an in vitro model of ischemia, SHH promotes neovascularization through inducing expression of vascular endothelial growth factor (VEGF), angiopoietin-1 (ANGPT-1), and angiopoietin-2 (ANGPT-2) in the interstitial mesenchymal cells (Pola *et al*., 2001). In human vascular smooth muscle cell (VSMC), SHH induces expression of beta-type platelet-derived growth factor (PDGFRβ) and the wrapping of VSMC around newly formed vessels (Frontini et al., 2011). Expression of mRNA for *Shh* and *hypoxia-induced factor 1* (*Hif1*) is induced by hypoxia in human pulmonary

arterial smooth muscle cells, and mediates proliferation of these cells through GLI1 (Wang *et al*., 2010). In a tumor xenograft model, HH ligand produced by tumor cells targets stromal perivascular cells and increases tumor vascular density (Chen *et al*., 2011). Furthermore, HH interacting protein 1 (Hhip1), which binds to HH ligands and limits the spatial distribution of the ligands, is expressed mainly in endothelial cells but not in other cell types in adult animals, and this is proposed to prevent HH signaling to the endothelial cells (Olsen *et al*., 2004). In summary, HH signaling controls vascular development by regulating both endothelial cells and vascular mesenchymal cells directly or indirectly, and it is an attractive candidate for tumor therapy and regenerative treatment.

The ovary is a unique organ compared to other adult tissues. Intensive cyclic vascular remodeling occurs in the ovary throughout an animal's reproductive life span, and the vascular system seems to be an active regulator of development and function of the ovary. Vasculature-associated factors such as platelet-derived growth factor (PDGF) and vascular endothelial growth factor (VEGF), are postulated to modulate follicle activation (Fortune et al, 2011; Kezele et al, 2005; Nilsson et al). As soon as follicles grow beyond the primary stage and start to acquire a second layer of granulosa cells, a capillary network forms within the theca-interstitial layer and is involved in further growth to the antral stage and in follicle selection (Acosta *et al*., 2004; Robinson *et al*., 2009; Zimmermann *et al*., 2003). In preparation for ovulation, multiple changes occur to the ovarian vasculature, such as changes in blood flow mediated by vasodilation and vasoconstriction, which modulate the

formation of the follicle rupture site (Dahm-Kahler *et al*., 2006; Koos *et al*., 1995; Macchiarelli *et al*., 2006; Zackrisson *et al*., 2000). Finally, the newly formed and steroidogenicaly active corpus luteum (CL) is one of the most highly vascularized structures in the body. Numerous studies indicate that vasculature is highly involved in, or perhaps regulates, the formation, function and degradation of the CL (Furukawa *et al*., 2007; Meidan & Levy, 2007; Wulff *et al*., 2001). It is not surprising that alterations in the vasculature are also involved in ovarian pathology, such as polycystic ovary syndrome and ovarian carcinoma (Delgado-Rosas *et al*., 2009; Schiffenbauer *et al*., 1997). Taken together, as the vascular system plays such important roles in the ovary, abnormality in the ovarian vasculature at any stage of follicular development could possibly affect fertility and induce pathogenesis. Therefore, new understanding of the potential role of HH signaling in development of the ovarian vasculature is of significant interest and importance.

Materials and Methods

Mouse strains and management

Procedures were performed as described in Chapter 2.

YFP expression

YFP expressed from the *SmoM2-Yfp* allele was examined using a Zeiss LSM 510 confocal microscope (Carl Zeiss Microimaging, Thornwood, NY). Ovaries were fixed in 4% paraformaldehyde for 1h, rinsed in PBS, counterstained with 1 μg/ml

Hoechst 33258 overnight, then mounted in aqueous mounting media and examined within 24h. YFP was excited at 514 nm and viewed using a 520-550 nm bandpass filter.

Real-time RT-PCR analysis of gene expression

RNA was prepared from whole ovaries using a RNeasy Micro Kit (QIAGEN, Valencia, CA). Reverse transcription was performed using a High Capacity cDNA Reverse Transcription Kit (Applied Biosystems, Foster City, CA). Real-time RT-PCR was performed on an ABI Prism 7000 using the mouse-specific assays listed in Table 3.1. A standard curve used in each assay was constructed by serial dilution of cDNA prepared from a RNA pool of immature (21-23 day old) mouse ovaries. The highest standard was assigned an arbitrary value of 20. In assays for each gene, values for standards and samples were standardized by dividing by that of the corresponding 18S rRNA and multiplying by 100. For assays of whole ovaries, samples from mice at each day of age were analyzed on the same assay plate.

In situ hybridization

Ovaries were collect on the day of birth, dissected in cold PBS on ice, and immediately fixed in 4 % paraformaldehyde in PBS at 4 ℃ for two hours. After fixation, ovaries were washed in PBS-0.1% Tween20, dehydrated, and then stored in 100% methanol at -20 ℃ until use. Whole-mount in situ hybridization was

Table 3.1. Quantitative real-time RT-PCR assays

Gene Symbol	Gene name	Assay ID[a]	Exons[b]
Dhh	desert hedgehog	Mm00432820_m1	2-3
Ihh	Indian hedgehog	Mm00439613_m1	2-3
Shh	sonic hedgehog	Mm00436527_m1	1-2
Ptch1	patched homolog 1	Mm00436026_m1	17-18
Hhip	hedgehog-interacting protein	Mm00469580_m1	12-13
Gli1	GLI-Kruppel family member GLI1	Mm00494645_m1	2-3
Gli2	GLI-Kruppel family member GLI2	Mm01293117_m1	8-9
Gli3	GLI-Kruppel family member GLI3	Mm00492333_m1	1-2
Smo	smoothened homolog	Mm01162710_m1	8-9
Star	steroidogenic acute regulatory protein	Mm00441558_m1	3-4
18s rRNA		4319413E	

[a] Taqman® Gene Expression Assays (Applied Biosystems)
[b] Exons in which forward and reverse primers anneal

performed using digoxigenin-labeled riboprobes and detected using BM purple substrate (Roche Bioscience, Palo Alto, CA) . Whole-mount stained ovaries were imaged using the differential interference contrast setting on a Nikon Eclipse E600 microscope. To better assess the location of mRNA, tissues were embedded in agarose blocks and cut into sections of 15 μm thickness using a vibratome. Ovaries from control and mutant mice were handled equally and were exposed for the same amount of time for each riboprobe. In addition, ovaries with no probe were used as negative controls and embryonic limb buds were used as positive controls.

Microarray analysis

RNA was prepared from ovaries from 2 day-old *Amhr2*$^{+/+}$*SmoM2* control and *Amhr2*$^{cre/+}$*SmoM2* mutant mice using a RNeasy Mini Kit (Qiagen, Valencia, CA). Each sample consisted of RNA from 16 ovaries from 8 mice. RNA quality was assessed by measurement of ribosomal RNA on an Agilent 2100 Bioanalyzer (Agilent Technologies, Santa Clara, CA). Microarray analyses were performed by the Microarray Core Facility of the Cornell University Life Sciences Core Laboratories Center using Affymetrix GeneChip Mouse Genome 430_2 chips (Affymetrix, Santa Clara, CA). Raw array data was processed by Affymetrix GCOS software to obtain signal values. The signals were log2-transformed after being offset by 64, and fold differences were calculated as the difference between mutant and control samples. Only probe sets having at least one Present call were included in the analysis. DAVID cluster analysis (Dahm-Kahler *et al.*, 2006) of Biological

Process terms from the Gene Ontology Consortium (Ashburner *et al*., 2000) was used to identify related groups of Biological Process terms that were over-represented (enriched) among the genes that were 2-fold higher in mutants compared to controls. For data presentation, Biological Process terms with extensive similarity were condensed by the authors into fewer categories (Table 3.2).

Histology and immunohistochemistry

Ovaries were fixed in Bouins and stained with hematoxylin and eosin (H&E) for histology or 2% paraformaldehyde for immunohistochemistry, and stored in ethanol at 4°C until use. Tissues were embedded in paraffin and 5 μm sections were prepared. For CYP17A and CYP21A immunohistochemistry, antigen retrieval was performed in citric acid buffer (pH=5.0) and sections were blocked with 2% normal goat serum (NGS). Sections were incubated overnight at 4°C with rabbit anti-mouse CYP17A (obtained from Dr. Alan J. Conley, University of California at Davis) or NRS diluted 1:200 in PBS-1% BSA. Sections were washed and incubated with 0.5 μg/ml Alexa 488 goat anti-rabbit IgG (Jackson ImmunoResearch, West Grove, PA) in PBS-1% BSA for 4 hours at room temperature and then counterstained with 1 μg/ml Hoechst 33258. Fluorescence was viewed using a Nikon Diaphot 300 microscope (Nikon Instruments, Melville, NY), and images were obtained using a Spot II Digital Camera (Diagnostic Instruments, Sterling Heights, MI).

For whole mount staining of platelet endothelial adhesion molecule (PECAM-1), ovaries were fixed and stored as above, rehydrated into PBS,

permeabilized in PBS-1% Triton X-100 (PBS-TX) and blocked in 5% NGS in PBS-0.1% Triton X-100 (PBS-TX). Ovaries were incubated overnight at 4°C with rat anti-mouse PECAM-1 (anti-mouse CD31,clone MEC 13.3, BD Pharmingen, San Jose, CA), diluted 1:25 in PBS-TX-1% BSA, followed by overnight incubation at 4°C with 1 μg/ml Alexa 488-conjugated goat anti-rat IgG (Molecular Probes) plus 1 μg/ml Hoechst 33258 in PBS-TX-1% BSA. Ovaries were mounted in aqueous mounting media between coverslips using 0.15 μm spacers to preserve depth and examined using a Zeiss LSM-510 confocal microscope with a 40x objective. In order to visualize the vascular system in areas of the cortex where follicle formation is occurring, a stack of 1 μm-thick images at intervals of 0.5 μm were obtained from the surface of the ovary through the cortex. For each ovary, 15 consecutive images, obtained from 6 to 20 μm inside the surface of the ovary, were flattened using a z-stack projection (ImageJ software, NIH). Three control and 3 mutant ovaries were examined on days 0, 2 and 4; ovaries were stained and images obtained in 3 runs, each run containing one of each day and type of ovary. Flattened images were processed and analyzed using Photoshop. Contrast and brightness were adjusted using the same settings for all ovaries stained in each run. Green fluorescence (PECAM-1) was selected using a set color definition, and the area in pixels of PECAM staining was measured and divided by the total area in pixels to determine percent PECAM staining.

Co-staining of PECAM and smooth muscle actin (SMA) was performed on frozen sections of ovaries from control and mutant mice after 48 hour of eCG

stimulation. Slides were removed from the freezer, dried in a vacuum oven, fixed in acetone at 0 ℃ for 2 minutes, and immediately transferred to PBS. Slides were blocked in 5% NGS in PBS, incubated overnight at room temperature with rat anti-mouse PECAM (anti-mouse CD31,clone MEC 13.3, BD Pharmingen, San Jose, CA) diluted 1:30 in PBS-TX-1% BSA, and rabbit anti-human SMA (ab15267, prediluted, Abcam Inc, Cambridge, MA), and followed by 2 hr incubation at room temperature with 1 μg/ml Alexa 488-conjugated goat anti-rat IgG, and Alexa 555-conjugated goat anti-rabbit IgG (Molecular Probes) plus 1 μg/ml Hoechst 33258 in PBS-TX-1% BSA.

For whole mount co-staining of SHH and CYP17A, ovaries were fixed, stored, rehydrated and permeabilized as above for whole mount staining of PECAM-1. Ovaries were blocked in PBS-TX-1% BSA and incubated overnight at 4°C with rabbit anti-mouse CYP17A and goat anti-rabbit SHH (sc-1194, Santa Cruz Biotechnology, Santa Cruz, CA), used at 1:200 dilution and 8 μg/ml, respectively. Alexa goat anti-rabbit 549 and Alexa donkey anti-goat 488 were used as second antibodies, and Hoechst 33258 was used for counter-staining. CYP17A and SHH expression in ovaries were examined using a Zeiss LSM-510 confocal microscope.

Multiple staining solution was used on a section adjacent to the section used for CYP17A staining according to the manufacturer's instructions (Polysciences, Warrington, PA).

Assessment of oocyte degeneration and the number of primordial follicles

Total oocytes and degenerating oocytes were counted in images of H&E-stained sections. Four slides containing 8 tissue sections/slide were prepared from ovaries of 3 control and 3 mutant mice at 17.5 dpc, and at 0, 2, 4 and 8 days of age. Digital images at 100x magnification were obtained of regions of the cortex in every 5^{th} section to obtain a total of 6 regions for each ovary. The morphological criteria used for assessing oocyte degeneration were described previously in detail (Beaumont & Mandl, 1961). Briefly, an oocyte was classified as degenerating if it had one or more features including condensed nuclei, pinkish eosinophilic cytoplasm, or if it was surrounded by red blood cells.

To determine the number of primordial follicles in ovaries of 24 day-old mice, serial H&E-stained sections were prepared from ovaries of 3 control and 3 mutant mice and analyzed using the method described here. Primordial follicles with a visible oocyte nucleus were counted in every 4th section under 100x magnification. The formula used to calculate the total number of primordial follicles in an ovary was: Total number of primordial follicles counted x (number of sections from an ovary that were counted/number of sections spanned by an oocyte). The number of sections spanned by an oocyte was determined by dividing the average diameter of the oocyte nucleus in a primordial follicle (12 μm, based on measurement of 12 primordial follicles) by the thickness of the section (5 μm).

Quantitative assessment of growing follicles

The percentage of growing follicles that contained more than one oocyte

(multiple oocyte follicles, MOF) and the percentage of growing follicles that were atretic were determined in ovaries of 3 control and 3 mutant mice at 16 days of age. Four H&E-stained slides containing 8 sections/slide were prepared from one ovary of each mouse. Images at 20x magnification were obtained of every growing follicle in each section (primary follicle or later stage of development) in which the oocyte nucleus was visible. Follicles were classified as atretic or healthy using a weighted scoring system as described previously (Boyer *et al*., 2010). Primary characteristics were: 1) presence of pycnotic granulosa cells; 2) loss of attachment of granulosa cells to the oocyte or loss of the cumulus cells; 3) presence of leukocytes; 4) presence of a misshaped, segmented or discolored oocyte or an oocyte with a condensed nucleus. Secondary characteristics were: 1) presence of vacuolated granulosa cells; 2) sparse granulosa cells; 3) presence of gaps in the basement membrane. Between 100 to 200 follicles from each ovary were scored.

Statistical analysis

Concentrations of mRNA in whole ovaries, density of theca capillary network, and oocyte degeneration data were analyzed by randomized (simple) two-way ANOVA. Concentrations of mRNA were log transformed prior to ANOVA. Student-Newman-Keuls test was used to compare individual means if ANOVA indicated overall significance. All other data were analyzed by unpaired t-test.

Results

Expression of SMOM2-YFP fusion protein

CRE-mediated recombination in ovaries of *Amhr2*$^{cre/+}$*SmoM2* mutant mice was assessed by detection of the SMOM2-YFP fusion protein by confocal microscopy of whole mount tissue. YFP was detected throughout the ovaries of mutant mice on day 2 of age. Signal was not detectable in *Amhr2*$^{+/+}$ *SmoM2* control mice (Fig. 3.1). These findings are in agreement with previous results using flow cytometry, in which 38% of cells from ovaries of newborn mutant mice were positive for YFP (Ren et al., 2009).

Levels of mRNA for genes within the HH signaling pathway

The levels of mRNA for genes within the HH pathway were determined during the first several weeks of age in the ovaries of control and mutant mice using real-time RT-PCR (Fig. 3.2). In *Amhr2*$^{+/+}$*SmoM2* control mice, expression of two of the HH ligands, *Dhh* and *Ihh*, increased soon after birth (day 0). Expression of *Dhh* increased between 17.5 dpc and day 0, continued to increase over time and remained elevated at day 16 of age. The pattern of expression of *Ihh* was similar except that expression increased slightly later, by day 2. The pattern of expression of *Shh* differed from that of *Dhh* and *Ihh* in that it decreased between 17.5 dpc and day 2 and remained at basal levels until day 8. Notably, mRNA of *Shh* was not detected until a great number of cycles of signal amplification (37~38 cycles in control mice), suggesting *Shh* mRNA may be present at a minimal level in the ovaries of control

mice. Genes for which transcription is known to be increased in response to HH signaling include *Gli1*, *Ptch1* and *Hhip* (Ingham & McMahon, 2001). *Gli1* and *Ptch1* increased by day 2 and *Hhip* increased by day 4 of age. Expression of *Gli2*, which is a major effector of HH signaling, increased by day 2 and remained elevated. Expression of *Gli3* and *Smo* remained relatively constant from 17.5 dpc through day 16.

In ovaries of *Amhr2*$^{cre/+}$*SmoM2* mutant mice, there were no major differences in expression of *Dhh* and *Ihh* compared to controls. In contrast, levels of *Shh* mRNA were dramatically elevated in ovaries of mutant mice compared to controls from 17.5 dpc through day 12. Levels of mRNA for genes that are transcriptional targets of HH signaling were increased in ovaries of mutant mice compared to controls between 17.5 dpc and day 0 (*Gli1*) or between 17.5 dpc and day 4 (*Ptch1* and *Hhip*). Thus, expression of these HH target genes, which increased in ovaries of control mice between day 0 and day 4 of age, was prematurely elevated in ovaries of mutant mice. Expression of *Gli2* was also elevated in ovaries of mutant mice during the neonatal time period and this was significant on day 0. Expression of *Gli3* and *Smo* did not differ in mutants and controls at each time point examined; however, the overall group mean for *Smo* mRNA levels in ovaries of mutant mice was significantly elevated compared to controls across all time points examined (<0.05).

Localization of cells expressing mRNA of Gli1, Ptch1 and Hhip

In situ hybridization showed the location of cells expressing mRNA of *Gli1*,

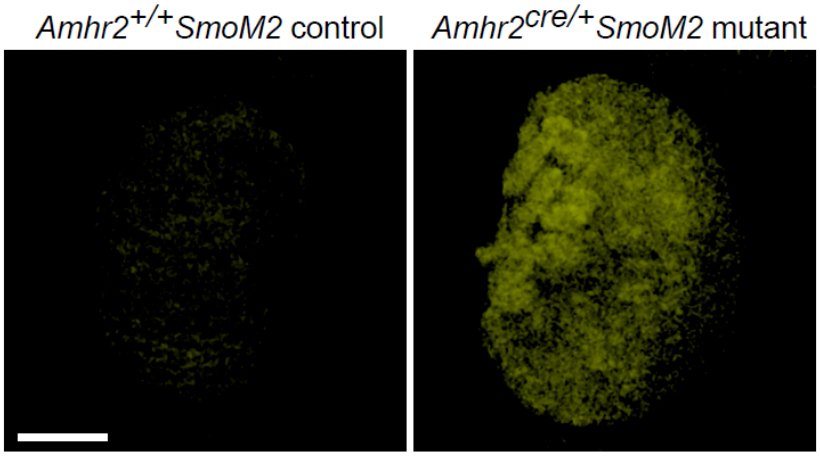

Fig.3.1. Expression of the *SmoM2-YFP* fusion gene in the ovaries of *Amhr2*$^{+/+}$ *SmoM2* control and *Amhr2*$^{cre/+}$*SmoM2* mutant mice. Ovaries were collected from mice at 2 days of age and examined using confocal microscopy. Scale bar represents 200μm. Images are representative of ovaries from two controls and two mutants.

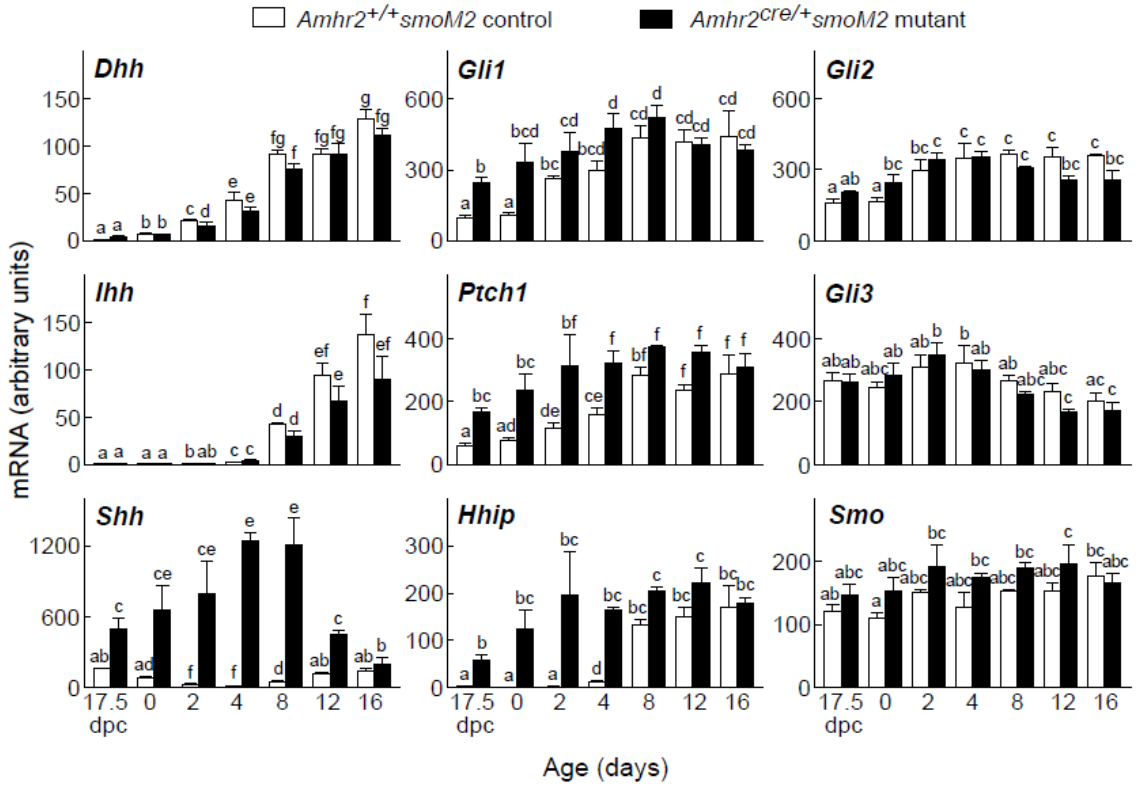

Fig.3.2. Expression of genes in the HH signaling pathway in whole ovaries of *Amhr2*$^{+/+}$ *SmoM2* control and *Amhr2*$^{cre/+}$*SmoM2* mutant mice. Ovaries were collected from mice at 17.5 dpc, and at days 0, 2, 4, 8, 12, and 16 of age. At each age ovaries from multiple mice were pooled to obtain sufficient quantities of RNA (3 mice at 17.5 dpc and at days 0, 2 and 4 of age; 2 mice at days 8, 12 and 16 of age). Total RNA was assayed by quantitative real-time RT-PCR. Data are mean ± SEM of assays performed on three RNA preparations. Within each panel, bars without common superscripts are significantly different ($P<0.05$).

Ptch1 and *Hhip* on the day of birth (Fig. 3.3). For *Gli1*, while low level of mRNA was present in the medullary region and the border region between the cortex and medulla of ovaries from control mice, mRNA appeared to be expressed at higher levels in these regions of the ovaries from mutant mice. For *Ptch1*, while low levels of mRNA were present in the cortex and little in the medulla of the ovaries from control mice, mRNA appeared to be expressed at higher levels in the cortex and medulla region of the ovaries from mutant mice. *Hhip* mRNA levels were minimal in the ovaries from control mice at this age but were considerable in the medullary region of ovaries from mutant mice (Fig. 3.2).

Microarray analysis

Microarray analysis of gene expression was performed on RNA prepared from ovaries of *Amhr2*$^{cre/+}$*SmoM2* mutant and control mice on day 2 of age in order to obtain insight into pathways altered by dominant activation of HH signaling. 416 transcripts representing 345 genes were expressed at least 2-fold higher in mutants compared to controls and 189 transcripts representing 180 genes were expressed at least 2-fold lower in mutants compared to controls. DAVID cluster analysis (Dahm-Kahler et al, 2006) of Biological Process terms from the Gene Ontology Consortium (Ashburner et al, 2000) was used to identify related groups of Biological Process terms that were over-represented (enriched) among the genes that were 2-fold higher in mutants compared to controls. Five highly enriched clusters of terms, with enrichment scores > 3.0, were identified and are shown in Table 3.2. The five

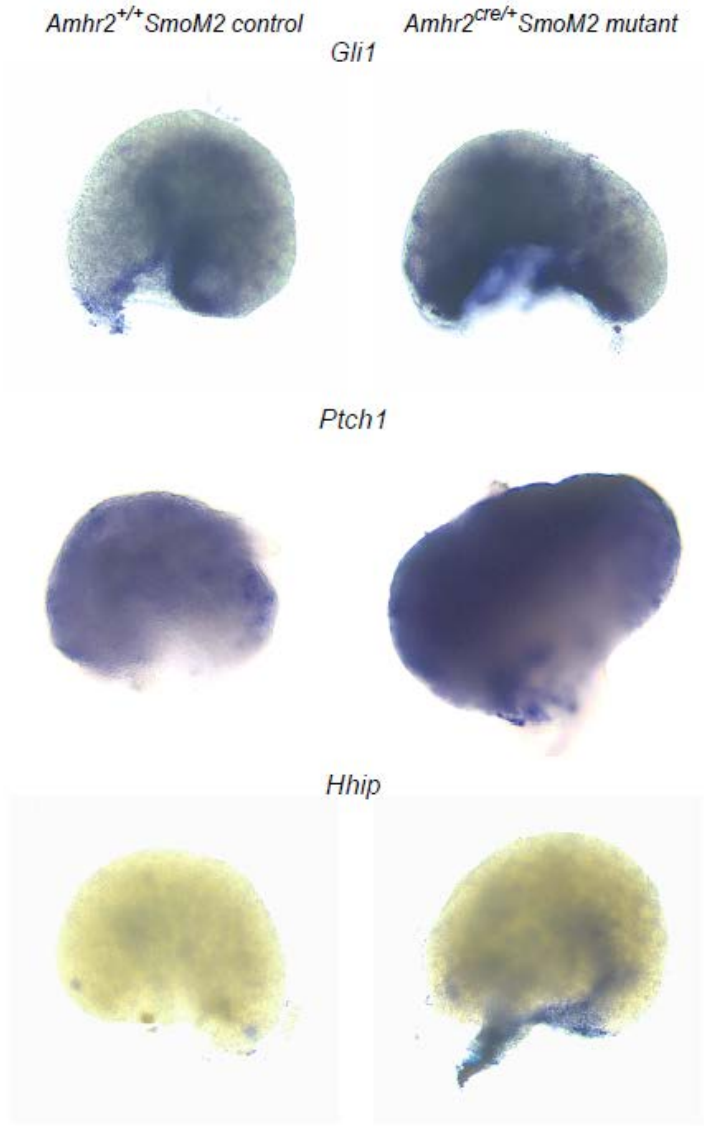

Fig.3.3. In situ hybridization for *Gli1*, *Ptch1* and *Hhip* in ovaries from *Amhr2*$^{+/+}$ *SmoM2* control and *Amhr2*$^{cre/+}$*SmoM2* mutant mice on day 0. All images are oriented with the medulla at the bottom. Images are representative of ovaries from at least two control and two mutants.

clusters were termed by the authors as hormone regulation, tube development, respiratory tube development, steroid production and vascular development. Examination of the genes that were expressed 2-fold higher in mutants and whose annotations included the Biological Process terms within each cluster showed that hormone regulation and steroid production were closely related; 10 of the 14 genes associated with hormone regulation were also associated with steroid production. The 28 genes associated with these two clusters are shown in Table 3.3. Similarly, the remaining 3 clusters were also closely related. All of the 21 genes associated with respiratory tube development were also associated with tube development, while 10 of the 16 genes associated with vascular development were also associated with tube development. The 38 genes that were associated with tube and vascular development and that were elevated at least 2-fold in mutants compared to controls are shown in Table 3.4. Among genes associated with vascular/tube development that were >2-fold higher in the mutants, some are involved in the formation of vascular network, and some are involved in interaction between endothelial cells and their surrounding mesenchymal cells (Table 3.5). When DAVID analysis was applied to genes whose mRNA levels were decreased 2-fold or more in mutants, only a single cluster of terms had an enrichment score > 3.0; this cluster was termed gamete development by the authors. Biological Process terms associated with this gamete development cluster are shown in Table 3.6, and genes with these terms in their annotations that were expressed 2-fold lower in mutants compared to controls are shown in Table 3.7.

Table 3.2. Results of DAVID analysis showing clusters of Biological Process terms associated with genes that were expressed at higher levels in ovaries of *Amhr2*$^{cre/+}$*SmoM2* mutant mice compared to *Amhr2*$^{+/+}$*SmoM2* control mice[a]

Gene Ontology Biological Process Term[b]	Significance (p)
Annotation Cluster 1 : Hormone regulation; enrichment score 6.73	
hormone metabolic process	$5.7x10^{-8}$
cellular hormone metabolic process	$2.7x10^{-7}$
regulation of hormone levels	$4.1x10^{-7}$
Annotation Cluster 2 : Tube development ; enrichment score 4.59	
tube development	$4.6x10^{-8}$
epithelium development	$3.4x10^{-7}$
morphogenesis of an epithelium	$4.2x10^{-7}$
tube morphogenesis	$2.0x10^{-6}$
morphogenesis of a branching structure	$2.1x10^{-6}$
branching morphogenesis of a tube	$5.5x10^{-6}$
tissue morphogenesis	$2.2x10^{-5}$
epithelial tube morphogenesis	$2.7x10^{-5}$
gland morphogenesis	$7.0x10^{-4}$
gland development	$7.6x10^{-4}$
urogenital system development	$4.4x10^{-3}$
regulation of cell proliferation	$3.5x10^{-1}$
Annotation Cluster 3 : Respiratory tube development ; enrichment score 4.24	
tube development	$4.6x10^{-8}$
respiratory system development	$3.5x10^{-4}$
lung development	$7.8x10^{-4}$
respiratory tube development	$8.8x10^{-4}$
Annotation Cluster 4 : Steroid production; enrichment score 3.92	
steroid biosynthetic process	$3.6x10^{-9}$
steroid metabolic process	$1.6x10^{-7}$
lipid biosynthetic process	$1.3x10^{-5}$
sterol metabolic process	$4.1x10^{-4}$
cholesterol metabolic process	$1.5x10^{-3}$
isoprenoid metabolic process	$1.7x10^{-3}$
sterol biosynthetic process	$1.8x10^{-3}$
cholesterol biosynthetic process	$7.4x10^{-3}$
isoprenoid biosynthetic process	$5.7x10^{-2}$

Annotation Cluster 5 : Vascular development; enrichment score 3.25	
blood vessel development	$2.9x10^{-5}$
vasculature development	$3.9x10^{-5}$
blood vessel morphogenesis	$2.8x10^{-3}$
angiogenesis	$3.1x10^{-2}$

[a] Genes expressed at least 2-fold higher in mutant ovaries compared to controls, as determined by microarray, were analyzed by DAVID analysis. Only clusters with an enrichment score > 3.0 are shown.

[b] Biological Process terms are from the Gene Ontology Consortium database.

Table 3.3. Genes associated with hormone regulation and steroid production that were expressed at higher levels in ovaries of *Amhr2*$^{cre/+}$*SmoM2* mutant mice compared to *Amhr2*$^{+/+}$*SmoM2* control mice[a]

Gene	Name	Fold[b]	Cluster[c]
Cyp17a1	cytochrome P450, family 17, subfamily a, polypeptide 1	73.89	H,S
Cyp11a1	cytochrome P450, family 11, subfamily a, polypeptide 1	61.58	H,S
Adh1	alcohol dehydrogenase 1 (class I)	39.56	H,S
Star	steroidogenic acute regulatory protein	13.20	H,S
Shh	sonic hedgehog	9.25	H,S
Ren1 /// Ren2	renin 1 structural /// renin 2 tandem duplication of Ren1	7.75	H
Scarb1	scavenger receptor class B, member 1	4.89	H,S
Hsd3b1	hydroxy-delta-5-steroid dehydrogenase, 3 beta- and steroid delta-isomerase 1	3.97	S
Sult1e1	sulfotransferase family 1E, member 1	3.90	H,S
Ddo	D-aspartate oxidase	3.89	H
Fabp3	fatty acid binding protein 3, muscle and heart	3.66	S
Cyp11b1	cytochrome P450, family 11, subfamily b, polypeptide 1	3.59	H,S
Idi1	isopentenyl-diphosphate delta isomerase	3.55	S
Scd1	stearoyl-Coenzyme A desaturase 1	3.52	S
Fads2	fatty acid desaturase 2	3.45	S
Sc4mol	sterol-C4-methyl oxidase-like	3.11	S
Cyp51	cytochrome P450, family 51	3.05	S
Agt	ensinogen (serpin peptidase inhibitor, clade A, member 8)	2.75	H
Aldh1a3	aldehyde dehydrogenase family 1, subfamily A3	2.75	H,S
Cyp26b1	cytochrome P450, family 26, subfamily b, polypeptide 1	2.61	H,S
Cyp21a1	cytochrome P450, family 21, subfamily a, polypeptide 1	2.40	S
Fads1	fatty acid desaturase 1	2.35	S
Elovl6	ELOVL family member 6, elongation of long chain fatty acids (yeast)	2.32	S
Tbx3	T-box 3	2.32	H
Hmgcr	3-hydroxy-3-methylglutaryl-Coenzyme A reductase	2.31	S
Lss	lanosterol synthase	2.26	S
Ldlr	low density lipoprotein receptor	2.17	S
Hmgcs1	oxy-3-methylglutaryl-Coenzyme A synthase 1 /// similar to Hmgcs1 protein	2.03	S

[a] Levels of mRNA expression were determined by microarray analysis. Biological Process terms associated with hormone regulation and steroid production are shown in Table 3.2; genes listed here have at least one of those terms included in their annotation.

[b] Fold increase in level of expression in mutants compared to controls.

[c] Cluster designation indicates: H, hormone regulation; S, steroid production. Designation with these letters indicates that the gene's annotation includes at least

one of the Biological Process terms associated with the respective cluster. Clusters are shown in Table 3.2.

Table 3.4. Genes associated with tube development and vascular development that were expressed at higher levels in ovaries of *Amhr2*$^{cre/+}$*SmoM2* mutant mice compared to *Amhr2*$^{+/+}$*SmoM2* control mice[a]

Gene	Name	Fold[b]	Cluster[c]
Hhip	Hedgehog-interacting protein	50.38	T
Shh	sonic hedgehog	9.25	T,V
Ren1 /// Ren2	renin 1 structural /// renin 2 tandem duplication of Ren1	7.75	T
Foxf1a	forkhead box F1a	6.02	T,V
Hk2	hexokinase 2	5.30	T
Enpep	glutamyl aminopeptidase	4.93	V
Prlr	prolactin receptor	4.57	T
Crispld2	cysteine-rich secretory protein LCCL domain containing 2	4.03	T
Tbx18	T-box18	3.70	T
Figf	C-fos induced growth factor	3.58	T,V
Ntrk2	neurotrophic tyrosine kinase, receptor, type 2	3.08	V
Angpt2	angiopoietin 2	2.97	V
Ptch1	patched homolog 1	2.84	T
Agt	angiotensinogen (serpin peptidase inhibitor, clade A, member 8)	2.75	T,V
Aldh1a3	aldehyde dehydrogenase family 1, subfamily A3	2.75	T
Nrp1	neuropilin 1	2.68	T,V
Ntn1	similar to Netrin-1 precursor /// netrin 1	2.49	T
Osr2	odd-skipped related 2 (Drosophila)	2.48	T
Ccl11	chemokine (C-C motif) ligand 11	2.48	T
Cxcr4	chemokine (C-X-C motif) receptor 4	2.47	T,V
Mef2c	myocyte enhancer factor 2C	2.47	V
Lox	lysyl oxidase	2.44	T,V
Adm	adrenomedullin	2.39	T
Gdnf	glial cell line derived neurotrophic factor	2.34	T
Ppap2b	phosphatidic acid phosphatase type 2B	2.33	V
Tbx3	T-box 3	2.32	T,V
Fzd2	frizzled homolog 2 (Drosophila)	2.30	T
Gja1	gap junction protein, alpha 1	2.27	T,V
Zeb2	zinc finger E-box binding homeobox 2	2.24	T
Igf1	insulin-like growth factor 1	2.23	T
Pdgfra	platelet derived growth factor receptor, alpha polypeptide	2.19	T
Sfrp1	secreted frizzled-related protein 1	2.17	T
Ctgf	connective tissue growth factor	2.15	T,V
Lipa	lysosomal acid lipase A	2.15	T
Wnt5a	wingless-related MMTV integration site 5A	2.14	T

Gpc3	glypican 3	2.09	T
Col1a1	collagen, type I, alpha 1	2.08	V
Hoxa9	homeo box A9	2.02	T

[a] Levels of mRNA expression were determined by microarray analysis. Biological Process terms associated with tube development and vascular development are shown in Table 3.2; genes listed here have at least one of those terms included in their annotation.

[b] Fold increase in level of expression in mutants compared to controls.

[c] Cluster designation indicates: T, tube development; V, vascular development. Designation with these letters indicates that the gene's annotation includes at least one of the Biological Process terms associated with the respective cluster. Clusters are shown in Table 3.2.

Table 3.5. Categories of genes involved in vascular development based on their major function in the development of blood vessels[a]

Formation of vascular networks	References
Figf	Marconcini *et al*., 1999; Girling *et al*., 2010
Cxcr4	Salcedo *et al*., 1999; Mirshahi *et al*., 2000; Salvucci *et al*., 2002
Nrp1	Gu *et al*., 2003; Gerhardt *et al*., 2004; Pan *et al*., 2007
Ctgf	Markiewicz *et al*., 2011; Shimo *et al*., 2001
Endothelial-mesenchymal cell interaction	
Foxf1a	Kalinichenko *et al*., 2001; Astorga and Carlsson 2007
Angpt2	Thomas and Augustin, 2009
Mef2c	Lin *et al*., 1998; Bi *et al*., 1999
Ntrk2	Donovan et al., 2000

[a] Genes involved in vascular development were identified by cluster analysis of genes >2-fold higher in the ovaries of mutant mice compared to controls.

Table 3.6. Results of DAVID analysis showing the cluster of Biological Process terms associated with genes that were expressed at lower levels in ovaries of *Amhr2*$^{cre/+}$*SmoM2* mutant mice compared to *Amhr2*$^{+/+}$*SmoM2* control mice[a]

Gene Ontology Biological Process Term[b]	Significance (p)
Annotation Cluster 1: Gamete development; Enrichment Score: 3.06	
reproductive developmental process	6.40×10^{-5}
multicellular organism reproduction	1.40×10^{-4}
reproductive process in a multicellular organism	1.40×10^{-4}
germ cell development	1.80×10^{-4}
sexual reproduction	3.40×10^{-4}
gamete generation	4.00×10^{-4}
reproductive cellular process	5.70×10^{-4}
male gamete generation	1.20×10^{-3}
spermatogenesis	1.20×10^{-03}
spermatid development	8.50×10^{-02}
spermatid differentiation	$9.50 \times 10\text{-}^{02}$

[a] Genes expressed at least 2-fold lower in mutant ovaries compared to controls, as determined by microarray, were analyzed by DAVID analysis. Only clusters with an enrichment score > 3.0 are shown.

[b] Biological Process terms are from the Gene Ontology Consortium database.

Table 3.7. Genes associated with gamete development that were expressed at lower levels in ovaries of *Amhr2*$^{cre/+}$*SmoM2* mutant mice compared to *Amhr2*$^{+/+}$*SmoM2* control mice[a]

Gene	Name	Fold[b]
Dazl	deleted in azoospermia-like	-2.67
Bbs4	Bardet-Biedl syndrome 4 (human)	-2.58
Taf7l	TAF7-like RNA polymerase II, TATA box binding protein (TBP)-associated factor	-2.52
Amhr2	anti-Mullerian hormone type 2 receptor	-2.44
Tdrd1	tudor domain containing 1	-2.37
Sohlh1	spermatogenesis and oogenesis specific basic helix-loop-helix 1	-2.19
Ube3a	ubiquitin protein ligase E3A	-2.19
Txnrd3	thioredoxin reductase 3	-2.16
Mov10l1	Moloney leukemia virus 10-like 1	-2.14
Asz1	ankyrin repeat, SAM and basic leucine zipper domain containing 1	-2.10
Med1	mediator complex subunit 1	-2.09
Ccnb1ip1	cyclin B1 interacting protein 1	-2.06

[a] Levels of mRNA expression were determined by microarray analysis. Biological process terms associated with gamete development are shown in Table 3.6. Genes listed here have at least one of those terms included in their annotation.

[b] Fold decrease in level of expression in mutants compared to controls.

Increased density of the capillary network in the ovarian cortex of mutant mice

To further investigate the finding that a class of genes enriched among those that are expressed at increased levels in ovaries of mutant mice compared to controls function in vascular development/tube formation, staining for the endothelial cell marker PECAM was performed on whole mounts of ovaries and examined by confocal microscopy. The appearance of the capillary network in stacks of confocal images was denser in the cortex region of ovaries of mutants compared to controls (Fig. 3.4A). The area of the cortex occupied by cells positive for PECAM staining was significantly elevated in mutants compared to controls on days 2 and 4 (Fig. 3.4B).

Reduced smooth muscle actin (SMA) is associated with theca vasculature in the ovaries of Amhr2$^{cre/+}$SmoM2 mutant mice

In a previous study, mRNA levels of genes expressed in smooth muscle cells were reduced in the ovaries of mutant mice, and immunohistochemistry of SMA showed that reduced SMA expression is in the thecal layer (Ren et al, 2009). At 48 hours after eCG stimulation, co-staining of PECAM-1 and SMA on ovarian sections showed intermingled localization of PECAM-1 and SMA in the theca layer in control mice but the SMA staining is significantly reduced in mutant mice (Fig. 3.5), indicating that reduced SMA is associated with thecal vasculature in ovaries of mutant mice.

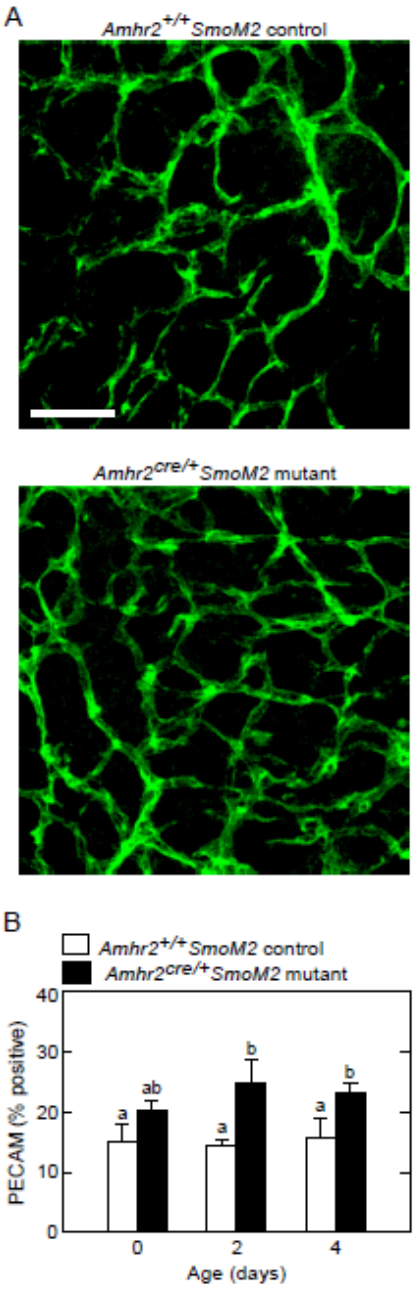
A
Amhr2+/+SmoM2 control
Amhr2cre/+SmoM2 mutant
B
Amhr2+/+SmoM2 control
Amhr2cre/+SmoM2 mutant
PECAM (% positive)
40
30
20
10
0
a
ab
a
b
a
b
0
2
4
Age (days)

Fig.3.4. Capillary density in the ovarian cortex of *Amhr2*$^{+/+}$ *SmoM2* control and *Amhr2*$^{cre/+}$*SmoM2* mutant mice. **A**) Representative whole mount immunofluorescence for PECAM-1 at 2 days of age. Scale bar represent 50 μm. Immunohistochemistry was repeated using three mice of each genotype. **B**) Quantitative comparison of density of capillaries in the ovarian cortex of *Amhr2*$^{+/+}$ *SmoM2* control and *Amhr2*$^{cre/+}$*SmoM2* mutant mice. Data are mean ± SEM for three mice. Bars without common superscripts are significantly different ($P<0.05$).

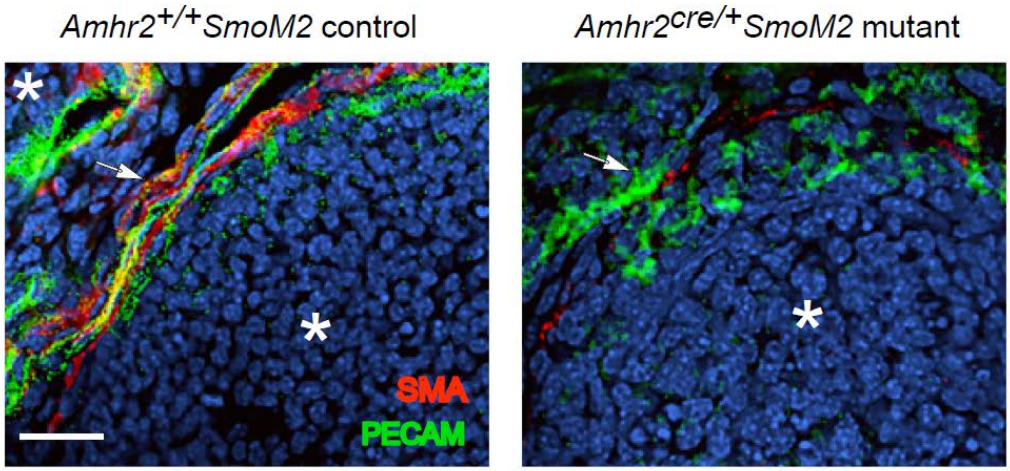

Fig.3.5. Whole-mount co-staining of PECAM-1 and SMA in the ovaries of *Amhr2*$^{+/+}$ *SmoM2* control and *Amhr2*$^{cre/+}$*SmoM2* mutant mice at 48 hours after eCG stimulation. Mice were at 21 days of age when treated with eCG. Asterisks mark granulosa cells. Arrows point to the thecal layer. Scale bar represents 50 μm. Sections were counterstained for nuclei with Hoechst 33342 (blue). Immunofluorescence was repeated using two mice of each genotype.

mRNA and protein of Star, Cyp17A, Cyp21A and Shh in the ovaries of *Amhr2$^{cre/+}$SmoM2 mutant mice*

According to the results of microarray analyses, mRNA levels for a number of genes for steroidogenic enzymes were elevated in ovaries of mutant mice compared to controls (Table 3) and are highlighted in a diagram of steroidogenic pathways in the adrenal gland and the gonad (Fig. 3.6). Among them, mRNA or protein of *Star*, *Cyp17a*, *Cyp21*a and *Shh* were analyzed in more detail. Real-time RT-PCR assays showed that in ovaries of control mice, levels of mRNA for *Star* were relatively low from 17.5 dpc through day 4, increased on day 8 and continued to rise between days 12 and 16 (Fig. 3.7A). In ovaries of mutant mice, mRNA levels of *Star* were significantly elevated from 17.5 dpc through day 8 and then became similar to levels in control ovaries on days 12 and 16.

CYP17A was not detectable by immunohistochemistry in ovaries of control mice between 17.5 dpc and day 16. In contrast, CYP17A-positive cells were present in ovaries from mutant mice and were most prominent on days 0 and 2 (Fig. 3.7B). On day 0, CYP17A-positive cells mostly localized in the medullary region while on day 2, CYP17A-positive cells were distributed in the border region between the medulla and the cortex. An enlarged image of CYP17A-postive cells shows the prominent cytoplasm typical of steroidogenic cells. Immunohistochemistry of CYP21A and CYP17A on adjacent sections indicated that the majority of CYP17A-positive cells also were positive for CYP21A. Whole-mount co-staining of CYP17A and SHH showed that while there were no cells expressing SHH in the ovaries of control mice,

there were a small number of cells in ovaries of mutant mice that expressed SHH primarily in the medullary region . SHH-positive cells in the ovaries of mutant mice were within close proximity to CYP17A-positive cells (Fig. 3.7C).

Early follicle development is altered in mutant mice

The breakdown of ovigerous cord and follicle formation are associated with a high frequency of oocyte death (Beaumont & Mandl, 1961; Pepling, 2006). Consistent with this, the percentages of oocytes that were clearly condensed and undergoing degeneration were substantial from 17.5 dpc through day 4 in *Amhr2*$^{+/+}$*SmoM2* control mice (Fig. 3.8A). The percent degenerating oocytes was higher in ovaries of control mice than in mutant mice at 17.5 dpc, and lower on day 0 (Fig. 3.8B). Counts of primordial follicles in serial sections of 24 day old mice indicated that there were 25% fewer primordial follicles in ovaries of mutant mice compared to controls (Fig. 3.8C).

During the first wave of follicle development, secondary and tertiary follicles with two or more layers of granulosa cells were observed in the ovaries of control mice as shown in ovaries of mice on 12 and 16 days of age (Fig. 3.9A). In ovaries of mutant mice, a large proportion of follicles with two layers of granulosa cells had an abnormal gap between cell layers (Fig. 3.9A), and there was a higher percentage of atretic follicles than in control mice (Fig. 3.9B). Abnormal follicles containing more than one oocyte (MOF) were present at a higher frequency in ovaries of mutant mice compared to controls (Fig. 3.9A and B). By 24 days of age, there were no obvious

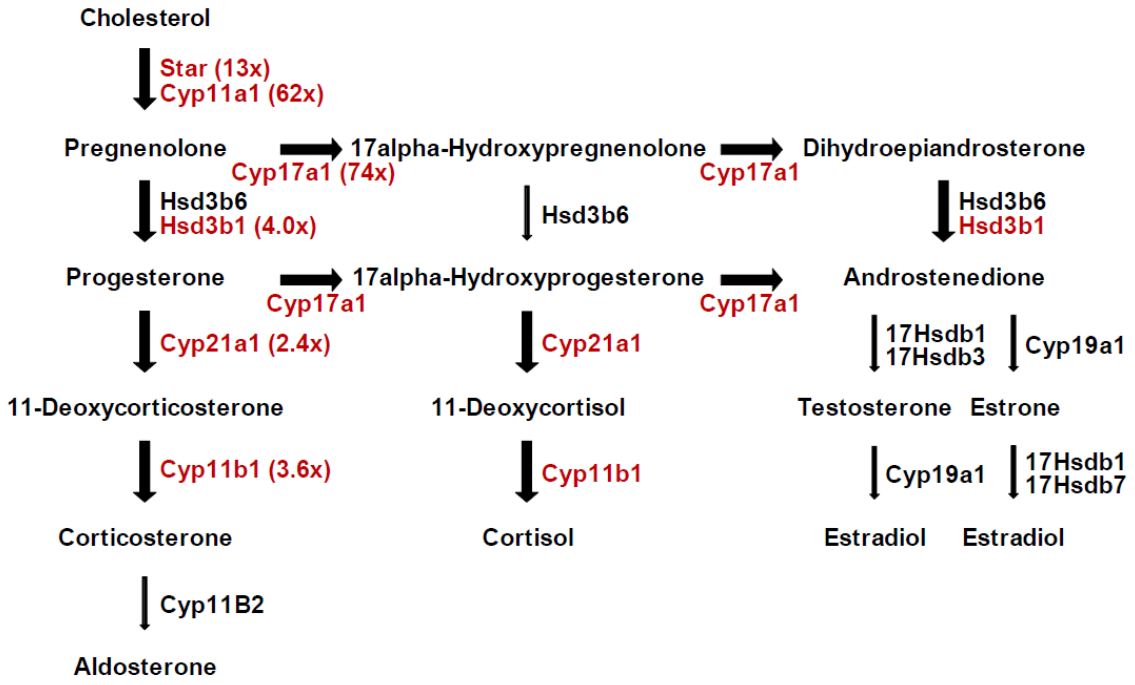

Fig. 3.6. Genes encoding key enzymes in the steroidogenic pathways in the gonad and adrenal gland. Levels of mRNA for genes highlighted in red are elevated in whole ovaries of mutant mice compared to controls based on the results of microarray analyses. The fold differences were indicated in parentheses.

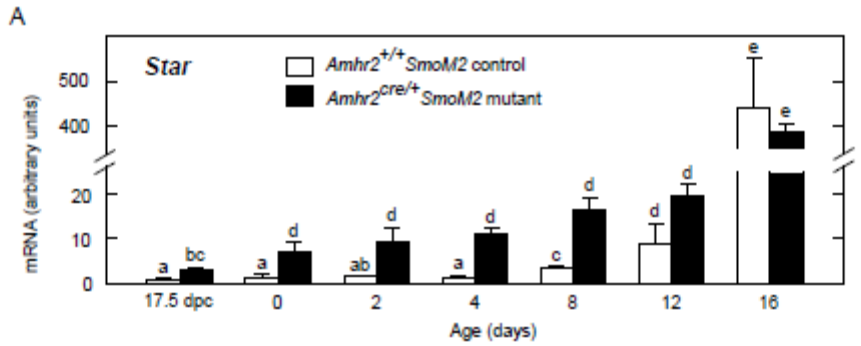

B CYP17A

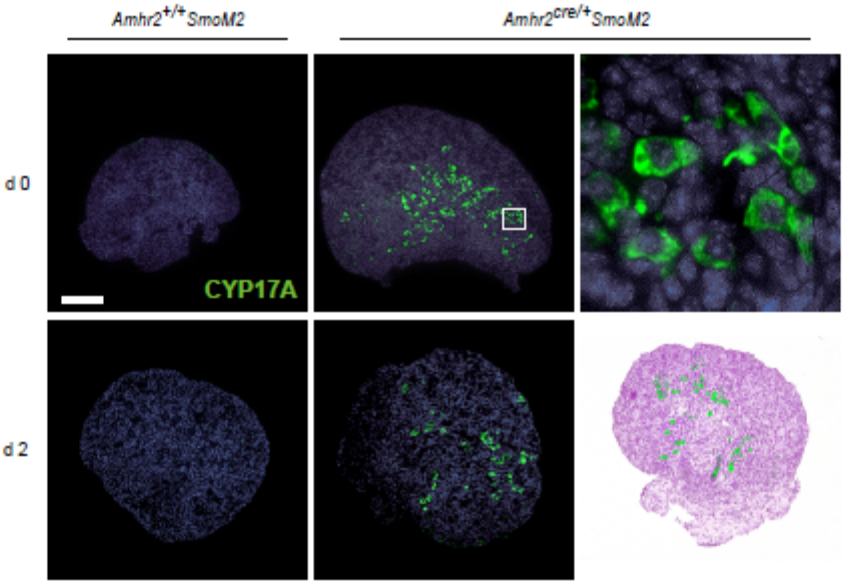

C CYP21A, CYP17A and SHH in *Amhr2*$^{cre/+}$*SmoM2*

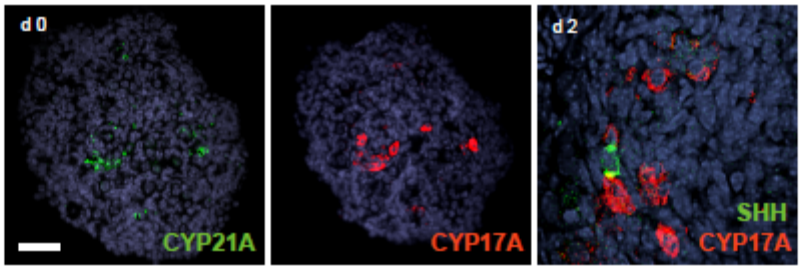

Fig. 3.7. Expression of *Star*, CYP17A, CYP21A and SHH in *Amhr2*$^{+/+}$ *SmoM2* control and *Amhr2*$^{cre/+}$*SmoM2* mutant mice. **A**) Expression of *Star* in whole ovaries. Ovaries were collected from mice at 17.5 dpc, and at days 0, 2, 4, 8, 12, and 16 of age. At each age ovaries from multiple mice were pooled to obtain sufficient quantities of RNA (3 mice at 17.5 dpc and at days 0, 2 and 4 of age; 2 mice at days 8, 12 and 16 of age). Total RNA was assayed by quantitative real-time RT-PCR. Data are mean ± SEM of assays performed on three RNA preparations. Within each panel, bars without common superscripts are significantly different ($P<0.05$). **B**) Immunofluorescence for CYP17A in ovaries of *Amhr2*$^{+/+}$ *SmoM2* control and *Amhr2*$^{cre/+}$*SmoM2* mutant mice at 0 and 2 days of age. The framed area is enlarged as the image on the right. Co-staining of CYP17A and multiple staining solution was performed on adjacent sections to show the localization of CYP17A-positive cells in the ovaries of mutant mice. All images are oriented with the medulla at the bottom. Scale bar represents 6 μm for the enlarged image and 100 μm for all the other images. Sections were counterstained for nuclei with Hoechst 33342 (blue). Immunofluorescence was repeated using more than four mice of each genotype and age and representative images are shown. **C**) Immunofluorescence for CYP21A, CYP17A and SHH. CYP21A and CYP17A staining were performed on adjacent sections of the same ovary on day 0. Co-staining of SHH and CYP17A was performed on ovaries from mice at 2 days of age. Sections were counterstained for nuclei with Hoechst 33342 (blue). Scale bar represents 50 μm for CYP21A and CYP17A, and 15 μm for co-staining of SHH and CYP17A.

differences in the histological appearance of follicles in mutant and control mice (Fig. 3.9A).

Discussion

The HH signaling pathway plays essential roles in the *Drosophila* ovary but its function in the mammalian ovary is undefined. One of the well-known and extensively studied functions of HH signaling is in regulating vascular development in multiple organs and tissues, during normal development and tumorigenesis. Multiple lines of investigation indicate that HH may exert its effect by promoting vascular outgrowth, patterning and remodeling through direct targeting of the vascular mesenchymal cells that surround the endothelial tubes. Consistent with this model, results of the present study show that levels of mRNA for genes involved in interaction between endothelial and surrounding mesenchymal cells are elevated in the ovaries of Amhr2$^{cre/+}$SmoM2 mutant mice compared to controls on day 2, and this alteration may contribute to defective maturation of thecal vasculature throughout life. Additionally, we identified a population of adrenal-like cells in ovaries of *Amhr2$^{cre/+}$SmoM2* mutant mice, providing evidence that HH signaling may be a mediator of cell sorting/migration in the adrenogonadal primordium, or alternatively, regulates differentiation of steroidogenic cells in the gonad.

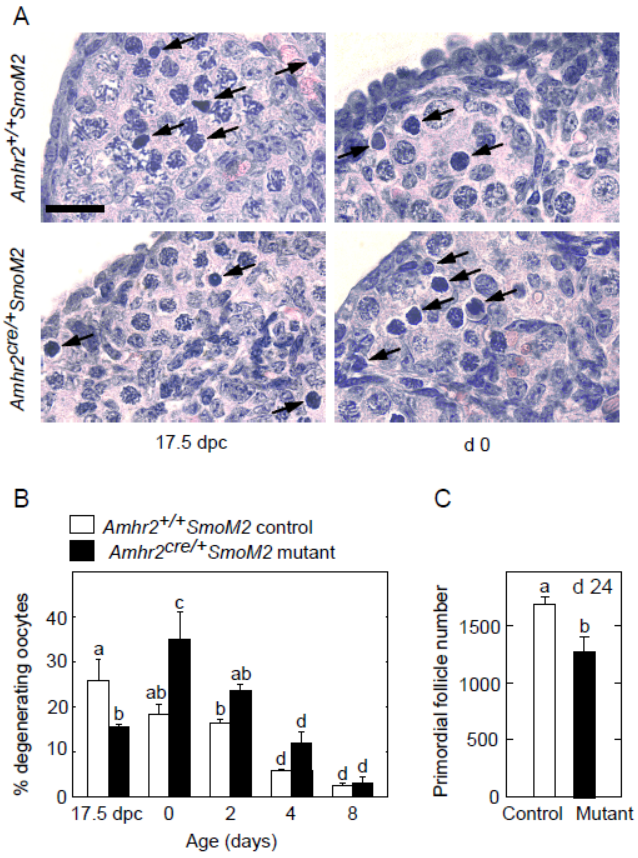

Fig.3.8. Increased degeneration of oocytes and reduced number of primordial follicles in *Amhr2*$^{cre/+}$*SmoM2* mutant mice compared to *Amhr2*$^{+/+}$ *SmoM2* controls.

A) H&E staining of representative fields of ovaries from control and mutant mice on 17.5 dpc and day 0. Arrows point to examples of degenerating oocytes. Scale bar represents 20µm. **B**) Quantification of the percentage of degenerating oocytes in the cortex. **C**) Numbers of primordial follicles counted in serial sections of ovaries of mice at 24 days of age. Data in B and C represent the mean ± SEM for 3 mice. Bars without common superscripts are significantly different ($P<0.05$).

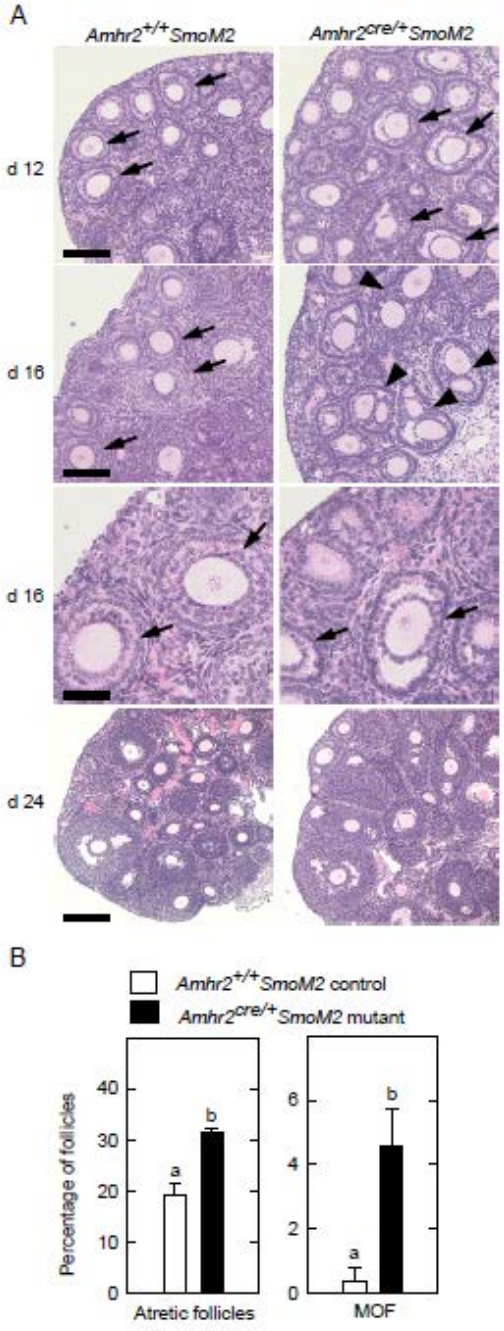
A
Amhr2+/+SmoM2
Amhr2cre/+SmoM2
d 12
d 16
d 16
d 24
B
Amhr2+/+SmoM2 control
Amhr2cre/+SmoM2 mutant
Percentage of follicles
40
30
20
10
0
a
b
Atretic follicles
6
4
2
0
a
b
MOF

Fig.3.9. Abnormal follicle morphology during the first wave of follicle development in *Amhr2*$^{cre/+}$*SmoM2* mutant mice. **A**) Representative H&E staining of ovaries from control and mutant mice. Arrows point to examples of follicles with two or more layers of granulosa cells. In mutant mice, these follicles have an abnormal gap between layers of granulosa cells. Arrowheads point to examples of MOF in *Amhr2*$^{cre/+}$*SmoM2* mutant mice. **B**) Quantification of atretic follicles and MOF as a percentage of growing follicles on day 16 of age. Data are mean ± SEM of 3 mice. Bars without common superscripts are significantly different ($P<0.05$).

Over-activation of HH signaling in Amhr2$^{cre/+}$SmoM2 mutant mice

Amhr2$^{cre/+}$SmoM2 mutant mice fail to ovulate and express reduced levels of genes typically expressed in vascular smooth muscle (Ren *et al*., 2009). In that study, we did not detect differences in HH signaling activity around the time of ovulation. Here, we have shown that in the *Amhr2$^{cre/+}$SmoM2* mutant mice, HH signaling is over-activated around the time of birth. Mutant mice have elevated levels of mRNA for HH transcriptional targets *Gli1*, *Ptch1* and *Hhip* measured using quantitative real-time PCR (Fig. 3.2), or by in situ hybridization (Fig. 3.3). In wild-type mice, components of the HH pathway are expressed in growing follicles and changes in HH signaling activity occur around the time of ovulation (Ren *et al*., 2009; Russell *et al*., 2007; Wijgerde *et al*., 2005). The function of HH signaling activity during follicle growth and the effect of changes in HH signaling activity around the time of ovulation remain to be defined. Results of the present study showed that in the neonatal ovary before the completion of follicle assembly, levels of mRNA for *Gli1*, *Ptch1* and *Hhip* gradually increased in whole ovaries of *Amhr2$^{+/+}$SmoM2* control mice, indicating a gradual increase in HH signaling activity. This signaling activity is likely due to HH ligands being produced in a small number of follicles that have transitioned to the primary stage and begun to grow in the border region between the cortex and medulla. In situ hybridization showed higher levels of mRNA for *Gli1*, *Ptch1* and *Hhip* in the medullary region and the border region between the cortex and medulla in the ovaries of mutant mice compared to controls, indicating a broad range of somatic cells with over-activated HH signaling activity in

the mutant mice. In summary, HH signaling is over-active in ovaries of *Amhr2*$^{cre/+}$*SmoM2* mutant mice compared to controls at around the time of birth.

Over-activation of HH signaling activity alters ovarian vascular development

HH ligands are potent pro-angiogenic factors during normal development and tumorigenesis (Byrd & Grabel, 2004; Nagase *et al*., 2008). Effects of HH signaling on vascular development can be achieved through targeting both endothelial cells and the vascular mesenchymal cells (vascular mural cells and the surrounding interstitum). In the present study, microarray analyses revealed that in ovaries of 2-day-old mutant mice, mRNA levels of genes recognized as critical factors promoting formation of capillary networks were elevated (Table 3.5). These genes included *Figf*, *Cxcr4*, *Nrp1*, and *Ctgf* (Gerhardt *et al*., 2004; Girling *et al*., 2010; Gu *et al*., 2003; Marconcini *et al*., 1999; Markiewicz *et al*., 2011 2001; Mirshahi *et al*., 2000; Pan *et al*., 2007; Salcedo *et al*., 1999; Salvucci *et al*., 2002). In addition, levels of mRNA for genes known to participate in endothelial-mesenchymal interaction were elevated. These gene included *Foxf1a*, *Angpt2*, *Mef2c*, and *Ntrk2* (Astorga & Carlsson, 2007; Bi *et al*., 1999; Donovan *et al*., 2000; Kalinichenko *et al*., 2001; Lin *et al*., 1998; Thomas & Augustin, 2009), in the mutants compared to controls. Moreover, PECAM-1 staining of neonatal ovaries demonstrated a capillary network of higher density in the ovarian cortex of mutants compared to controls. Co-staining of ovaries for PECAM-1 and SMA showed that in preovulatory follicles, reduced SMA

is associated with the thecal vasculature, indicating defects in vascular maturation in the ovaries of mutant mice. Based on these results, HH may promote the formation of vascular networks through targeting both endothelial cells and vascular mesenchymal cells, directly or indirectly. The results from the present study do not favor either endothelial cells or vascular mesenchymal cells as the direct target of altered HH signaling activity. However, based on the fact that expression of vascular smooth muscle genes are reduced in growing follicles of *Amhr2*$^{cre/+}$*SmoM2* mutant mice (Ren *et al*., 2009), we postulate that over-activation of HH signaling around the time of birth directly targets and affects the programming of cells destined to become vascular mesenchymal cells. Vascular mesenchymal cells are active regulators of vascular growth and remodeling (Armulik *et al*., 2005; Jain, *et al*., 2003); thus, through targeting and regulating functions of these cells, the HH signaling pathway may participate in the remodeling of ovarian vasculature during normal ovarian function and pathology.

Interestingly, major ovarian blood vessels that are not directly associated with growing follicles appear to have a normal complement of vascular mural cells. In addition, neonatal ovaries treated with cyclopamine in culture or mice with genetically reduced HH signaling activity showed a decreased number of mesenchymal cells (Quirk laboratory). Although it has not been directly tested, these mesenchymal cells may be vascular cells. These findings lead to two speculations: first, the source of VSMCs for each growing follicle is highly unlikely to be derived from the circulation but rather is likely to be generated *de novo*, such as

in the form of mesenchymal precursor cells within the ovarian interstitum (Chambers *et al*., 2003; Elenbaas & Weinberg, 2001; Hungerford & Little, 1999; Sartore *et al*., 2001; Tomasek *et al*., 2002). Second, the hypothetical mesenchymal precursor cells of VSMC in the ovary probably have self-renewal ability in order to sustain each new wave of follicle growth during the entire reproductive lifespan. In summary, our findings suggest that HH signaling may regulate the maintenance or differentiation of VSMC precursors needed for the maturation of the thecal vasculature around each growing follicles.

Over-activation of HH signaling induces the presence of adrenal-like cells in the ovary of Amhr2$^{cre/+}$SmoM2 mutant mice

Microarray analyses revealed elevated mRNA levels for genes within the steroidogenic pathways in whole ovaries of mutants compared to controls on day 2, such as *Star*, *Cyp11a1*, *Cyp17a*, *Cyp21*a, *Cyp11b1* and *Hsd3b1* (Fig. 3.6). Real-time RT-PCR analysis of the gene *Star* confirmed the results of microarray analyses (Fig. 3.7A). Immunohistochemistry indicated the presence of CYP17A/CYP21A-positive cells in the ovaries of mutant mice (Fig. 3.6B). Moreover, *Shh* mRNA and SHH protein are expressed at a significant level in the ovaries of mutant mice in a small number of cells within close proximity to the CYP17A/CYP21A-positive cells in the medullary region (Fig. 3.6C). While there is no evidence for the expression of *Shh* in the fetal or neonatal mouse ovary, *Shh* is known to be expressed in the fetal and

adult adrenal and is proposed to regulate expansion of adrenal cortical progenitor cells that are in the adrenal capsule (Ching & Vilain, 2009; Guasti *et al*., 2010; Huang et al, 2010; King *et al*, 2009). As *Shh* and *Cyp21* are normally expressed in the adrenal gland but not the ovary, our results indicate that adrenal-like cells are present in ovaries of the *Amhr2*$^{cre/+}$*SmoM2* mutant mice around the time of birth.

The presence of adrenal-like cells in the fetal ovary was observed in *Wnt4* knockout mice and in *β-catenin* conditional knockout mice created using steroidogenic factor 1/Cre (SF1/Cre) (Heikkila *et al*., 2002; Liu *et al*., 2009). The authors of these two papers provided evidence that the WNT4/β-catenin pathway may regulate migration and/or sorting of adrenal and gonadal cells. The adrenal gland and gonad share the same origin: the adrenogonadal primordium (Huang *et al*., 2010). Shortly after the expression of *SF1* is switched on at 9.5 dpc (Ikeda *et al*, 1994), an unknown mechanism induces specification of SF1-positive cells as adrenal or gonadal cells, and the fetal adrenal and fetal gonad diverge from the adrenogonadal primordium around 11- 12 dpc (Hatano *et al*., 1996). Expression of *Gli1* and *Gli2* was detected in the gonad/mesonephros complex from 11.5-13.5 dpc (Pazin & Albrecht, 2009), and the investigators hypothesized that HH signaling may be active in the diverging adrenogonadal primordium. The presence of adrenal-like cells in the ovary of *Amhr2*$^{cre/+}$*SmoM2* mutant mice supports this hypothesis and suggests that HH signaling may be involved in migration or/and sorting of cells in the adrenogonadal primordium.

An alternative explanation for the presence of adrenal-like cells in the ovary of mutant mice is that expression of dominant active SMOM2 induced differentiation of ovarian cells into adrenal type cells. Steroidogenic cells of the adrenal cortex and the gonad share common precursors, the SF1-positive cells in the adrenogonadal primordium. While the fetal ovary remains quiescent for steroidogenesis, DHH secreted from Sertoli cells induces steroidogenic differentiation of Leydig cells in the fetal testis (Bitgood *et al*., 1996). In the fetal adrenal gland, SHH secreted from the adrenal cortex induces expression of *Gli1* and *Ptch1* in the capsule cells surrounding the gland (Ching & Vilain, 2001; Guasti *et al*., 2010; Huang *et al*., 2010; King *et al*., 2009). These cells then proliferate, migrate centripetally into the adrenal cortex, and further differentiate into steroidogenic cells as well as give rise to new SHH-producing cells. Accordingly, expression of *SmoM2* in the ovary may induce expression of *Gli1* and *Ptch1* as well as differentiation of ovarian cells into adrenal-like cells in a cell-autonomous manner. In turn, cells expressing *Gli1* and *Ptch1* might proliferate and differentiate into steroidogenic cells, and give rise to a small number of SHH-positive cells. This model is based on the assumption that there is a progenitor cell population in the fetal ovary that has the potential to differentiate into adrenal type steroidogenic cells upon certain stimulation, such as HH signaling. The same population of progenitor cells in the fetal ovary may also contain the precursor for steroidogenic theca cells. However, further studies are needed to test this hypothesis.

One previous study concluded that abnormal activation of HH signaling in the embryonic ovary induces differentiation of Leydig cells (Barsoum *et al*., 2009). In mice expressing the *YFP-SmoM2* fusion gene under the regulation of the *SF-1* promoter in the ovary, expression of *Gli1*, *Cyp17, Insl3* and *Hsd3b* were detected in the fetal ovary, and the mice had partial female-to-male sex reversal as indicated by the presence of Wolffian duct derivatives and descent of the gonads into the abdominal cavity. In the study by Barsoum *et al*., expression of *Gli1*, *Cyp17a*, and *Hsd3b* do not validate the presence of Leydig cells since these genes are also expressed in the fetal adrenal (Heikkila *et al*., 2002). In the same study, it is not reported whether CYP17A-positive cells also expressed adrenal markers such as CYP21A or CYP11B1. In the current study, adrenal-like cells are present in the ovaries of *Amhr2*$^{cre/+}$*SmoM2* mutant mice and there are no apparent signs of masculinization of the reproductive tract in mutant mice. The *SF1* promoter is active in the adrenogonadal primordium but not the mesonephros beginning between 9.5 to 10.5 dpc and continuing until 13.5 to 16.5 dpc (Ikeda *et al*., 1994), while the *Amhr2* promoter is active in the somatic cells of the gonads and the mesenchymal cells of the Mullerian duct beginning at about 11.5 dpc (Jamin *et al*.,2002). Thus, differences in the timing and location of CRE activity may contribute to the different effects of *SmoM2* expression. In the current study, because levels of mRNA for *Hsd3b1* and *Cyp17A*, and levels of mRNA for genes of enzymes needed for the production of corticosterone and cortisol are elevated, assays directly measuring steroid levels in serum or ovarian tissue are needed to conclude whether the levels of

testosterone, estradiol, corticosterone and cortisol are elevated in the mutant mice compared to controls. On balance, more detailed characterization is needed to explain the similarities and differences in phenotypes observed in these two studies.

The increased rate of oocyte degeneration and the abnormal first wave of follicular development in the mutant mice compared to controls might be the result of the abnormal vascular development, the presence of ectopic SHH-positive cells, or potentially abnormal levels of steroids produced by the CYP17A/CYP21A-positive cells in the ovaries of mutant mice. The abnormal development of the first wave of follicles may be associated with altered vascular development in the ovaries of mutant mice; alternatively it may be a secondary effect of excessive oocyte death in the ovaries of mutant mice.

In summary, the present study uncovered a potential regulatory role of HH signaling in the development of the ovarian vasculature, in particular the maturation of thecal vasculature. We also identified adrenal-like cells in the ovaries of mice with dominantly active HH signaling, suggesting that HH signaling may be involved in cell migration or/and sorting in the adrenogonadal primordium, or alternatively, that HH signaling is involved in the differentiation of steroidogenic cells in the gonad.

Acknowledgement

We thank Dr. Richard R. Behringer, University of Texas M.D. Anderson Cancer Center, Houston Texas, for providing *Amhr2*$^{cre/+}$ mice. I thank Robert Cowan for advice and help in experimental procedures used for work reported in this chapter,

and Fernando Migone for performing the in situ hybridization procedure.

References

Acosta TJ, Gastal EL, Gastal MO, Beg MA, Ginther OJ (2004) Differential blood flow changes between the future dominant and subordinate follicles precede diameter changes during follicle selection in mares. *Biol Reprod* **71:** 502-507

Armulik A, Abramsson A, Betsholtz C (2005) Endothelial/pericyte interactions. *Circ Res* **97:** 512-523

Asai J, Takenaka H, Kusano KF, Ii M, Luedemann C, Curry C, Eaton E, Iwakura A, Tsutsumi Y, Hamada H, Kishimoto S, Thorne T, Kishore R, Losordo DW (2006) Topical sonic hedgehog gene therapy accelerates wound healing in diabetes by enhancing endothelial progenitor cell-mediated microvascular remodeling. *Circulation* **113:** 2413-2424

Ashburner M, Ball CA, Blake JA, Botstein D, Butler H, Cherry JM, Davis AP, Dolinski K, Dwight SS, Eppig JT, Harris MA, Hill DP, Issel-Tarver L, Kasarskis A, Lewis S, Matese JC, Richardson JE, Ringwald M, Rubin GM, Sherlock G (2000) Gene ontology: tool for the unification of biology. The Gene Ontology Consortium. *Nat Genet* **25:** 25-29

Astorga J, Carlsson P (2007) Hedgehog induction of murine vasculogenesis is mediated by Foxf1 and Bmp4. *Development* **134:** 3753-3761

Barsoum IB, Bingham NC, Parker KL, Jorgensen jS, Yao HHC (2009) Activation of the hedgehog pathway in the mouse fetal ovary leads to ectopic appearance of fetal leydig cells and female pseudohermaphroditism. *Developmental Biology* **329:** 96-103

Beaumont HM, Mandl AM (1961) A quantitavive and cytological study of oogonia and oocytes in the foetal and neonetal rat. *Proceedings of the Royal Society of London***:** 557-579

Bi W, Drake CJ, Schwarz JJ (1999) The transcription factor MEF2C-null mouse exhibits complex vascular malformations and reduced cardiac expression of angiopoietin 1 and VEGF. *Dev Biol* **211:** 255-267

Bitgood MJ, Shen L, McMahon AP (1996) Sertoli cell signaling by Desert hedgehog regulates the male germline. *Current Biology* **6:** 298-304

Boyer A, Lapointe E, Zheng X, Cowan RG, Li H, Quirk SM, DeMayo FJ, Richards JS, Boerboom D (2010) WNT4 is required for normal ovarian follicle development and

female fertility. *FASEB Journal* **24:** 3010-3025

Byrd N, Becker S, Maye P, Narasimhaiah R, St-Jacques B, Zhang X, McMahon J, McMahon A, Grabel L (2002) Hedgehog is required for murine yolk sac angiogenesis. *Development* **129:** 361-372

Byrd N, Grabel L (2004) Hedgehog signaling in murine vasculogenesis and angiogenesis. *Trends in Cardiovascular Medicine* **14:** 308-313

Chambers RC, Leoni P, Kaminski N, Laurent GJ, Heller RA (2003) Global expression profiling of fibroblast responses to transforming growth factor-beta1 reveals the induction of inhibitor of differentiation-1 and provides evidence of smooth muscle cell phenotypic switching. *Am J Pathol* **162:** 533-546

Chen W, Tang T, Eastham-Anderson J, Dunlap D, Alicke B, Nannini M, Gould S, Yauch R, Modrusan Z, Dupree KJ, Darbonne WC, Plowman G, de Sauvage FJ, Callahan CA (2011) Canonical hedgehog signaling augments tumor angiogenesis by induction of VEGF-A in stromal perivascular cells. *Proc Natl Acad Sci U S A* **108:** 9589-9594

Ching S, Vilain E (2009) Targeted disruption of Sonic Hedgehog in the mouse adrenal leads to adrenocortical hypoplasia. *Genesis* **47:** 628-637

Dahm-Kahler P, Lofman C, Fujii R, Axelsson M, Janson PO, Brannstrom M (2006) An intravital microscopy method permitting continuous long-term observations of ovulation in vivo in the rabbit. *Hum Reprod* **21:** 624-631

Delgado-Rosas F, Gaytan M, Morales C, Gomez R, Gaytan F (2009) Superficial ovarian cortex vascularization is inversely related to the follicle reserve in normal cycling ovaries and is increased in polycystic ovary syndrome. *Hum Reprod* **24:** 1142-1151

Donovan MJ, Lin MI, Wiegn P, Ringstedt T, Kraemer R, Hahn R, Wang S, Ibanez CF, Rafii S, Hempstead BL (2000) Brain derived neurotrophic factor is an endothelial cell survival factor required for intramyocardial vessel stabilization. *Development* **127:** 4531-4540

Elenbaas B, Weinberg RA (2001) Heterotypic signaling between epithelial tumor cells and fibroblasts in carcinoma formation. *Exp Cell Res* **264:** 169-184

Fortune JE, Yang MY, Muruvi W (2011) In vitro and in vivo regulation of follicular formation and activation in cattle. *Reprod Fertil Dev* **23:** 15-22

Frontini MJ, Nong Z, Gros R, Drangova M, O'Neil C, Rahman MN, Akawi O, Yin H,

Ellis CG, Pickering JG (2011) Fibroblast growth factor 9 delivery during angiogenesis produces durable, vasoresponsive microvessels wrapped by smooth muscle cells. *Nat Biotechnol* **29:** 421-427

Furukawa K, Fujiwara H, Sato Y, Zeng BX, Fujii H, Yoshioka S, Nishi E, Nishio T (2007) Platelets are novel regulators of neovascularization and luteinization during human corpus luteum formation. *Endocrinology* **148:** 3056-3064

Geng L, Cuneo KC, Cooper MK, Wang H, Sekhar K, Fu A, Hallahan DE (2007) Hedgehog signaling in the murine melanoma microenvironment. *Angiogenesis* **10:** 259-267

Gerhardt H, Ruhrberg C, Abramsson A, Fujisawa H, Shima D, Betsholtz C (2004) Neuropilin-1 is required for endothelial tip cell guidance in the developing central nervous system. *Dev Dyn* **231:** 503-509

Girling JE, Donoghue JF, Lederman FL, Cann LM, Achen MG, Stacker SA, Rogers PA (2010) Vascular endothelial growth factor-D over-expressing tumor cells induce differential effects on uterine vasculature in a mouse model of endometrial cancer. *Reprod Biol Endocrinol* **8:** 84

Gu C, Rodriguez ER, Reimert DV, Shu T, Fritzsch B, Richards LJ, Kolodkin AL, Ginty DD (2003) Neuropilin-1 conveys semaphorin and VEGF signaling during neural and cardiovascular development. *Dev Cell* **5:** 45-57

Guasti L, Paul A, Laufer E, King P (2010) Localization of Sonic hedgehog secreting and receiving cells in the developing and adult rat adrenal cortex. *Mol Cell Endocrinol* **336** (1-2): 117-22

Hatano O, Takakusu A, Nomura M, Morohashi K (1996) Identical origin of adrenal cortex and gonad revealed by expression profiles of Ad4BP/SF-1. *Genes Cells* **1:** 663-671

Heikkila M, Peltoketo H, Leppaluoto J, Ilves M, Vuolteenaho O, Vainio S (2002) Wnt-4 deficiency alters mouse adrenal cortex function, reducing aldosterone production. *Endocrinology* **143:** 4358-4365

Huang CC, Miyagawa S, Matsumaru D, Parker KL, Yao HH (2010) Progenitor cell expansion and organ size of mouse adrenal is regulated by sonic hedgehog. *Endocrinology* **151:** 1119-1128

Hungerford JE, Little CD (1999) Developmental biology of the vascular smooth muscle cell: building a multilayered vessel wall. *J Vasc Res* **36:** 2-27

Ikeda Y, Shen WH, Ingraham HA, Parker KL (1994) Developmental expression of mouse steroidogenic factor-1, an essential regulator of the steroid hydroxylases. *Mol Endocrinol* **8:** 654-662

Ingham PW, McMahon AP (2001) Hedgehog signaling in animal development: paradigms and principles. *Genes and Development* **15:** 3059-3087

Jain RK (2003) Molecular regulation of vessel maturation. *Nature Medicine* **9:** 685-693

Jamin SP, Arango NA, Mishina Y, Hanks MC, Behringer RR (2002) Requirement of Bmpr1a for Mullerian duct regression during male sexual development. *Nature Genetics* **32:** 408-410

Joeng KS, Long F (2009) The Gli2 transcriptional activator is a crucial effector for Ihh signaling in osteoblast development and cartilage vascularization. *Development* **136:** 4177-4185

Kalinichenko VV, Lim L, Stolz DB, Shin B, Rausa FM, Clark J, Whitsett JA, Watkins SC, Costa RH (2001) Defects in pulmonary vasculature and perinatal lung hemorrhage in mice heterozygous null for the Forkhead Box f1 transcription factor. *Dev Biol* **235:** 489-506

Kezele PR, Ague JM, Nilsson E, Skinner MK (2005) Alterations in the ovarian transcriptome during primordial follicle assembly and development. *Biol Reprod* **72:** 241-255

King P, Paul A, Laufer E (2009) Shh signaling regulates adrenocortical development and identifies progenitors of steroidogenic lineages. *Proc Natl Acad Sci U S A* **106:** 21185-21190

Koos RD (1995) Increased expression of vascular endothelial growth/permeability factor in the rat ovary following an ovulatory gonadotropin stimulus: potential roles in follicle rupture. *Biology of Reproduction* **52:** 1426-1435

Lin Q, Lu J, Yanagisawa H, Webb R, Lyons GE, Richardson JA, Olson EN (1998) Requirement of the MADS-box transcription factor MEF2C for vascular development. *Development* **125:** 4565-4574

Liu CF, Bingham N, Parker K, Yao HH (2009) Sex-specific roles of beta-catenin in mouse gonadal development. *Hum Mol Genet* **18:** 405-417

Macchiarelli G, Jiang JY, Nottola SA, Sato E (2006) Morphological patterns of angiogenesis in ovarian follicle capillary networks. A scanning electron microscopy

study of corrosion cast. *Microscopy Research and Technique* **69:** 459-468

Marconcini L, Marchio S, Morbidelli L, Cartocci E, Albini A, Ziche M, Bussolino F, Oliviero S (1999) c-fos-induced growth factor/vascular endothelial growth factor D induces angiogenesis in vivo and in vitro. *Proc Natl Acad Sci U S A* **96:** 9671-9676

Markiewicz M, Nakerakanti SS, Kapanadze B, Ghatnekar A, Trojanowska M (2011) Connective tissue growth factor (CTGF/CCN2) mediates angiogenic effect of S1P in human dermal microvascular endothelial cells. *Microcirculation* **18:** 1-11

Meidan R, Levy N (2007) The ovarian endothelin network: an evolving story. *Trends in Endocrinology and Metabolism* **18:** 379-385

Mirshahi F, Pourtau J, Li H, Muraine M, Trochon V, Legrand E, Vannier J, Soria J, Vasse M, Soria C (2000) SDF-1 activity on microvascular endothelial cells: consequences on angiogenesis in in vitro and in vivo models. *Thromb Res* **99:** 587-594

Nagase M, Nagase T, Koshima I, Fujita T (2006) Critical time window of hedgehog-dependent angiogenesis in murine yolk sac. *Microvascular Research* **71:** 85-90

Nagase T, Nagase M, Machida M, Fujita T (2008) Hedgehog signalling in vascular development. *Angiogenesis* **11:** 71-77

Nielsen CM, Dymecki SM (2010) Sonic hedgehog is required for vascular outgrowth in the hindbrain choroid plexus. *Dev Biol* **340:** 430-437

Nilsson EE, Detzel C, Skinner MK (2006) Platelet-derived growth factor modulates the primordial to primary follicle transition. *Reproduction* **131:** 1007-1015

Olsen CL, Hsu PP, Glienke J, Rubanyi GM, Brooks AR (2004) Hedgehog-interacting protein is highly expressed in endothelial cells but down-regulated during angiogenesis and in several human tumors. *BMC Cancer* **4:** 43

Pan Q, Chathery Y, Wu Y, Rathore N, Tong RK, Peale F, Bagri A, Tessier-Lavigne M, Koch AW, Watts RJ (2007) Neuropilin-1 binds to VEGF121 and regulates endothelial cell migration and sprouting. *Journal of Biological Chemistry* **282:** 24049-24056

Pazin DE, Albrecht KH (2009) Developmental expression of Smoc1 and Smoc2 suggests potential roles in fetal gonad and reproductive tract differentiaton. *Developmental Dynamics* **238:** 2877-2890

Pepling ME (2006) From primordial germ cell to primordial follicle: mammalian

female germ cell development. *Genesis* **44:** 622-632

Pola R, Ling LE, Silver M, Corbley MJ, Kearney M, Pepinsky RB, Shapiro R, Taylor FR, Baker DP, Asahara T, Isner JM (2001) The morphogen Sonic hedgehog is an indirect angiogenic agent upregulating two families of angiogenic growth factors. *Nature Medicine* **7:** 706-711

Ren Y, Cowan RG, Harman RM, Quirk SM (2009) Dominant activation of the hedgehog signaling pathway in the ovary alters theca development and prevents ovulation. *Molecular Endocrinology* **23:** 711-723

Robinson RS, Woad KJ, Hammond AJ, Laird M, Hunter MG, Mann GE (2009) Angiogenesis and vascular function in the ovary. *Reproduction* **138:** 869-881

Russell MC, Cowan RG, Harman RM, Walker AL, Quirk SM (2007) The hedgehog signaling pathway in the mouse ovary. *Biology of Reproduction* **77:** 226-236

Salcedo R, Wasserman K, Young HA, Grimm MC, Howard OM, Anver MR, Kleinman HK, Murphy WJ, Oppenheim JJ (1999) Vascular endothelial growth factor and basic fibroblast growth factor induce expression of CXCR4 on human endothelial cells: In vivo neovascularization induced by stromal-derived factor-1alpha. *Am J Pathol* **154:** 1125-1135

Salvucci O, Yao L, Villalba S, Sajewicz A, Pittaluga S, Tosato G (2002) Regulation of endothelial cell branching morphogenesis by endogenous chemokine stromal-derived factor-1. *Blood* **99:** 2703-2711

Sartore S, Chiavegato A, Faggin E, Franch R, Puato M, Ausoni S, Pauletto P (2001) Contribution of adventitial fibroblasts to neointima formation and vascular remodeling: from innocent bystander to active participant. *Circ Res* **89:** 1111-1121

Schiffenbauer YS, Abramovitch R, Meir G, Nevo N, Holzinger M, Itin A, Keshet E, Neeman M (1997) Loss of ovarian function promotes angiogenesis in human ovarian carcinoma. *Proc Natl Acad Sci U S A* **94:** 13203-13208

Thomas M, Augustin HG (2009) The role of the Angiopoietins in vascular morphogenesis. *Angiogenesis* **12:** 125-137

Tomasek JJ, Gabbiani G, Hinz B, Chaponnier C, Brown RA (2002) Myofibroblasts and mechano-regulation of connective tissue remodelling. *Nat Rev Mol Cell Biol* **3:** 349-363

van Tuyl M, Groenman F, Wang J, Kuliszewski M, Liu J, Tibboel D, Post M (2007) Angiogenic factors stimulate tubular branching morphogenesis of sonic

hedgehog-deficient lungs. *Dev Biol* **303:** 514-526

Vokes SA, Yatskievych TA, Heimark RL, McMahon J, McMahon AP, Antin PB, Krieg PA (2004) Hedgehog signaling is essential for endothelial tube formation during vasculogenesis. *Development* **131:** 4371-4380

Wang G, Zhang Z, Xu Z, Yin H, Bai L, Ma Z, Decoster MA, Qian G, Wu G (2010) Activation of the sonic hedgehog signaling controls human pulmonary arterial smooth muscle cell proliferation in response to hypoxia. *Biochim Biophys Acta* **1803:** 1359-1367

White AC, Lavine KJ, Ornitz DM (2007) FGF9 and SHH regulate mesenchymal Vegfa expression and development of the pulmonary capillary network. *Development* **134:** 3743-3752

Wijgerde M, Ooms M, Hoogerbrugge JW, Grootegoed JA (2005) Hedgehog signaling in mouse ovary: Indian hedgehog and desert hedgehog induce target gene expression in developing theca cells. *Endocrinology* **146:** 3558-3566

Williams C, Kim SH, Ni TT, Mitchell L, Ro H, Penn JS, Baldwin SH, Solnica-Krezel L, Zhong TP (2010) Hedgehog signaling induces arterial endothelial cell formation by repressing venous cell fate. *Dev Biol* **341:** 196-204

Wulff C, Dickson SE, Duncan WC, Fraser HM (2001) Angiogenesis in the human corpus luteum: simulated early pregnancy by HCG treatment is associated with both angiogenesis and vessel stabilization. *Hum Reprod* **16:** 2515-2524

Zackrisson U, Mikuni M, Peterson MC, Nilsson B, Janson PO, Brannstrom M (2000) Evidence for the involvement of blood flow-related mechanisms in the ovulatory process of the rat. *Hum Reprod* **15:** 264-272

Zimmermann RC, Hartman T, Kavic S, Pauli SA, Bohlen P, Sauer MV, Kitajewski J (2003) Vascular endothelial growth factor receptor 2-mediated angiogenesis is essential for gonadotropin-dependent follicle development. *J Clin Invest* **112:** 659-669

CHAPTER FOUR:

OVARIAN PATHOLOGY IN AGED MICE WITH DOMINANT ACTIVATION OF THE HEDGEHOG SIGNALING PATHWAY IN THE OVARY

Summary

Virgin female *Amhr2*$^{+/+}$ *SmoM2* control mice and *Amhr2*$^{cre/+}$*SmoM2* mutant mice were caged together and maintained until advanced age in order to test for the occurrence of ovarian cancer. By 1.5 years of age, *Amhr2*$^{cre/+}$*SmoM2* mutant mice had ovaries containing an abnormal complement of stromal-like cells, but they did not develop epithelial-derived cancer. The present study determined the timeline of the pathological development and provided insight into the cause of this phenotype based on histological and immunohistochemical characteristics. Histological examination at a series of time points showed that pathological changes in the ovary of mutant mice started between 60 and 120 days of age and progressed over time, with the major phenotype being abnormal clusters of cells within the ovarian stroma that histologically resemble steroidogenic cells. These clusters of cells were still present at 1.5 years of age. At one year of age, cells positive for CYP17A were present sporadically in the ovarian stroma of mutant mice but not controls. At 1.5 years of age, ovarian and oviductal tissue merged and multiple cystic structures were present. Taken together, these results indicate that the pathology in the ovary of mutant mice is associated with the abnormal presence of steroidogenic-like cells but not with the development of epithelial-derived ovarian cancer.

Introduction

Female reproductive aging has many manifestations, including that it is associated with increased incidences of tumorigenesis within the ovary (Broekmans *et*

al., 2007). In female primates, a relatively sharp decline in fertility occurs in middle age, followed by a complete loss of fertility, termed menopause. In comparison, female rodents do not have a distinct physiological transition equivalent to menopause, and remain fertile until late in life. This difference presents limitations in using rodents as models to study human female reproductive aging; hence, our current knowledge of reproductive aging is gained primarily from clinical data of human samples and experimental data from primates. Before sterility associated with aging is reached, changes at all levels of the hypothalamic-pituitary-gonad (HPG) axis occur in a comparable manner in primates and rodents, such as elevated levels of circulating follicle-stimulating hormone (FSH) and anti-Mullerain hormone (AMH) (Broekmans *et al.*, 2007), and increasingly compromised quality of the remaining oocytes. Moreover, the exact processes and conditions associated with reproductive aging are strongly influenced by intrinsic and extrinsic factors, such as genetics, maternal-fetal interaction in utero, diabetes, smoking and alcohol intake, etc (Ottinger, 2010). Therefore, as a powerful tool for genetic, environmental and pharmaceutical manipulations, the mouse model is capable of providing insights into the molecular basis of reproductive aging and associated pathological changes in humans.

Aberrant HH signaling activity is associated with numerous types of cancer (Merchant & Matsui, 2010; Rubin & de Sauvage, 2006; Taipale & Beachy, 2001), including several types of ovarian cancer (Bhattacharya *et al.*, 2008; Chen *et al.*, 2007; Liao *et al.*, 2009), such as ovarian dermoids and fibromas (Cretnik *et al.*, 2007;

Levanat *et al.*, 2004), granulosa cell tumors (Papanastasopoulos *et al.*, 2008), and ovarian surface epithelial (OSE) cell-derived tumors (Schmid *et al.*, 2011). Evidence indicates that *Amhr2*$^{cre/+}$ is expressed in the OSE cells , thus dominant activation of HH signaling may occur in OSE cells in *Amhr2*$^{cre/+}$*SmoM2* mutant mice (Fan *et al.*, 2009; Mullany *et al.*, 2011). Accordingly, we hypothesized that *Amhr2*$^{cre/+}$*SmoM2* mutant mice might develop OSE cell-derived epithelial ovarian tumors at advanced age. Based on this hypothesis, virgin female *Amhr2*$^{+/+}$ *SmoM2* control mice and *Amhr2*$^{cre/+}$*SmoM2* mutant mice were caged together to test for the occurrence of ovarian cancer. No evidence of OSE-derived ovarian cancer was detected by 1.5 years of age; nonetheless, virgin female *Amhr2*$^{cre/+}$*SmoM2* mutant mice developed ovarian pathology associated with the abnormal presence of steroidogenic-like cells with high penetrance. This chapter describes the timeline of the pathological development, and histological and immunohistochemical characteristics of the ovaries from aged *Amhr2*$^{cre/+}$*SmoM2* mutant mice.

Materials and Methods

Mouse Strains and Management

Procedures were performed as described in Chapter 2.

Histology and Immunohistochemistry

Ovarian histology and immunohistochemistry of CYP17A were performed as described in Chapter 3.

Results

Ovarian pathology of aged Amhr2$^{cre/+}$SmoM2 mutant mice

Virgin female *Amhr2$^{+/+}$ SmoM2* control mice and *Amhr2$^{cre/+}$SmoM2* mutant mice were caged together until they were 1.5 years of age. Four out of four *Amhr2$^{cre/+}$SmoM2* mutant mice developed pathological changes in their ovaries (Fig. 4.1A). Histological assessment revealed that while ovaries in controls appeared normal, ovaries of mutant mice became cystic and deformed (Fig 4.1B and C; asterisk indicates cyst, arrow points to follicle). Minimal solid ovarian tissue remained and seemed to be stretched due to the presence of multiple cysts. In an ovary from a different mutant mouse, ovarian and oviductal tissue merged (Fig. 4.1D; arrowhead points to oviductal lumen); regions with clusters of cells resembling steroidogenic cells and tissue infiltrated with a pool of blood cells were present (Fig. 4.1D, framed regions; 4.1E is the enlarged image of clusters of cells resembling steroidogenic cells; 4.1F is the enlarged image of a pool of blood cells).

Development of ovarian pathology in the ovary of Amhr2$^{cre/+}$SmoM2 mutant mice during aging

Histology of ovaries from *Amhr2$^{+/+}$ SmoM2* control mice and *Amhr2$^{cre/+}$SmoM2* mutant mice of various ages were examined and compared (Fig. 4.2). At 60 days of age, no apparent difference was observed between ovaries of controls and mutants (Fig.4.2 A and B). Nonetheless, at 120 days of age, excessive stromal tissue was

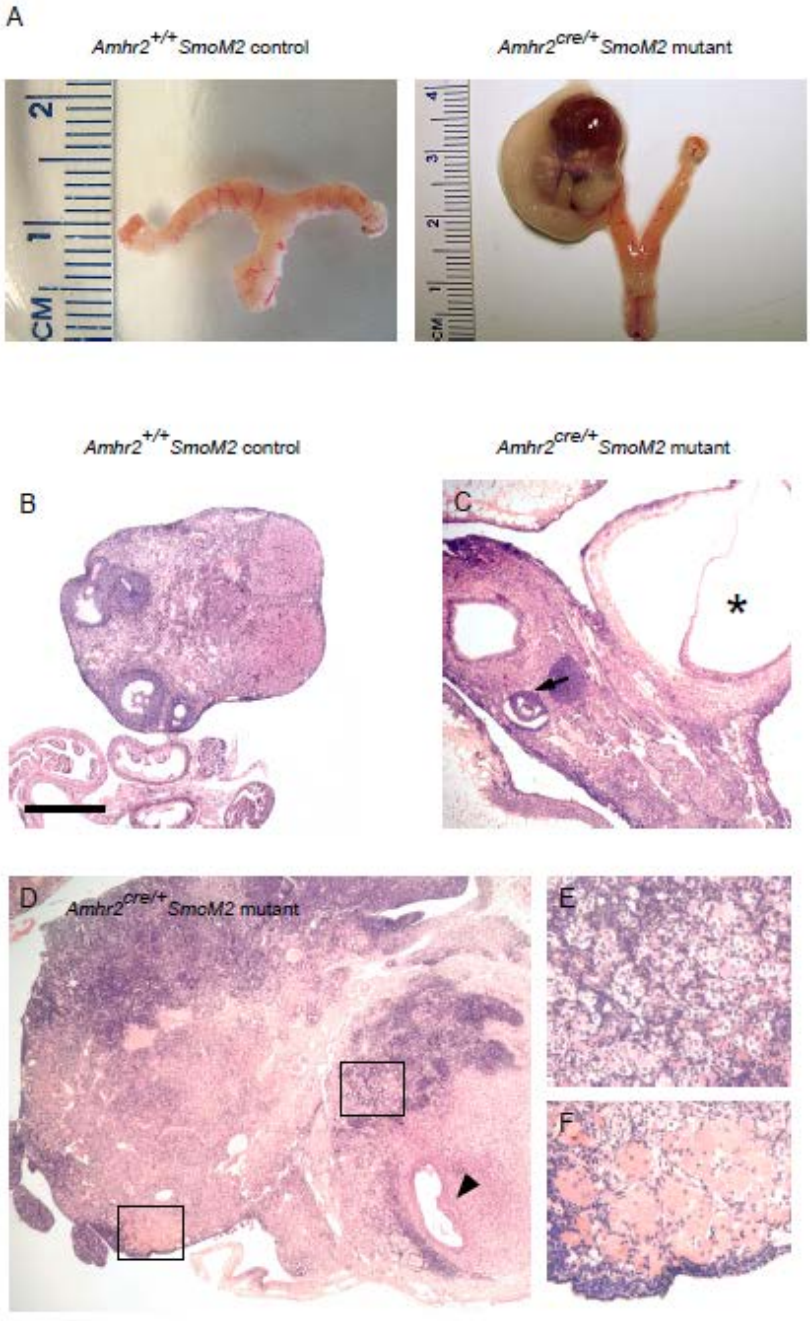
A
Amhr2+/+SmoM2 control
Amhr2cre/+SmoM2 mutant
B
Amhr2+/+SmoM2 control
C
Amhr2cre/+SmoM2 mutant
*
D
Amhr2cre/+SmoM2 mutant
E
F

Fig.4.1. Gross morphology and histology of ovaries from *Amhr2*$^{+/+}$ *SmoM2* control and *Amhr2*$^{cre/+}$*SmoM2* mutant mice at 1.5 years of age. **A**) Gross morphology of ovaries from *Amhr2*$^{+/+}$ *SmoM2* control and *Amhr2*$^{cre/+}$*SmoM2* mutant mice at 1.5 years of age. **B, C, D**) Histology of ovaries from *Amhr2*$^{+/+}$ *SmoM2* control and *Amhr2*$^{cre/+}$*SmoM2* mutant mice at 1.5 years of age. Inserts are enlarged images of framed fields. C and D represent images from the ovaries of two different mutant mice. Arrowhead, lumen of oviduct; arrow, follicle; asterisk, cystic structure. Scale bar represents 125 μm in enlarged panels and 500 μm in all other panels.

readily seen in ovaries of mutant mice compared to those of controls. A closer examination showed that the excessive stromal tissue in the mutants was primarily composed of clusters of cells with abundant cytoplasm and outlined by spindle-shaped mesenchymal cells (Fig. 4.2C and D; enlarged image shown in the insert). These cells with abundant cytoplasm resemble steroidogenic cells morphologically and will be termed steroidogenic-like cells in the following discussion. At one year of age, steroidogenic-like cells became more prominent compared to 120 days of age (Fig. 4.2E and F; enlarged image of the framed region in F is shown as Fig. 4.3B). In addition, numerous regions in the ovary of mutant mice seemed to be infiltrated by pools of blood (Fig. 4.2E and F; arrows).

Abnormal steroidogenic activity and infiltration of blood cells in the ovary of aged *Amhr2*$^{cre/+}$*SmoM2 mutant mice*

Regions of steroidogenic-like cells in the ovaries of mutant mice were further examined at one year of age (Fig. 4.3). Images at higher magnification showed that these cells had abundant cytoplasm characteristic of steroidogenic cells and were frequently in close proximity with tissues infiltrated with blood cells (Fig. 4.3 B, D and E; E is enlarged image of steroidogenic-like cells in B; D is enlarged image of infiltrated blood cells in B). Immunohistochemistry of CYP17A showed that only theca cells were positive for CYP17A in ovaries of controls (Fig. 4.3C), but CYP17A-positive cells not associated with follicles were sporadically present in small clusters in ovaries of mutant mice (Fig. 4.3G).

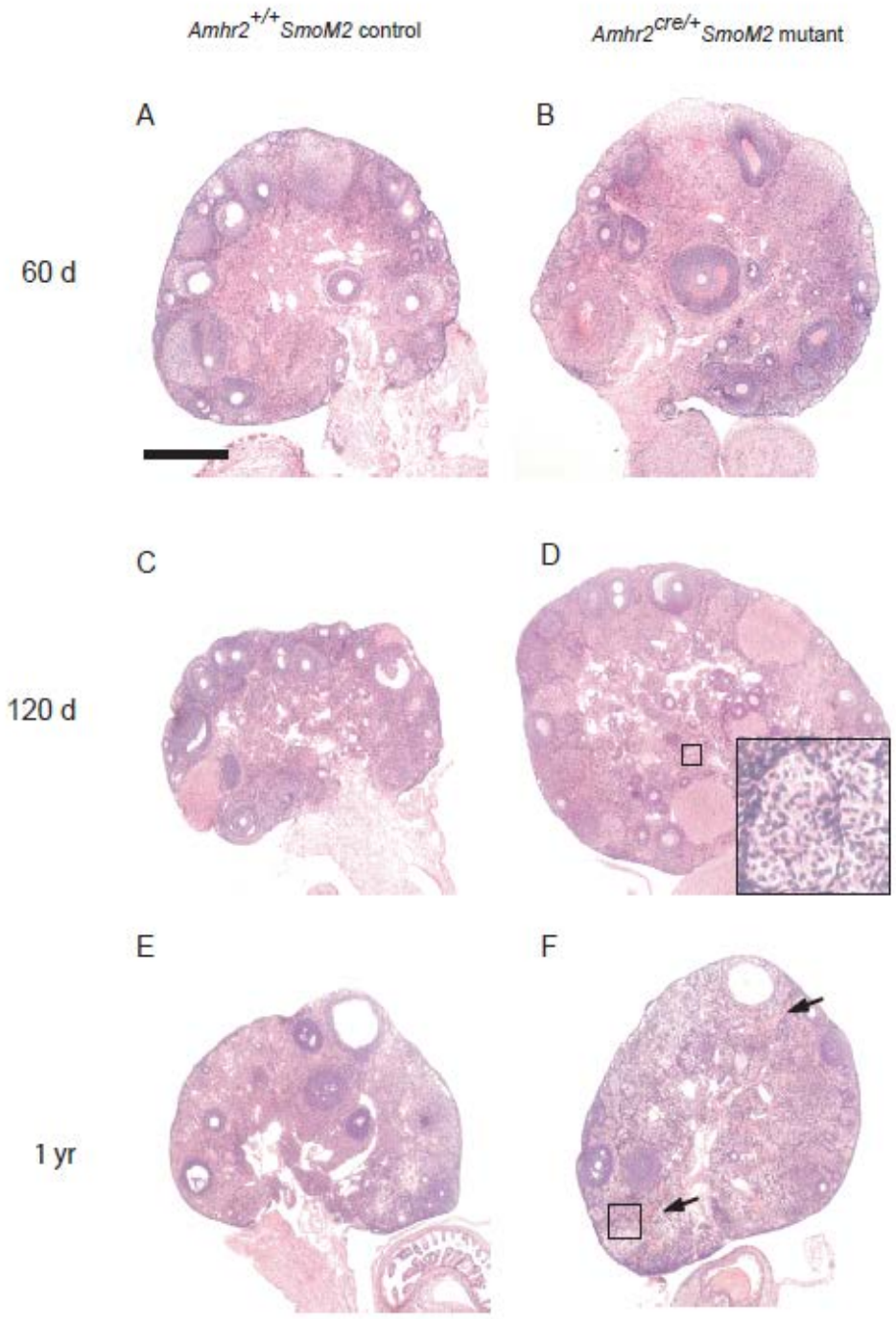
Amhr2+/+SmoM2 control
Amhr2cre/+SmoM2 mutant
A
B
60 d
C
D
120 d
E
F
1 yr

Fig.4.2. Histology of ovaries from *Amhr2*$^{+/+}$ *SmoM2* control and *Amhr2*$^{cre/+}$*SmoM2* mutant mice at 60, 120 days, and one year of age. In panel D, the insert is an enlarged image of the framed region. The framed area in panel F is enlarged in Fig. 3B. Arrows point to regions of tissue infiltrated by pools of red blood cells. Scale bar represents 60 μm for the enlarged insert and 500 μm in all other panels. Framed region in F is enlarged as Fig.4.3B.

Discussion

By 1.5 years of age, virgin female *Amhr2*$^{cre/+}$*SmoM2* mutant mice developed severe ovarian pathology. Histological examination at a series of time points showed that pathological changes in the ovary of mutant mice started between 60 and 120 days of age and progressed over time. The major phenotype in ovaries of mutant mice that persisted from 120 days to 1.5 years of age was the presence of clusters of steroidogenic-like cells in the ovarian stroma, some of which were positive for CYP17A. From one to 1.5 years of age, regions close to clusters of steroidogenic-like cells in the ovaries of mutant mice were frequently infiltrated by pools of red blood cells. Because steroidogenic-like cells were present before infiltration of red blood cells, the latter might be a secondary effect. Overall, data from the present study indicate that the pathology in the ovary of aged mutant mice is associated with abnormal steroidogenic-like cells.

Tumors in the ovary can be very difficult to classify based on morphological features and immunohistochemical markers, which may vary not only in different types of tumors but also at different stages of pathological progression (Scully, 1978). This is especially true for ovarian steroid cell tumors, in which tumor cells very often resemble adrenal cortical cells, and multiple terms have been given to the tumors including lipoid cell tumor, adrenal rest tumor, adrenal-like tumor, hypernephroid tumor, luteoma and masculinovoblastoma (Lin *et al.*, 2000). In the present study, excessive stromal tissue containing clusters of cells with abundant cytoplasm typical of steroidogenic cells was observed in the ovaries of aged mutants but not controls

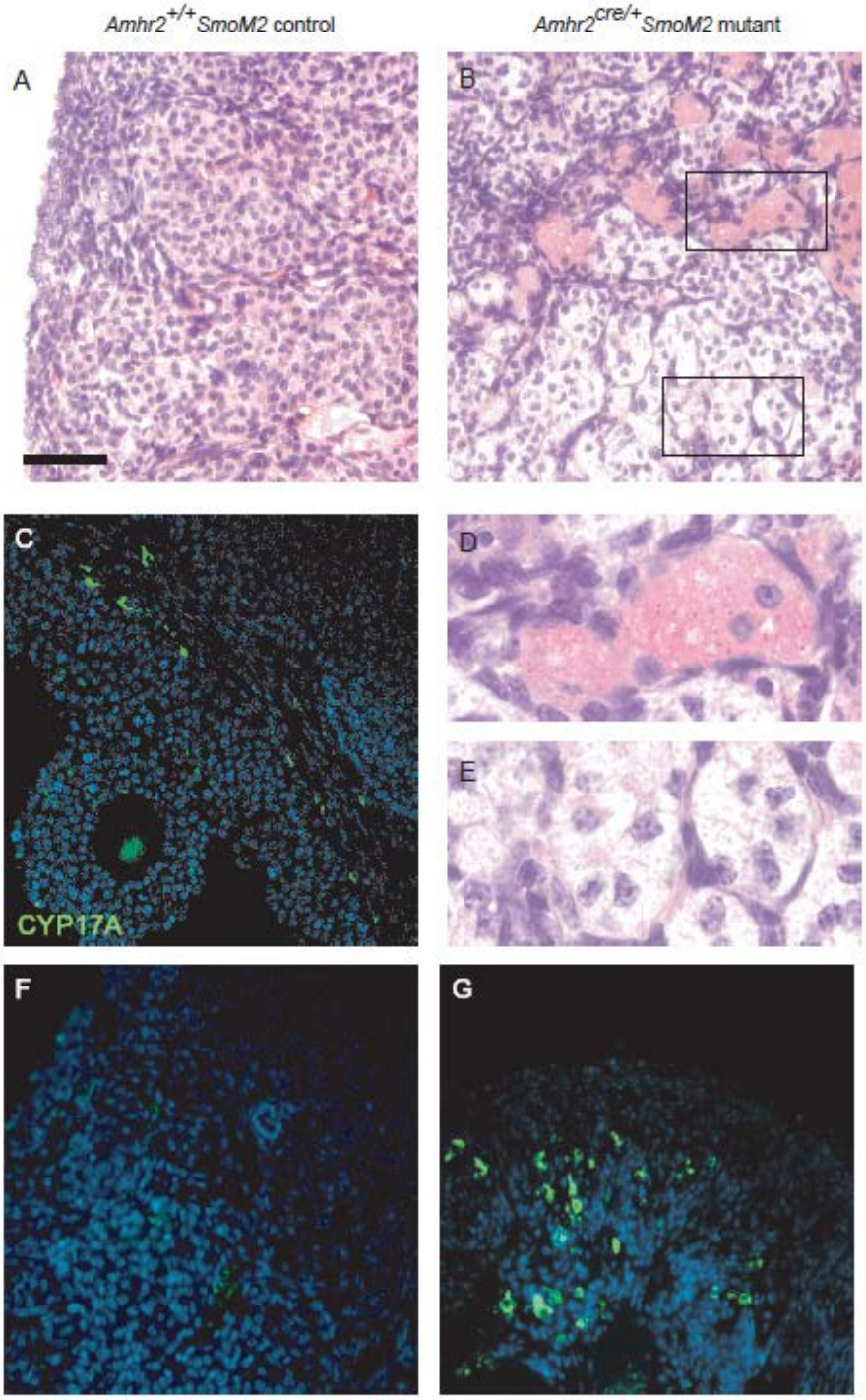
Amhr2+/+SmoM2 control
Amhr2cre/+SmoM2 mutant
A
B
C
CYP17A
D
E
F
G

Fig.4.3. Histology and immunohistochemistry for CYP17A of ovaries from *Amhr2*$^{+/+}$ *SmoM2* control and *Amhr2*$^{cre/+}$*SmoM2* mutant mice at one year of age. **A** and **B**) Histology of ovaries from *Amhr2*$^{+/+}$ *SmoM2* control and *Amhr2*$^{cre/+}$*SmoM2* mutant mice at one year of age. **D** and **E**) Enlarged images of framed regions in panel B. **C**, **F** and **G**) Immunohistochemistry for CYP17A (green) of ovaries from *Amhr2*$^{+/+}$ *SmoM2* control and *Amhr2*$^{cre/+}$*SmoM2* mutant mice. Scale bar represents 50 μm in A, B, C, F, and G; 20 μm in D and E.

between 120 days and 1.5 years of age. At one year of age, those clusters of stromal cells in the ovaries of mutant mice expressed CYP17A, consistent with their histological feature as steroidogenic cells. A pathologist, Dr. Alexander Nikitin, College of Veterinary Medicine, Cornell University, examined ovarian histology of mutant mice at one year of age and concluded that the excessive stromal tissue represented a luteoma. Although the clusters of stromal cells with steroidogenic features are morphologically similar to adrenal rest tumors of the ovary (Adashi *et al.*, 1979) and adrenalcortical neoplasia (Bielinska *et al.*, 2006), adrenal-specific markers such as *Cyp11b* and *Cyp21a* are needed to test whether the cells have characteristics of adrenal cells.

Adrenal rest tumors in the ovary seem to be rare and much less frequent than in the testis (Adashi *et al.*, 1979; Stikkelbroeck *et al.*, 2004). In the testis, the tumor is frequently found in patients with congenital adrenal hyperplasia, a condition characterized by a chronic high level of adrenocorticotrophic hormone (ACTH) (Clark *et al.*, 1990; Srikanth *et al.*, 1992). It was hypothesized that adrenal rest tumors of the gonad originate from a pluripotential cell population that can respond to ACTH stimulation and differentiate into adrenal-like cells (Srikanth *et al.*, 1992). This hypothesis was supported by a study showing that cells expressing the adrenal markers *Cyp21a* and *Cyp11*b are rare but present in the interstitium of fetal and adult mouse testes, and treatment with ACTH or hCG can induce the presence of more cells positive for these two adrenal markers (Val *et al.*, 2006). The normal ovary seems to lack a similar population of ACTH-responsive cells (Val *et al.*, 2006). A study of

ovarian adrenal rest tumor showed that tumor tissue expressed mRNA of *Mc2r (melanocortin 2 receptor)*, *Cyp21a* and *Cyp11b*, providing strong evidence that the tumor might be of adrenal origin (Lin *et al.*, 2000). Interestingly, adrenal-like cells are present in the neonatal ovaries of *Amhr2*$^{cre/+}$*SmoM2* mutant mice and these cells gradually disappear by 16 days of age. If the steroidogenic-like cells expressing CYP17A in the ovaries of aged mutant mice also express adrenal-specific marker genes, such as CYP21A, it would suggest a potential connection between abnormal differentiation/migration of adrenal-like cells in the embryonic and neonatal ovary and pathology in aged mice resembling adrenal rest tumors.

As we have not determined whether the steroidogenic-like cells in ovaries of aged mutant mice express adrenal markers, it is possible that these cells resemble or represent cells in stromal-leydig cell tumors (Kohn *et al.*, 1995). The presence of the Reinke crystals, which are naturally only seen in leydig cells, can be used to distinguish this possibility from the current hypothesis that they are of adrenal origin (Yoon *et al.*, 2010; Zhang *et al.*, 1982). Worth noting, loss of heterozygosity in the *Ptch* gene increases the occurrence of ovarian fibromas and dermoids (Cretnik *et al.*, 2007; Levanat *et al.*, 2004; Tsuji *et al.*, 2005), such as in the case of Basal Nevus (Gorlin) Syndrome (Ball *et al.*, 2011). Expression of the dominantly active *SmoM2* allele may have a similar effect in the ovary as heterozygosity in the *Ptch* gene, and could possibly induce the development of fibromas and dermoids. Further examination is needed to access this possibility. Limitations of the current study are the small sample size and the need to examine multiple biological markers.

An interesting comparison can be made between the ovarian phenotypes in *Amhr2*$^{cre/+}$*SmoM2* mutant mice that develops after breeding and what occurs during aging of virgin mice. Upon breeding, an abnormal inflammatory reaction of the uterine horn occurred in the mutant mice (Migone, *et al.*, 2011). As early as three to four days after breeding with intact males, the ovarian bursa of mutant mice became thickened and filled with transparent or yellowish fluid. Infiltration of neutrophils and necrosis in the oviduct and the ovarian tissue were observed. It is likely that ovarian pathology upon breeding originates from the abnormal inflammatory reaction in the uterine horn and the oviduct. Compared to the pathological changes after breeding, the ovarian abnormality in aged *Amhr2*$^{cre/+}$*SmoM2* mutant mice does not seem to originate from the reproductive tracts, because until one year of age, the oviduct and the ovary were still clearly separated, and the reproductive tract appeared to be normal morphologically. However, in aged *Amhr2*$^{cre/+}$*SmoM2* mutant mice, merging of the ovary and the oviduct also occurred. The fact that in both cases pathological development involved the ovary and the oviduct supports the idea that coordination between internal organs is tightly regulated during development and pathological changes, such as in the case of the ovary and the oviduct (Winnard *et al.*, 2006).

In conclusion, the results of the current study described in this chapter show that pathology in ovaries of aged *Amhr2*$^{cre/+}$*SmoM2* virgin females is associated with the presence of abnormal steroidogenic-like cells in the stromal tissue. The present study is preliminary and further examination is needed to more accurately define the

pathology associated with aging in the ovary of mutant mice.

Acknowledgement

We thank Dr. Richard R. Behringer, University of Texas M.D. Anderson Cancer

Center, Houston Texas, for providing *Amhr2*$^{cre/+}$ mice.

References

Adashi EY, Rosenwaks Z, Lee PA, Jones GS, Migeon CJ (1979) Endocrine features of an adrenal-like tumor of the ovary. *J Clin Endocrinol Metab* **48**: 241-245

Ball A, Wenning J, Van Eyk N (2011) Ovarian fibromas in pediatric patients with basal cell nevus (Gorlin) syndrome. *J Pediatr Adolesc Gynecol* **24**: e5-7

Bhattacharya R, Kwon J, Ali B, Wang E, Patra S, Shridhar V, Mukherjee P (2008) Role of hedgehog signaling in ovarian cancer. *Clin Cancer Res* **14**: 7659-7666

Bielinska M, Kiiveri S, Parviainen H, Mannisto S, Heikinheimo M, Wilson DB (2006) Gonadectomy-induced adrenocortical neoplasia in the domestic ferret (Mustela putorius furo) and laboratory mouse. *Vet Pathol* **43**: 97-117

Broekmans FJ, Knauff EA, te Velde ER, Macklon NS, Fauser BC (2007) Female reproductive ageing: current knowledge and future trends. *Trends Endocrinol Metab* **18**: 58-65

Chen X, Horiuchi A, Kikuchi N, Osada R, Yoshida J, Shiozawa T, Konishi I (2007) Hedgehog signal pathway is activated in ovarian carcinomas, correlating with cell proliferation: it's inhibition leads to growth suppression and apoptosis. *Cancer Sci* **98**: 68-76

Clark RV, Albertson BD, Munabi A, Cassorla F, Aguilera G, Warren DW, Sherins RJ, Loriaux DL (1990) Steroidogenic enzyme activities, morphology, and receptor studies of a testicular adrenal rest in a patient with congenital adrenal hyperplasia. *J Clin Endocrinol Metab* **70**: 1408-1413

Cretnik M, Musani V, Oreskovic S, Leovic D, Levanat S (2007) The Patched gene is epigenetically regulated in ovarian dermoids and fibromas, but not in basocellular carcinomas. *Int J Mol Med* **19**: 875-883

Fan HY, Liu Z, Paquet M, Wang J, Lydon JP, DeMayo FJ, Richards JS (2009) Cell type-specific targeted mutations of Kras and Pten document proliferation arrest in granulosa cells versus oncogenic insult to ovarian surface epithelial cells. *Cancer Res* **69**: 6463-6472

Kohn AD, Kovacina KS, Roth RA (1995) Insulin stimulates the kinase activity of RAC-PK, a pleckstrin homology domain containing ser/thr kinase. *EMBO Journal* **14**: 4288-4295

Levanat S, Musani V, Komar A, Oreskovic S (2004) Role of the hedgehog/patched signaling pathway in oncogenesis: a new polymorphism in the PTCH gene in ovarian fibroma. *Ann N Y Acad Sci* **1030**: 134-143

Liao X, Siu MK, Au CW, Wong ES, Chan HY, Ip PP, Ngan HY, Cheung AN (2009) Aberrant activation of hedgehog signaling pathway in ovarian cancers: effect on prognosis, cell invasion and differentiation. *Carcinogenesis* **30**: 131-140

Lin CJ, Jorge AA, Latronico AC, Marui S, Fragoso MC, Martin RM, Carvalho FM, Arnhold IJ, Mendonca BB (2000) Origin of an ovarian steroid cell tumor causing isosexual pseudoprecocious puberty demonstrated by the expression of adrenal steroidogenic enzymes and adrenocorticotropin receptor. *J Clin Endocrinol Metab* **85**: 1211-1214

Merchant AA, Matsui W (2010) Targeting Hedgehog--a cancer stem cell pathway. *Clinical Cancer Research* **16**: 3130-3140

Mullany LK, Fan HY, Liu Z, White LD, Marshall A, Gunaratne P, Anderson ML, Creighton CJ, Xin L, Deavers M, Wong KK, Richards JS (2011) Molecular and functional characteristics of ovarian surface epithelial cells transformed by KrasG12D and loss of Pten in a mouse model in vivo. *Oncogene* **30(32)**: 3522-36

Ottinger MA (2010) Mechanisms of reproductive aging: conserved mechanisms and environmental factors. *Ann N Y Acad Sci* **1204**: 73-81

Papanastasopoulos P, Repanti M, Damaskou V, Bravou V, Papadaki H (2008) Investigating differentiation mechanisms of the constituent cells of sex cord-stromal tumours of the ovary. *Virchows Arch* **453**: 465-471

Rubin LL, de Sauvage FJ (2006) Targeting the Hedgehog pathway in cancer. *Nature Reviews Drug Discovery* **5**: 1026-1033

Schmid S, Bieber M, Zhang F, Zhang M, He B, Jablons D, Teng NN (2011) Wnt and Hedgehog Gene Pathway Expression in Serous Ovarian Cancer. *Int J Gynecol Cancer*

Srikanth MS, West BR, Ishitani M, Isaacs H, Jr., Applebaum H, Costin G (1992) Benign testicular tumors in children with congenital adrenal hyperplasia. *J Pediatr Surg* **27**: 639-641

Stikkelbroeck NM, Hermus AR, Schouten D, Suliman HM, Jager GJ, Braat DD, Otten BJ (2004) Prevalence of ovarian adrenal rest tumours and polycystic ovaries in females with congenital adrenal hyperplasia: results of ultrasonography and MR imaging. *Eur Radiol* **14**: 1802-1806

Taipale J, Beachy PA (2001) The Hedgehog and Wnt signalling pathways in cancer. *Nature* **411**: 349-354

Tsuji T, Catasus L, Prat J (2005) Is loss of heterozygosity at 9q22.3 (PTCH gene) and 19p13.3 (STK11 gene) involved in the pathogenesis of ovarian stromal tumors? *Human Pathology* **36**: 792-796

Val P, Jeays-Ward K, Swain A (2006) Identification of a novel population of adrenal-like cells in the mammalian testis. *Dev Biol* **299**: 250-256

Winnard KP, Dmitrieva N, Berkley KJ (2006) Cross-organ interactions between reproductive, gastrointestinal, and urinary tracts: modulation by estrous stage and involvement of the hypogastric nerve. *Am J Physiol Regul Integr Comp Physiol* **291**: R1592-1601

Yoon BS, Seong SJ, Park CT, Park H, Shim JY, Kim JY (2010) Cellular fibroma of the ovary containing Leydig cell hyperplasia: a case report. *J Gynecol Oncol* **21**: 56-58

Zhang J, Young RH, Arseneau J, Scully RE (1982) Ovarian stromal tumors containing lutein or Leydig cells (luteinized thecomas and stromal Leydig cell tumors)--a clinicopathological analysis of fifty cases. *Int J Gynecol Pathol* **1**: 270-285

CHAPTER FIVE:

OVERALL CONCLUSIONS AND DISCUSSION

When this project was initiated, a significant amount was known about the critical roles of HH signaling in the *Drosophila* ovary, but there was no information about whether HH signaling played a role in the mammalian ovary. My results suggest that HH signaling is also important for the development of the mammalian ovary. I found that HH signaling may regulate the development of the thecal vasculature in the mouse ovary. In addition, HH signaling may control steroidogenic activity in the ovary, through its regulation of cell migration or/and sorting in the adrenogonadal primordium, or alternatively, by its effect on differentiation of steroidogenic cells in the ovary.

With the presence of key components within the HH signaling pathway identified in the mouse ovary, we set out to examine the in vivo function of HH signaling. We took advantage of the *Amhr2*$^{cre/+}$ transgenic mouse line created in Dr. Richard Behringer's laboratory. Two transgenic mouse lines were created around the same time in the Quirk laboratory, namely *Amhr2*$^{cre/+}$Smo$^{null/flox}$ and *Amhr2*$^{cre/+}$*SmoM2* mouse lines. In *Amhr2*$^{cre/+}$Smo$^{null/flox}$ mouse line, the HH signal transducer *Smo* is conditionally deleted in the somatic cells of the ovary and in the mesenchyme of the Mullerian duct . Deferred implantation (Harman *et al.*, 2011), reduced follicular vascular formation, as well as increased atresia of primary and secondary follicles in the ovary are observed in the mutant mice with reduced HH signaling activity (ongoing project conducted by other members in the Quirk laboratory). The focus of this dissertation is *Amhr2*$^{cre/+}$*SmoM2* mice in which HH signaling is abnormally activated in the ovary and the reproductive tract. In addition to the complete loss of fertility and failure of ovulation, development of the reproductive tract is altered in *Amhr2*$^{cre/+}$*SmoM2* mutant mice, as described in Migone *et al*., 2011. This dissertation focuses on the ovarian phenotypes of *Amhr2*$^{cre/+}$*SmoM2* mutant mice.

The *Amhr2*$^{cre/+}$ transgenic mouse line is a powerful tool to conditionally express or delete genes of interest in the ovary and the reproductive tract, and it has been utilized in multiple studies (Deutscher & Hung-Chang Yao, 2007; Jeyasuria *et al.*, 2004; Jorgez *et al.*, 2004; Lei *et al.*, 2010; Mullany *et al.*, 2011; Pangas *et al.*, 2004). The current project utilized this mouse line to express a fusion gene of *YFP* and the dominantly active allele of *Smo*, named *SmoM2*, in the ovary and the Mullerian duct. Data from the present study demonstrate that the *SmoM2-Yfp* fusion gene is expressed in somatic cells of neonatal ovary, and in theca and granulosa cells of preovulatory follicles (Chapter 3). In addition, although we did not obtain direct evidence that the *SmoM2-Yfp* fusion gene is also expressed in the ovary during embryonic development, the fact that HH signaling activity is already elevated in mutant mice at 17.5 dpc indicates that the *SmoM2-Yfp* fusion gene is expressed during embryonic development. This pattern of CRE-mediated recombination, as manifested by the expression of the *SmoM2/Yfp* fusion gene, is consistent with several other studies. Jamin *et al*. (2002) showed that *Amhr2* is expressed as early as 11.5 dpc in somatic cells of the gonads and in the mesenchymal cells of the Mullerian duct. Expression of *Amhr2* during early embryonic life was further demonstrated by data from several other studies (di Clemente *et al.*, 1994; Jeyasuria *et al.*, 2004; Pastorelli *et al.*, 2009). Results of the present study also indicate that *Amhr2*$^{cre/+}$ is expressed in granulosa and theca cells of preovulatory follicles (Chapter 2). Activity of *Amhr2*$^{cre/+}$ in granulosa and theca cells is consistent with results of other studies (Daikoku *et al.*, 2011; Jorgez *et al.*, 2004). Furthermore, *Amhr2*$^{cre/+}$ is active in CL (Daikoku *et al.*, 2011). Interestingly, in a double-mutant mouse model using *Amhr2*$^{cre/+}$ to delete the *Pten* gene and to express a stable form of *Kras*, ovarian surface epithelial (OSE) tumors occurred with 100% penetrance, suggesting *Amhr2*$^{cre/+}$ is also expressed in the OSE

cells (Fan *et al.*, 2009; Mullany *et al.*, 2011). In summary, based on information obtained to date, *Amhr2*$^{cre/+}$ is expressed in somatic cells of embryonic gonad starting from 11.5 dpc; postnatally, *Amhr2*$^{cre/+}$ is expressed in granulosa and theca cells of preovulatory follicles, in OSE cells, and CL. This temporal and spatial pattern of expression is important when interpreting ovarian phenotypes in transgenic mouse lines with *Amhr2*$^{cre/+}$ -mediated recombination. For instance, potential defects that may have occurred during embryonic and neonatal development should not be ignored when analyzing phenotypes observed during adult life, as exemplified in the present study.

Because cellular response to HH signaling activity is temporally and spatially restricted, cells expressing *SmoM2-Yfp* do not necessary have elevated HH signaling activity. In the neonatal ovaries of *Amhr2*$^{cre/+}$*SmoM2* mutant mice, although the majority of somatic cells express *SmoM2-Yfp* and no distinct pattern of spatial distribution of YFP-positive cells is observed, the cells with elevated HH signaling activity as indicated by elevated levels of mRNA for *Gli1*, *Ptch1* or *Hhip*, are only a portion of somatic cells in the medullary region or between ovigerous cords (Chapter 3). In the preovulatory follicles of *Amhr2*$^{cre/+}$*SmoM2* mutant mice, although both granulosa cells and theca cells express *SmoM2-Yfp*, neither of these two cell types has over-activated HH signaling. The difference between expression of the dominantly active SMOM2 and over-activation of HH signaling is also exemplified by data from other tissues. In the reproductive tracts of sexually mature female mice, CRE expression driven by the promoter of the *progesterone receptor gene* (*Pgr*) occurs in the luminal and glandular epithelial cells, as well as in the subepithelial stroma and myometrium (Soyal *et al.*, 2005); yet expression of SMOM2 only induced elevated HH signaling activity in the stroma and myometrium, not the luminal and glandular

epithelial cells (Franco *et al.*, 2010). Pancreatic ductal epithelial cells are incapable of transducing HH signaling and expression of SMOM2 in these cells did not induce expression of *Ptch-LacZ*; instead, an elevated level of mRNA for *Gli1* was detected in the SMA-positive cells within the stroma in close proximity to the ductal epithelium, indicating responsiveness to HH signaling activity is restricted to the stromal compartment in the pancreas (Artac *et al.*, 2009). To date, although a number of studies suggest an autocrine effect of HH signaling activity in development and tumorigenesis, such as acting as a survival factor for tumor cells and as a regulator of the self-renewal of cancer stem cells (Dierks *et al.*, 2008; Handrigan & Richman, 2010; Tzelepi *et al.*, 2011; Zhao *et al.*, 2009), results from the majority of related studies argue that HH signaling function in a paracrine manner (Bailey *et al.*, 2009; Nolan-Stevaux *et al.*, 2010; Singh *et al.*, 2011; Theunissen & de Sauvage, 2009). As in the ovary, uterus and pancreas discussed above, most often the mesenchymal compartment is the direct target and is responsive to changes in HH signaling activity from the nearby epithelium. The same logic may explain the absence of OSE-derived tumor in aged *Amhr2*$^{cre/+}$*SmoM2* mutant mice (Chapter 4). Although it is highly likely that SMOM2 is expressed in OSE cells, whether these cells are responsive to HH signaling is questionable and can be tested by examining levels of mRNA for *Gli1* and *Ptch1* using methods such as RT-PCR and in situ hybridization. Furthermore, crossing the *Amhr2*$^{cre/+}$*SmoM2* mouse line with mice carrying *Ptch-lacZ* allele may provide an effective way of identifying cells that are responsive to expression of dominantly active *SmoM2*, thus facilitating the accurate detection of cells types affected in the *Amhr2*$^{cre/+}$*SmoM2* mutant mice.

In chapter 2, we reported that *Amhr2*$^{cre/+}$*SmoM2* mutant mice fail to ovulate and this anovulation phenotype is highly likely due to the fact that the vasculature in

growing and preovulatory follicles of mutant mice fails to mature. This finding is novel in that the importance of a mature vasculature in the process of ovulation has not been recognized. Based on morphological characteristics and the expression of smooth muscle cell markers in the theca-interstitial layer, it was postulated that there is a layer of smooth muscle cells that contracts at the time of ovulation to release the oocyte-cumulus complex (Ko *et al.*, 2006; Okamura *et al.*, 1972; Talbot *et al.*, 1987). In the current study, we did not observe the presence of a layer of smooth muscle cells independent of the thecal vasculature, and data presented in Chapter 3 showed that in *Amhr2*$^{cre/+}$*SmoM2* mutant mice, reduced smooth muscle around growing follicles likely represents vascular smooth muscle in the theca layer. In fact, in multiple studies markers for smooth muscle cells have been used in the ovary as markers for the vascular mural cells (Inzunza *et al.*, 2007; Redmer *et al.*, 2001; Vorontchikhina *et al.*, 2005). Hence, the results of the current study support a role of the vascular mural cells in successful ovulation. Multiple changes occur to the ovarian vasculature in preparation for ovulation, such as changes in blood flow mediated by vasodilation and vasoconstriction, which modulate the formation of the follicle rupture site (Dahm-Kahler *et al.*, 2006; Koos; Macchiarelli *et al.*, 2006; Zackrisson *et al.*, 2000). Therefore, one potential mechanism through which vascular mural cells may participate in the process of ovulation is through their regulation of vasodilation and vasoconstriction before ovulation.

Results of the current study provide strong evidence that HH signaling regulates vascular development in the mouse ovary. HH signaling is over-activated in neonatal ovaries of the *Amhr2*$^{cre/+}$*SmoM2* mutant mice compared to controls. Levels of mRNA for genes involved in vascular network formation are elevated in whole ovaries of mutant mice compared to controls. A capillary network of higher density

forms in the cortex of newborn ovaries from mutant mice compared to controls. With reduced HH signaling activity in the *Amhr2*$^{cre/+}$Smo$^{null/flox}$ mutant mice, a lower density of capillary network forms (data from Quirk Laboratory). Thus, HH signaling is critical for vascular network formation in the neonatal ovary. Accumulating evidence suggests that the effect of HH ligands on promoting vasculogenesis and angiogenesis is often not through direct targeting to the endothelial cells, but to the mesenchymal cells surrounding the endothelial tube (Chen *et al.*, 2011; Frontini *et al.*, 2011; Pola *et al.*, 2001; Wang *et al.*, 2010; White *et al.*,2007). In the present study, levels of mRNA for genes involved in the interaction between endothelial and mesenchymal cells are elevated in whole ovaries of mutant mice compared to controls, such as *Foxf1a*, *Angpt-2*, *Mef2c* and *Ntrk2* (Chapter 3). During development, adult homeostasis and tumorigenesis, HH signaling plays important roles in the maintenance of progenitor cell populations in various tissues and organs (Beachy *et al.*, 2004). It is likely that HH regulates maintenance and/or differentiation of precursor cells for vascular mural cells, thereby participating in formation of vascular networks in the neonatal ovaries and in the maturation of thecal vasculature later in life.

Notably, dynamic changes in HH signaling activity seem to occur in the ovary in a temporally and spatially regulated manner (Ren *et al.*, 2009; Wijgerde *et al.*, 2005). Briefly, while levels of mRNA for *Ihh* and transcriptional targets *Ptch1* and *Gli1* decreased in the theca-interstitial tissue shortly after hCG treatment, the level of mRNA for *Gli3* sharply increased in granulosa cells at around 4 hr after hCG treatment, and the level of mRNA for *Hhip* increased in the granulosa cells from 4 to 12 hr after hCG treatment. HHIP binds to HH ligands and restricts their spatial distribution, functioning as an inhibitor of HH signaling (Ribes & Briscoe, 2009);

GLI3 is proteolytically cleaved and functions as a transcriptional repressor in the presence of decreasing HH signaling activity (Dessaud *et al.*, 2007). Thus, the decrease in mRNA levels of *Ihh* and increase in mRNA levels of *Hhip* and *Gli3* suggests an inhibition of HH signaling activity before ovulation occurs. This potential change in HH signaling activity may be important for successful ovulation to occur. As phenotypes in the *Amhr2*$^{cre/+}$*SmoM2* mutant mice are the result of long-term developmental defects, additional approaches are needed to more directly test this hypothesis.

Detection of adrenal-like cells in the ovaries of mutant mice around the time of birth suggests that HH signaling may play a role in the process of cell migration or/and sorting in the adrenogonadal primordium, or alternatively, elevated HH signaling activity may lead to steroidogenic differentiation of cells in the fetal and neonatal ovary into adrenal-like cells. A potential role of HH signaling in the cell migration or/and sorting of the adrenogonadal primordium can be tested in future studies and the first step would be to determine whether components of the HH signaling pathway are present in the adrenogonadal primordium within the time window (9.5 to 12 dpc) of cell migration/sorting. The alternative hypothesis, that elevated HH signaling activity may lead to steroidogenic differentiation of cells in the fetal and neonatal ovary into adrenal-like cells, is equally interesting. In the fetal adrenal gland, SHH regulates the steroidogenic differentiation of adrenal cortical cells, mainly through inducing expression of *Gli1* and *Ptch1* in the capsule cells surrounding the gland, which proliferate and differentiate into steroidogenic cells of the adrenal cortex (Ching & Vilain, 2009; Guasti *et al.*, 2010; Huang *et al.*, 2010; King *et al.*, 2009). If abnormally elevated HH signaling activity in the embryonic and neonatal ovary induced differentiation of ovarian cells into adrenal-like cells, it

would suggest that there is a population of precursor cells in the fetal and neonatal ovary that can respond to HH signaling and differentiate into adrenal-like cells. Whether this population of precursor cells also contains the precursors for theca cells will be an interesting subject for future studies. Interestingly, cells expressing *Gli1* and *Ptch1* in response to the expression of SMOM2 in *Amhr2*$^{cre/+}$*SmoM2* mutant mice may likely represent an excessive population of steroidogenic precursor cells, and these cells may contribute to the ovarian pathology in aged mice that is associated with steroidogenic-like cells (Chapter 4).

Overall, the current project establishes that HH signaling activity is an important regulator of vascular development in the mouse ovary. The results from this project also point to a potential role of HH signaling in cell migration or/and sorting within the adrenogonadal primordium, or alternatively, in the differentiation of steroidogenic cells in the ovary.

References

Artac RA, McFee RM, Smith RA, Baltes-Breitwisch MM, Clopton DT, Cupp AS (2009) Neutralization of vascular endothelial growth factor antiangiogenic isoforms is more effective than treatment with proangiogenic isoforms in stimulating vascular development and follicle progression in the perinatal rat ovary. *Biol Reprod* **81:** 978-988

Bailey JM, Mohr AM, Hollingsworth MA (2009) Sonic hedgehog paracrine signaling regulates metastasis and lymphangiogenesis in pancreatic cancer. *Oncogene* **28:** 3513-3525

Beachy PA, Karhadkar SS, Berman DM (2004) Tissue repair and stem cell renewal in carcinogenesis. *Nature* **432:** 324-331

Chen W, Tang T, Eastham-Anderson J, Dunlap D, Alicke B, Nannini M, Gould S, Yauch R, Modrusan Z, Dupree KJ, Darbonne WC, Plowman G, de Sauvage FJ, Callahan CA (2011) Canonical hedgehog signaling augments tumor angiogenesis by induction of VEGF-A in stromal perivascular cells. *Proc Natl Acad Sci U S A* **108:** 9589-9594

Ching S, Vilain E (2009) Targeted disruption of Sonic Hedgehog in the mouse adrenal leads to adrenocortical hypoplasia. *Genesis* **47:** 628-637

Dahm-Kahler P, Lofman C, Fujii R, Axelsson M, Janson PO, Brannstrom M (2006) An intravital microscopy method permitting continuous long-term observations of ovulation in vivo in the rabbit. *Hum Reprod* **21:** 624-631

Daikoku T, Jackson L, Besnard V, Whitsett J, Ellenson LH, Dey SK (2011) Cell-specific conditional deletion of Pten in the uterus results in differential phenotypes. *Gynecol Oncol* **122(2)**:424-9

Dessaud E, Yang LL, Hill K, Cox B, Ulloa F, Ribeiro A, Mynett A, Novitch BG, Briscoe J (2007) Interpretation of the sonic hedgehog morphogen gradient by a temporal adaption mechanism. *Nature* **450:** 717-721

Deutscher E, Hung-Chang Yao H (2007) Essential roles of mesenchyme-derived beta-catenin in mouse Mullerian duct morphogenesis. *Dev Biol* **307:** 227-236

di Clemente N, Wilson C, Faure E, Boussin L, Carmillo P, Tizard R, Picard JY, Vigier B, Josso N, Cate R (1994) Cloning, expression, and alternative splicing of the receptor for anti-Mullerian hormone. *Mol Endocrinol* **8:** 1006-1020

Dierks C, Beigi R, Guo GR, Zirlik K, Stegert MR, Manley P, Trussell C, Schmitt-Graeff A, Landwerlin K, Veelken H, Warmuth M (2008) Expansion of Bcr-Abl-positive leukemic stem cells is dependent on Hedgehog pathway activation. *Cancer Cell* **14:** 238-249

Fan HY, Liu Z, Paquet M, Wang J, Lydon JP, DeMayo FJ, Richards JS (2009) Cell type-specific targeted mutations of Kras and Pten document proliferation arrest in granulosa cells versus oncogenic insult to ovarian surface epithelial cells. *Cancer Res* **69:** 6463-6472

Franco HL, Lee KY, Rubel CA, Creighton CJ, White LD, Broaddus RR, Lewis MT, Lydon JP, Jeong JW, DeMayo FJ (2010) Constitutive activation of smoothened leads to female infertility and altered uterine differentiation in the mouse. *Biology of Reproduction* **85:** 991-999

Frontini MJ, Nong Z, Gros R, Drangova M, O'Neil C, Rahman MN, Akawi O, Yin H, Ellis CG, Pickering JG (2011) Fibroblast growth factor 9 delivery during angiogenesis produces durable, vasoresponsive microvessels wrapped by smooth muscle cells. *Nat Biotechnol* **29:** 421-427

Guasti L, Paul A, Laufer E, King P (2010) Localization of Sonic hedgehog secreting

and receiving cells in the developing and adult rat adrenal cortex. *Mol Cell Endocrinol* **336(1-2)**: 117-22

Handrigan GR, Richman JM (2010) Autocrine and paracrine Shh signaling are necessary for tooth morphogenesis, but not tooth replacement in snakes and lizards (Squamata). *Dev Biol* **337:** 171-186

Harman RM, Cowan RG, Ren Y, Quirk SM (2011) Reduced signaling through the hedgehog pathway in the uterine stroma causes deferred implantation and embryonic loss. *Reproduction* **141:** 665-674

Huang CC, Miyagawa S, Matsumaru D, Parker KL, Yao HH (2010) Progenitor cell expansion and organ size of mouse adrenal is regulated by sonic hedgehog. *Endocrinology* **151:** 1119-1128

Inzunza J, Morani A, Cheng G, Warner M, Hreinsson J, Gustafsson JA, Hovatta O (2007) Ovarian wedge resection restores fertility in estrogen receptor á knockout (ERá -/-) mice. *Proceedings of the National Academy of Sciences* **104:** 600-605

Jeyasuria P, Ikeda Y, Jamin SP, Zhao L, de Rooij DG, Themmen APN, Behringer RR, Parker KL (2004) Cell-specific knockout of steroidogenic factor 1 reveals its essential roles in gonadal function. *Molecular Endocrinology* **18:** 1610-1619

Jorgez CJ, Klysik M, Jamin SP, Behringer RR, Matzuk MM (2004) Granulosa cell-specific inactivation of follistatin causes female fertility defects. *Molecular Endocrinology* **18:** 953-967

King P, Paul A, Laufer E (2009) Shh signaling regulates adrenocortical development and identifies progenitors of steroidogenic lineages. *Proc Natl Acad Sci U S A* **106:** 21185-21190

Ko CM, Gieske MC, Al-Alem L, Hahn YK, Su W, Gong MC, Iglarz M, Koo Y (2006) Endothelin-2 in ovarian follicle rupture. *Endocrinology* **147:** 1770-1779

Koos RD (1995) Increased expression of vascular endothelial growth/permeability factor in the rat ovary following an ovulatory gonadotropin stimulus: potential roles in follicle rupture. *Biology of Reproduction* **52:** 1426-1435

Lei L, Jin S, Gonzalez G, Behringer RR, Woodruff TK (2010) The regulatory role of Dicer in folliculogenesis in mice. *Mol Cell Endocrinol* **315:** 63-73

Macchiarelli G, Jiang JY, Nottola SA, Sato E (2006) Morphological patterns of angiogenesis in ovarian follicle capillary networks. A scanning electron microscopy study of corrosion cast. *Microscopy Research and Technique* **69:** 459-468

Mullany LK, Fan HY, Liu Z, White LD, Marshall A, Gunaratne P, Anderson ML, Creighton CJ, Xin L, Deavers M, Wong KK, Richards JS (2011) Molecular and functional characteristics of ovarian surface epithelial cells transformed by KrasG12D and loss of Pten in a mouse model in vivo. *Oncogene* [Epub ahead of print]

Nolan-Stevaux O, Lau J, Truitt ML, Chu GC, Hebrok M, Fern ndez-Zapico ME, Hanahan D (2010) GLI1 is regulated through Smoothened-independent mechanisms in neoplastic pancreatic ducts and mediates PDAC cell survival and transformation. *Genes and Development* **23:** 24-36

Okamura H, Virutamasen P, Wright KH, Wallach EE (1972) Ovarian smooth muscle in the human being, rabbit, and cat. Histochemical and electron microscopic study. *Am J Obstet Gynecol* **112:** 183-191

Pangas SA, Jorgez CJ, Matzuk MM (2004) Growth differentiation factor 9 regulates expression of the bone morphogenic protein antagonist Gremlin. *Journal of Biological Chemistry* **279:** 32281-32286

Pastorelli LM, Wells S, Fray M, Smith A, Hough T, Harfe BD, McManus MT, Smith L, Woolf AS, Cheeseman M, Greenfield A (2009) Genetic analyses reveal a requirement for Dicer1 in the mouse urogenital tract. *Mamm Genome* **20:** 140-151

Pola R, Ling LE, Silver M, Corbley MJ, Kearney M, Pepinsky RB, Shapiro R, Taylor FR, Baker DP, Asahara T, Isner JM (2001) The morphogen Sonic hedgehog is an indirect angiogenic agent upregulating two families of angiogenic growth factors. *Nature Medicine* **7:** 706-711

Redmer DA, Doraiswamy V, Bortnem BJ, Fisher K, Jablonka-Shariff A, Grazul-Bilska AT, Reynolds LP (2001) Evidence for a role of capillary pericytes in vascular growth of the developing ovine corpus luteum. *Biology of Reproduction* **65:** 879-889

Ren Y, Cowan RG, Harman RM, Quirk SM (2009) Dominant activation of the hedgehog signaling pathway in the ovary alters theca development and prevents ovulation. *Molecular Endocrinology* **23:** 711-723

Ribes V, Briscoe J (2009) Establishing and interpreting graded sonic hedgehog signaling during vertebrate neural tube patterning: the role of negative feedback. *Cold Spring Harbor Perspectives in Biology* **1:a002014**

Singh S, Wang Z, Liang Fei D, Black KE, Goetz JA, Tokhunts R, Giambelli C, Rodriguez-Blanco J, Long J, Lee E, Briegel KJ, Bejarano PA, Dmitrovsky E, Capobianco AJ, Robbins DJ (2011) Hedgehog-Producing Cancer Cells Respond to

and Require Autocrine Hedgehog Activity. *Cancer Res* **71:** 4454-4463

Soyal SM, Mukherjee A, Lee KY, Li J, Li H, DeMayo FJ, Lydon JP (2005) Cre-mediated recombination in cell lineages that express the progesterone receptor. *Genesis* **41:** 58-66

Talbot P, Martin GG, Ashby H (1987) Formation of the rupture site in preovulatory hamster and mouse follicles: loss of the surface epithelium. *Gamete Research* **17:** 287-302

Theunissen JW, de Sauvage FJ (2009) Paracrine Hedgehog signaling in cancer. *Cancer Res* **69:** 6007-6010

Tzelepi V, Karlou M, Wen S, Hoang A, Logothetis C, Troncoso P, Efstathiou E (2011) Expression of hedgehog pathway components in prostate carcinoma microenvironment: shifting the balance towards autocrine signalling. *Histopathology* **58:** 1037-1047

Vorontchikhina MA, Zimmermann RC, Shawber CJ, Tang H, Kitajewski J (2005) Unique patterns of Notch1, Notch4 and Jagged1 expression in ovarian vessels during folliculogenesis and corpus luteum formation. *Gene Expression Patterns* **5:** 701-709

Wang G, Zhang Z, Xu Z, Yin H, Bai L, Ma Z, Decoster MA, Qian G, Wu G (2010) Activation of the sonic hedgehog signaling controls human pulmonary arterial smooth muscle cell proliferation in response to hypoxia. *Biochim Biophys Acta* **1803:** 1359-1367

White AC, Lavine KJ, Ornitz DM (2007) FGF9 and SHH regulate mesenchymal Vegfa expression and development of the pulmonary capillary network. *Development* **134:** 3743-3752

Wijgerde M, Ooms M, Hoogerbrugge JW, Grootegoed JA (2005) Hedgehog signaling in mouse ovary: Indian hedgehog and desert hedgehog induce target gene expression in developing theca cells. *Endocrinology* **146:** 3558-3566

Zackrisson U, Mikuni M, Peterson MC, Nilsson B, Janson PO, Brannstrom M (2000) Evidence for the involvement of blood flow-related mechanisms in the ovulatory process of the rat. *Hum Reprod* **15:** 264-272

Zhao C, Chen A, Jamieson CH, Fereshteh M, Abrahamsson A, Blum J, Kwon HY, Kim J, Chute JP, Rizzieri D, Munchhof M, VanArsdale T, Beachy PA, Reya T (2009) Hedgehog signalling is essential for maintenance of cancer stem cells in myeloid leukaemia. *Nature* **458:** 776-779